ANNA OLEKSANDRIVNA STRYZHAK

ESTUDO DA EXECUÇÃO E CONTROLO DA PROLIFERAÇÃO DE CÉLULAS HUMANAS

UNIVERSIDADE DO ALGARVE

Mestrado em Oncobiologia – Mecanismos Moleculares do Cancro

Faro

2021

ANNA OLEKSANDRIVNA STRYZHAK

ESTUDO DA EXECUÇÃO E CONTROLO DA PROLIFERAÇÃO DE CÉLULAS HUMANAS

MESTRADO EM ONCOBIOLOGIA, 2º ANO

Dissertação para obtenção do título de Mestre em Oncobiologia – Mecanismos Moleculares do Cancro

Cell Cycle and Cancer Biology Group, CBMR

Faculdade de Medicina e Ciências Biomédicas, UALG

Trabalho efetuado sob a orientação de:

Orientador: Professor Doutor Álvaro Tavares

Co-orientador: Doutor Juan Garrido-Maraver

UNIVERSIDADE DO ALGARVE

Mestrado em Oncobiologia – Mecanismos Moleculares do Cancro

Faro

2021

Estudo da execução e controlo da proliferação de células humanas

Declaração de autoria de trabalho

Declaro ser a autora deste trabalho, que é original e inédito. Autores e trabalhos consultados estão devidamente citados no texto e constam na listagem de referências incluída.

_____

Anna Oleksandrivna Stryzhak

"We are a family, and the loyalty of the family must come before anything and everyone else. For if we honour that commitment, we will never be vanquished – but if we falter in that loyalty, we will all be condemned."

Mario Puzo – The family (2001)

Agradecimentos / Acknowledgements

Quero agradecer a todos que duma forma ou doutra contribuíram para a realização deste trabalho.

Acima de tudo quero agradecer ao professor Álvaro Tavares, por me ter aceitado no seu laboratório. Pelo apoio, motivação, disponibilidade e por todos os conselhos. Pela partilha de conhecimento científico e por histórias de vida que contava durante o café da manhã.

Um obrigado especial à Inês Santos, pela ajuda, paciência e disponibilidade durante este ano. Por me ter ensinado os aspetos práticos do laboratório.

Ao Juan Garrido-Maraver, pela ajuda no laboratório e conversas interessantes.

À Cláudia Florindo, uma mulher e profissional que eu admiro.

À Andreia Colaço, colega de laboratório e de bancada, pela partilha de momentos altos e baixos neste mundo da ciência.

Às minhas amigas, Alene, Alexandra e Gisela, pelo apoio, conversas ao almoço e bons mementos que passámos durante esta saga. À Iasmina, Carla e Filipa, pela amizade que trago comigo pela vida.

Aos meus pais e irmão, longe da vista, mas sempre tão perto no meu coração. Graças a eles sou quem sou e estou onde estou. Uma eterna saudade.

ABSTRACT

Regulation of cell proliferation is of crucial importance to all multicellular organisms. The faithful transmission of genetic material relies upon the connection between chromosomes and the mitotic spindle. Errors can result in aneuploidy with consequent cell death or cancer formation.

This work was dedicated to studying a human MOB4, an uncharacterised member of the MOB-like proteins family. Preliminary results from our laboratory point for MOB4 localisation at the mitotic spindle, MOB4 was observed at centrosomes. In the absence of MOB4, CENP-A is lost from kinetochores. MOB4 downregulation causes severe mitotic defects, mitotic block, and cell death. However, the mechanism by which this protein acts is undetermined.

To better understand MOB4 function, nocodazole assays were held to study if MOB4 localisation could be altered when microtubules are depolymerised. Results suggest that MOB4 still localises at centrosomes. Afterwards, cells were treated with MG132 for metaphase block and analysis of MOB4 localisation at kinetochores. MOB4 does not appear to be localised at kinetochores in my working conditions. In addition, in cells treated with MG132, I observed MOB4 accumulations in the nucleus periphery of interphase cells. These results suggest that MOB4 accumulates in Golgi Complex during G2. In order to understand if these aggregates result from the MOB4 levels increase, I compared MOB4 protein levels of interphase cells and cells blocked in mitosis. Western blot results indicate that MOB4 concentration is stable during the cell cycle.

Furthermore, I wanted to know if these aggregates are dependent on microtubules. Cells were incubated with MG132 and nocodazole. MOB4 aggregates were observed in cells with and without microtubules. Additionally, some cells with depolymerised microtubules present separate accumulations of MOB4.

With this work, I can conclude that, in mitosis, MOB4 localises at centrosomes with and without the microtubules. MOB4 accumulates in Golgi Complex during G2, and these aggregates are independent of microtubules. Levels of MOB4 protein are stable during the cell cycle.

Keywords: MOB4, microtubules, mitotic spindle, Golgi, interphase

RESUMO

Regulação de proliferação celular é de importância crucial para todos os organismos multicelulares. A transmissão fiel do material genético para as células filhas depende da ligação correta entre os cromossomas e o fuso mitótico. Erros aqui podem resultar na morte celular ou podem levar à formação de cancro. A segregação cromossómica é conseguida pela interação entre os microtúbulos do fuso e os cinetocoros nos centrómeros. Os centrómeros em células humanas são definidos epigeneticamente por nucleossomas contendo CENP-A, que define o local de montagem do cinetocoro. A segregação cromossómica é conseguida através da regulação fina das interações cinetocoro-microtúbulo e a atividade correta de ativadores ou inibidores em estádios específicos da mitose. Apesar de sua importância, como os cinetocoros são montados, regulados e como funcionam durante a segregação cromossómica, estes são fenómenos ainda não totalmente compreendidos.

MOB4 é um membro essencial, que pertence a uma família de proteínas do tipo MOB, requerido para a transição entre metáfase e anáfase. A sua depleção resulta em defeitos severos na congregação e alinhamento dos cromossomas, e bloqueio mitótico. Para além de que células depletadas de MOB4 apresentam perda de CENP-A dos cinetocoros mitóticos. Ao mesmo tempo, CENP-E, membro de cinetocoro externo não é afetado. Também foi identificada a localização de MOB4 no fuso mitótico, MOB4 foi observado nos centrossomas. No contexto fisiológico, MOB4 apresenta ser um gene essencial sendo a sua deleção em *D. melanogaster* mutantes letal na fase de larva. Estas apresentavam tumores melanocíticos, mais uma vez alertando à conexão entre MOB4 e carcinogénese. Bases de dados de proteínas mostram que a proteína MOB4 é altamente expressa em vários tipos de cancro, sugerindo o seu papel proto-oncogénico. O mecanismo pelo qual MOB4 contribui para a evolução e a progressão tumoral ainda é por ser definido.

Um dos objetivos deste trabalho foi identificar se o MOB4 é essencial para a ligação entre cinetocoro e microtúbulo. Células foram submetidas a despolimerização de microtúbulos no gelo, com consequente recuperação de microtúbulos. Este processo permitiu determinar tempo necessário para completa despolimerização de microtúbulos e para aparecimento de primeiros microtúbulos nucleados.

Para a melhor compreensão da função de MOB4, células foram tratadas com nocodazole, para identificar se a localização centrosomal de MOB4 em células mitóticas é alterada na ausência

de microtúbulos. Nas condições de trabalho realizado, consegui demonstrar que MOB4 continua a ser localizado nos centrossomas na presença e na ausência de microtúbulos.

Resultados prévios a este trabalho, sugerem que MOB4 tem um papel importante para a acumulação de CENP-A nos cinetocoros. Estes dados deram origem à hipótese de que o MOB4 pode estar localizado nos cinetocoros. Para testar esta hipótese, as células foram tratadas com MG132, para bloqueio em metáfase e análise da possível localização de MOB4 nos cinetocoros. Nas minhas condições de trabalho, os resultados sugerem que MOB4 não se localiza nos cinetocoros. Contudo, em células tratadas com MG132 foi possível observar um elevado número de células interfásicas com MOB4 localizado na região perinuclear. Este resultado indica que esta localização correspondente ao Complexo Golgi, e estes agregados de MOB4 são formados durante G2, o que está de acordo com os resultados prévios do nosso laboratório.

Para compreender se os agregados de MOB4 são resultado do aumento dos seus níveis na célula, células foram tratadas com timidina e STLC, para o bloqueio em mitose. A análise proteica de células não tratadas e de células bloqueadas em mitose foi feita por meio de Western blot. Os resultados obtidos sugerem que os níveis de MOB4 são estáveis durante o ciclo celular. Este resultado é comum para pelo menos duas linhas celulares diferentes.

Para prosseguir com a análise dos agregados de MOB4, células foram incubadas com MG132 na presença de nocodazole, para identificar se estes agregados são dependentes de microtúbulos. Foi possível observar agregados de MOB4 no Complexo Golgi na presença e na ausência de microtúbulos. Estes resultados indicam que a localização de MOB4 aparenta ser independente da presença de microtúbulos. Além disso, foram observadas células com mais que uma acumulação de MOB4 na zona perinuclear de células quando estas foram tratadas com MG132 e nocodazole. Este acontecimento não teve lugar em células tratadas com MG132. Células incubadas com nocodazole apresentam baixo número de células interfásicas com agregados de MOB4 no Complexo Golgi. Este número é comparável ao controlo.

Para a localização e estudo de proteína de interesse, foram usadas células CRAL1, que expressam MOB4-GFP, geradas a partir de células HCT116. Esta linha celular permitiu amplamente identificar a localização e o comportamento da proteína MOB4. Como trata-se duma linha celular originadas por meio de isolamento clonal, é necessário criar várias linhas celulares criadas sob condições similares. Foi usada a tecnologia CRISPR/Cas9, para inserção da sequência de interesse pela recombinação homóloga para criar clones que expressam a

proteína MOB4 acoplada com uma proteína de fluorescência que torne possível a visualização desta proteína na célula.
Este trabalho permitiu mostrar que MOB4 permanece localizado nos centrossomas de células interfásicas na ausência de microtúbulos. A proteína MOB4 forma agregados no Complexo Golgi durante G2, sendo acumulação destes agregados independente dos microtúbulos. Os níveis proteicos de MOB4 são estáveis durante o ciclo celular.

Palavras-chave: MOB4, microtúbulos, fuso mitótico, Golgi, interfase

List of contents

List of figures

List of tables

List of abbreviations, acronyms, and symbols

APC/C	Anaphase promoting complex/cyclosome
ATP	Adenosine triphosphate
Bub	Budding uninhibited by benzimidazole
BubR1	Budding uninhibited by benzimidazole-related 1
C-terminus	Carboxyl-terminus
CBB	Coomassie brilliant blue
CCAN	Constitutive centromere-associated network
CCM	Cerebral cavernous malformation
Cdks	Cyclin-dependent kinases
CENP	Centromere-associated protein
CPC	Chromosomal passenger complex
CTTNBP2	Cortactin binding protein 2
DAPI	4′,6-diamidino-2-phenylindole
DMEM	Dulbecco's Modified Eagle's Medium
DNA	Deoxyribonucleic acid
dNTP	Deoxyribonucleotide triphosphate
E3	Ubiquitin ligase enzyme
ECL	Enhanced Chemiluminescence
EDTA	Ethylenediamine tetraacetic acid
EGFP	Enhanced green fluorescent protein
FBS	Fetal bovine serum
FITC	Fluorescein isothiocyanate
G0	Gap 0
G1	Gap 1
G2	Gap 2
GCK	Germinal centre kinase
GDP	Guanosine diphosphate
GFP	Green fluorescent protein
GTP	Guanosine triphosphate
HCl	Hydrochloric acid
HRP	Horseradish peroxidase
IP	Immunoprecipitation

KMN	KNL-1/Mis12 complex/Ndc80 complex
LATS	Large tumour suppressor
Mad	Mitotic arrest deficient
MAPs	Microtubule-associated proteins
MCC	Mitotic checkpoint complex
mCherry	monomeric Cherry
MG132	Carbobenzoxy-Leu-Leu-leucinal
uM	Micromolar
mM	Millimolar
MOB	Mps One Binder 1 kinase activator
M-phase	Mitosis
MPF	Mitosis-Promoting Factor
Mps1	Monopolar spindle 1 kinase
MST	Mammalian Ste20-like protein kinase
mRNA	Messenger ribonucleic acid
N-terminus	Amino-terminus
NaCl	Sodium chloride
NEB	Nuclear envelope breakdown
NDR	Nuclear Dbf2-related
nM	Nanomolar
OA	Okadaic acid
PAGE	Polyacrylamide gel electrophoresis
PBS	Phosphate-buffered saline
PCM	Pericentriolar material
PCR	Polymerase chain reaction
Plk	Polo-like kinase
PP2A	Protein phosphatase 2A
PP2A A	Protein phosphatase 2A adaptor subunit
PP2Ac	Protein phosphatase 2A catalytic subunit
PVDF	Polyvinylidene Difluoride
RNA	Ribonucleic acid
RNAi	RNA interference
RNase	Ribonuclease
S-phase	Synthesis-phase

SAC	Spindle assembly checkpoint
SDS	Sodium dodecyl sulphate
SIKE	Suppressor of IKK epsilon
siRNA	Small interfering RNA
SLMAP	Sarcolemma membrane associated protein
STK	Serine/threonine kinase
STLC	S-trityl-L-cysteine
STRIP	STRiatin interacting protein
STRIPAK	Striatin interacting phosphatase and kinase
STRN	Striatin
TEMED	N,N,N',N'-tetamethylethylenediamine
YAP	Yes-associated protein
γ-TuRC	γ-tubulin ring complex
γ-TuSC	γ-tubulin small complex

CHAPTER I

INTRODUCTION

1. Introduction

1.1. The cell cycle

From the simplest unicellular organisms to higher eukaryotes as mammals, the cell is the essential element whose primary function is to maintain its specific genetic information and propagate to subsequent generations (Alberts, Johnson *et al*., 2015).

It is estimated that the human body is composed of about $3x10^{13}$ cells. In addition, new cells are constantly being reproduced to replace damaged or shed (Bianconi *et al*., 2013). The cell cycle is an essential mechanism for the reproduction of all living organisms. It refers to the ordered series of events that lead to cell division and the production of two daughter cells, each containing chromosomes identical to those of the parental cell (Cooper & Hausman, 2013; Lodish *et al*., 2016).

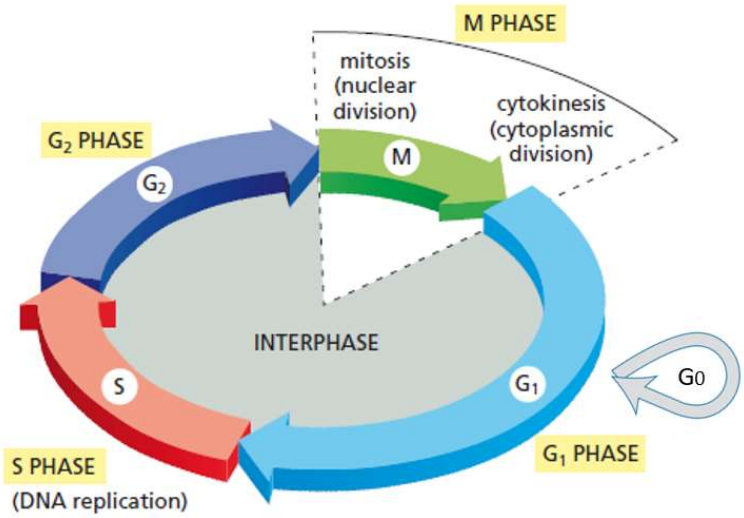

Figure I.1 – Representation of the cell cycle phases.
The interphase consists of growth and metabolic activity, called gap1 (G1), followed by a DNA synthesis phase, called the S phase, followed by a second gap phase, called G2. The nucleus division occurs in mitosis, and the cytoplasm division has a place in cytokinesis, and these two phases have a name of M phase. Most nonproliferating cells enter a specialised resting stage known as G zero (G0), in which they can stay for extended periods (days, weeks, or even years) before returning to proliferation (adapted from Alberts, Bray *et al*., 2014).

In eukaryotes, the cell cycle is a highly conserved process with a well-coordinated sequence of events (Lodish *et al*., 2016). Two main molecular processes occur during the cell cycle: the interphase, the more extended phase in the cell cycle, which contributes by cell growth, DNA

replication, and the distribution of duplicated chromosomes to daughter cells and mitosis (M phase), cell division (figure I.1). Mitosis is the shortest phase but with the most stunning cytological events that can be visualised under microscopy. The cells not only duplicate their genome but also duplicate their other organelles and mass of proteins. Approximately 95 % of the cell cycle is spent in the interphase (Cooper & Hausman, 2013; Alberts, Johnson *et al*., 2015).

1.1.1. Interphase

The remainder of the cell cycle, called interphase, is divided into three distinct stages, termed G1, S, and G2. Interphase is generally a time of high metabolic activity, during which DNA replication occurs in an orderly manner in preparation for cell division. The cells grow and double in size during interphase between one mitosis and the next (Alberts, Johnson *et al*., 2015; Cooper & Hausman, 2013).

There is an initial time gap, called G1, which corresponds to the interval (gap) between mitosis and the initiation of DNA replication. In G1, cells grow, metabolise, and perform their designated functions for the organism. Also, in G1, the cell can receive external signals that predict their future: enter a quiescent phase of the cell cycle called G zero (G0) or proceed to the S-phase. Following the G1 is a period of DNA synthesis, designated S, in which the entire genome is duplicated. Another gap phase completes DNA synthesis, G2, during which cell growth continues, proteins are synthesised, followed by the subsequent mitotic division (Alberts, Bray *et al*., 2014; Cooper & Hausman, 2013 & Lodish *et al*., 2016).

1.1.2. Mitosis

Human cells are extraordinarily complex machines being built from thousands of proteins with a wide range of functions. Perhaps the essential requirement is to replicate and duplicate itself and do so with high fidelity and efficiency. Indeed, errors in these processes are linked to the development of cancer, ageing and multiple human diseases states. The most remarkable part of this process is mitosis, nuclear division. It corresponds to the process in which each chromosome in the nucleus duplicates longitudinally. Then this double structure separates to become two daughter chromosomes, each going to a different daughter nucleus.

Mitosis produces two daughter nuclei identical genetically to each other and the progenitor nucleus (Alberts, Johnson, *et al*., 2015, Cooper & Hausman, 2013).

In higher eukaryotes, mitosis can be divided into several distinct phases with different characteristics, listed in chronological sequence as prophase, prometaphase, metaphase, anaphase, and telophase. These phases are very short and merge one into another, but each has definite characteristics, particularly concerning chromosomal behaviour, helpful in identifying each of these stages (figure I.2) (Alberts, Bray *et al*., 2014; Alberts, Johnson *et al*., 2015; Karp *et al*., 2016).

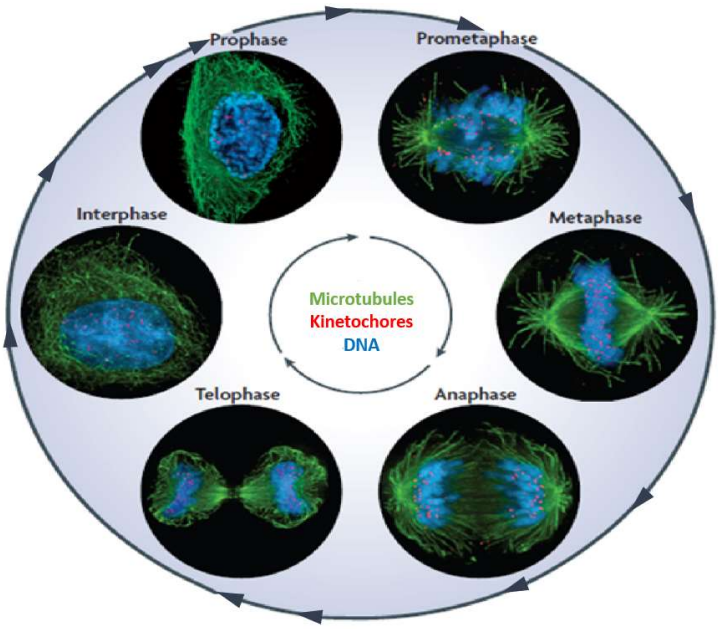

Figure I.2 - The human, mitosis-centric cell cycle.
An interphase human cell and cells in the five stages of mitosis are shown (adapted from Cheeseman & Desai, 2008).

The chromosomes condense at the prophase, the beginning of mitosis. The centrosome pair moves to opposite sides of the nucleus and nucleate microtubules and organise mitotic spindle. The two sister chromatids that have been replicated are attached at the centromere (Alberts, Johnson *et al*., 2015). The chromatids are identical and result from the DNA replication in the earlier S phase of the cell cycle. Also, during prophase, the nucleolus disappears, the Golgi complex breaks down into vesicles and nuclear envelope breakdown has a place. Almost all organelles are rebuilt or modified (Lodish *et al*., 2016).

In prometaphase, a new structure, the mitotic spindle, composed of a series of microtubules that stretch to the poles of the cell, appears. Centrosomes emanate spindle microtubules to search and capture the sister chromatids through association with kinetochores. The mitotic spindle is fundamental to the correct and active movement of the chromosomes to the two poles later in mitosis. The nuclear membrane completely disappears during metaphase, and the microtubules reorganise to form the mitotic spindle. The spindle microtubules are attached to the centromere of the chromosomes on opposite poles of the spindle (bipolar attachment). Furthermore, to become bi-oriented on the spindle centre, the chromosomes move to the metaphase plate, an imaginary region midway between the two poles (Alberts, Bray *et al*., 2014; Alberts, Johnson *et al*., 2015; Karp *et al*., 2016).

Anaphase is the shortest period of mitosis. It starts with the abrupt shortening of the kinetochore Microtubules which contributes to the synchronous separation of sister chromatids that are pulled in the direction of the spindle pole to which they are coupled. The spindle microtubules shortening contributes to chromosome segregation, with the two identical daughter chromosomes moving to opposite poles of the spindle. The interpolar (pole-to-pole) microtubules progressively extend to push two spindle poles further away from each other (Alberts, Bray *et al*., 2014; Alberts, Johnson *et al*., 2015; Karp *et al.*, 2016; Lodish *et al*., 2016).

The last phase of mitosis, telophase, is marked by the two sets of daughter chromosomes reaching opposite spindle poles, where they begin to decondense. The spindle has dispersed, and the nuclear envelope of the daughter cells reappears and surrounds the chromosomes, and the nucleoli are re-formed. The cytoplasm division with the assembly of contractile ring culminates the cell division (Alberts, Bray *et al*., 2014; Alberts, Johnson *et al*., 2015; Karp *et al.*, 2016; Lodish *et al*., 2016).

1.1.3. Centrosomes

Known as the major microtubule organising centre (MTOC) of animal cells, the centrosome participates in the organisation of the microtubule network within the cell (Lodish *et al*., 2016). Each centrosome in an animal cell comprises a pair of right-angled assembled cylindrical centrioles enclosed by a structured matrix of proteins called pericentriolar material. The centrioles are established, and stable structures composed of nine

sets of three laterally fused microtubules (Alberts, Johnson *et al*., 2015; Lodish *et al*., 2016), which are involved in recruiting the proteins that form the pericentriolar material. Furthermore, the direct function of pericentriolar material is nucleating and anchoring microtubules (Alberts, Bray *et al*., 2019; Lodish *et al*., 2016). The pericentriolar material contains a vast number of proteins, some of them with permanent function, such as γ-tubulin, and others with temporary action (Schatten, 2008). The *γ-tubulin ring complex (γ-TuRC)* is a ring-shaped, macromolecular complex located in the pericentriolar material. It comprises numerous copies of γ-tubulin complex proteins which minus (−) end is associated with γ-TuRC, and on which plus (+) end the first row of αβ-tubulin dimers assemble (Alberts, Bray *et al*., 2019; Karp *et al.*, 2016; Lodish *et al*., 2016).

During interphase, the centrosome is generally located near the nucleus, producing an array of microtubules with their plus ends radiating toward the cell periphery. Additionally, it influences cell shape, motility, polarity, and intracellular transport (Tang & Marshall, 2012).

In mitosis, two centrosomes, or spindle poles, are the microtubule organising centres that nucleate the microtubules of the mitotic spindle in animal cells. The assembly of microtubules, anchoring, and regulation of the microtubule minus-end dynamics are the main functions of the centrosomes (Alberts, Johnson *et al*., 2015; Lodish *et al*., 2016).

1.1.4. Microtubules

The microtubules are highly dynamic cytoskeletal structures that serve critical roles in all eukaryotic cells, including organelle transport, DNA segregation during mitosis, motility, organisation, and structure. Microtubules must assemble into distinctive structures to facilitate this wide range of functions, such as the tracks for intracellular transport, spindle for mitosis, and the basal body. Their length can vary from a fraction of a micrometre to hundreds of micrometres and is stiff due to their tubular construction (Alberts, Johnson *et al*., 2015; Bodakuntla *et al*., 2019; Lodish *et al*., 2016).

Two main concepts relating to microtubule organisation and dynamics: microtubules are assembled from localised sites known as microtubule organising centres, and individual microtubules can undergo dynamic instability (Lodish *et al*., 2016).

1.1.4.1. Microtubule structure and assembly

Microtubules are polymers of globular tubulin subunits, which by themselves are heterodimers. Each heterodimer is formed by two 55 kDa monomers, α-tubulin and β-tubulin, non-covalently bonded (Alberts, Johnson *et al.*, 2015, Lodish *et al.*, 2016). These heterodimers form cylindrical hollow structures composed of 13 parallel protofilaments, each composed of αβ-tubulin heterodimers pointing in the same direction. The external diameter of microtubules is about 25 nm and have distinct structural polarity. Within each dimer, the β subunit is the plus (+) end, preferential for polymerisation and the α is the minus (-) end, preferential for depolymerisation (figure I.3) (Karp *et al.*, 2016; Lodish *et al.*, 2016). This organisation means that guanosine-5'-triphosphate (GTP) bound to α-tubulin cannot be hydrolysed and is thus a structural component of a microtubule. β-tubulin subunits account for GTP-hydrolysis within the microtubule. Microtubules originate via nucleation and grow in a plus-end manner. The microtubule nucleation can occur in vitro from pure β-tubulin dimers (Desai & Mitchison, 1997).

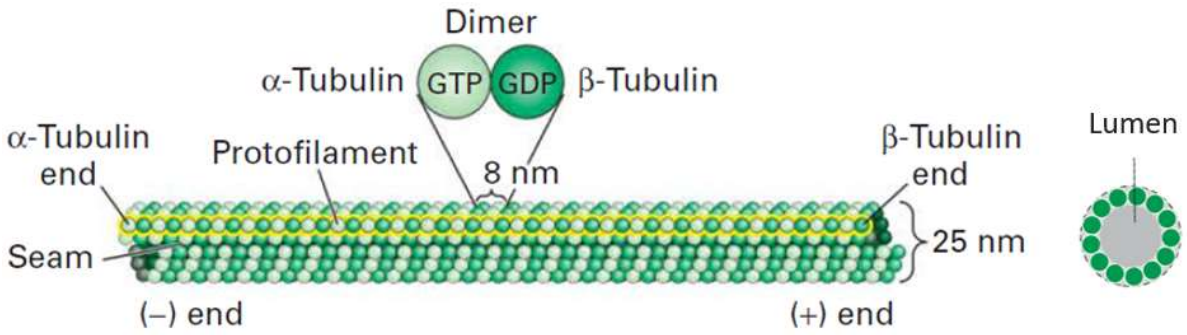

Figure I.3 - The organisation of tubulin subunits in a microtubule.
The dimers are aligned end to end into protofilaments, which pack side by side to form the microtubule wall. The protofilaments are slightly staggered so that α-tubulin in one protofilament is in contact with α-tubulin in the neighbouring protofilaments, except at the seam, where an α-tubulin contacts β-tubulin. The 13 protofilaments are assembled in the cylinder shape, forming the lumen in the middle (adapted from Lodish *et al.*, 2016).

The dynamics of microtubules allows them the rapid assembly or disassembly at their ends, with an extensively varying half-life, less than 60 seconds for mitotic cells and 5 to 10 minutes in interphase cells (Kirschner & Mitchison, 1986). Microtubule polymerisation is

highly regulated throughout the cell cycle. γ-tubulin is considered the primary microtubule nucleation protein. As a part of the γ-TuRC, γ is present at the microtubule minus-end and directs the polymerisation of new microtubules (Luders & Stearns, 2007).

The microtubules help eukaryotic cells maintain their shape and assist in forming the cell spindle during cell division. During mitosis, cells completely reorganise their microtubules to form a bipolar spindle extending from two centrosomes, also known as spindle poles, that can accurately segregate copies of the duplicated chromosomes. The Microtubule Associated Proteins (MAPs) are crucial for this process; they bind and modulate microtubules depending on the cell cycle-specific signalling (Lodish *et al*., 2016).

1.1.4.2. Dynamic instability

Dynamic instability of microtubules was first observed in vitro under appropriate conditions. Within a population of microtubules, no microtubule exhibits a steady-state length. Instead, they were regularly transitioning between shrinkage and rescue phases (figure I.4). Since the minus end of microtubules in animal cells are generally attached to a microtubule organising centre (MTOC), this dynamism is most relevant to the microtubule plus end (Mitchison & Kirschner, 1984). The growth of a microtubule plus-end is dependent on the concentration of free GTP-tubulin, which covers the growing microtubule plus end. GTPase activity of β-tubulin initiates the microtubule shrinkage. Hydrolysis of GTP results in guanosine diphosphate (GDP) bound tubulin within the microtubule, producing an unstable microtubule conformation and consequent catastrophe. Furthermore, these depolymerising microtubules are occasionally rescued by adding GTP-bound tubulin (Desai & Mitchision, 1997). This transient transitioning from microtubule growth to shrinkage is highly modulated by MAPs and increases dramatically as the cell enters mitosis (Lodish *et al*., 2016).

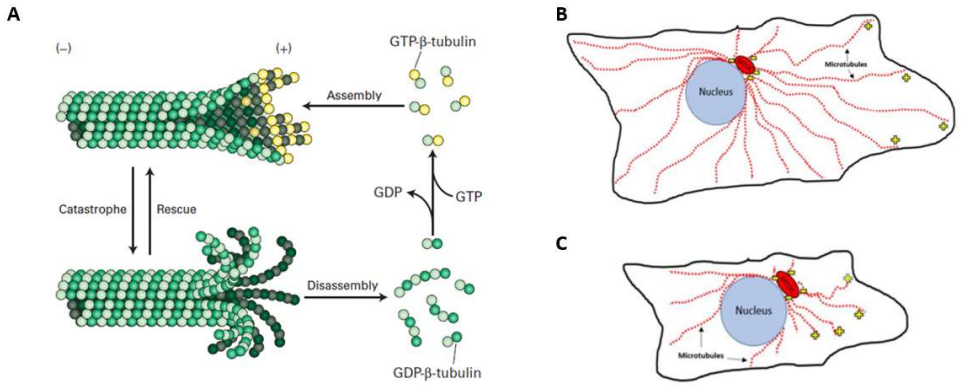

Figure I.4 - Diagram of microtubule dynamic instability.

A – diagram showing the dynamics of microtubule growth (top) and microtubule decay (bottom). GTP-b-tubulin adds to the growing plus-end of the microtubule when tubulin dimers are incorporated, and they transition from the GTP to GDP bound state. If enough GDP-b-tubulin is exposed at the plus-end, the microtubule will shrink in the process of catastrophe. The microtubule can also begin growth again in a process called rescue. Switches between rescues and catastrophes occur frequently, and associated proteins regulate the rate of switching. **B** – eukaryotic cells under normal physiological conditions exhibit a normal distribution of established microtubules. Free tubulin heterodimers are added to the plus-end (yellow plus sign) of the growing microtubule strand, extending to the cell's periphery. The microtubule minus-end (yellow minus sign) is located at the MTOC. **C** – Microtubules destabilise in the cells under non-physiological conditions (e. g. cold or drug presence). In this process, tubulin is removed at the plus-end, thus shrinking the microtubule towards the minus-end near the MTOC (adapted from Bowne-Anderson *et al*., 2013; Lodish *et al*., 2016).

1.1.5. Kinetochore

Human kinetochores are located at the centromeric domains that range from ~240 kb to more than 4 000 kb in size. Direct observation by electron microscopy using chemical fixation revealed a differentiated chromosomal region that connects to spindle fibres during mitosis, termed the kinetochore. The kinetochore consists of a plate-like structure around 300 nm wide and 150 nm deep (Jokelainen, 1967; Roos; 1973). It was demonstrated that microtubules plus ends are directly embedded in the outer kinetochore plate (Rieder, 1982). Nevertheless, high-pressure freezing, which better preserves kinetochore structure, shows that the tri-laminar plate structure is likely to be an artefact. The kinetochore instead appears as a fibrous network. Though these are not static attachments, chromosome movement is intimately coupled to changes in the polymerization dynamics of kinetochore-bound microtubules (Black, 2017).

The kinetochore is a macromolecular complex that mediates the connection between chromosomal DNA and microtubule polymers (Cheeseman, 2014; Cheeseman & Desai, 2008) (Figure I.5). The kinetochore is composed of over 100 proteins and is highly dynamic in humans due to its mitotic role. The kinetochore assembles, performs multiple functions, and then disassembles, all within 60 minutes. There are three kinetochore proteins, classified as the inner kinetochore, outer kinetochore, and dynamic kinetochore proteins (Black, 2017; Cheeseman & Desai, 2008).

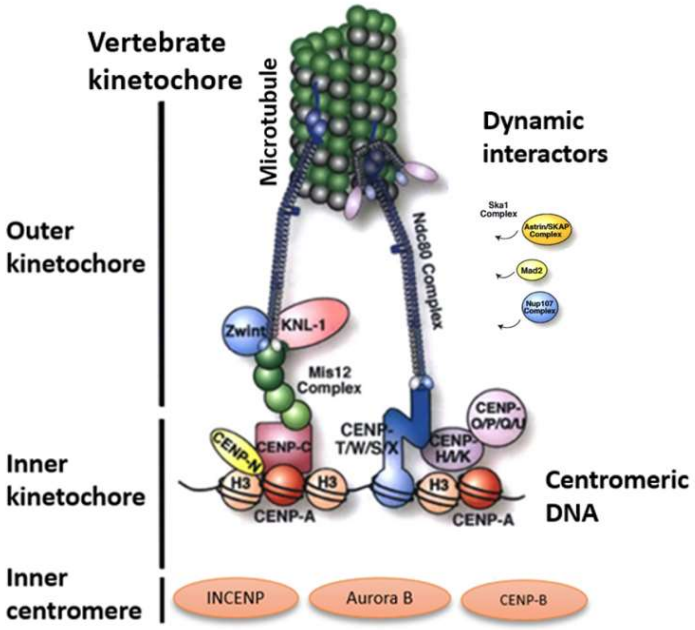

Figure I.5 - The vertebrate kinetochore. Schematic model of the tri-laminar structure of the kinetochore.

The sister-chromatids area is the inner centromere zone, which is defined by the chromosome passenger complex (CPC), and consists of Aurora B, INCENP, CENP-B, and condensin. The inner kinetochore consists of 5 groups of CENPs known as CCAN (CENP-C, CENP-T/W/S/X, CENP-N/L/M, CENP-H/I/K, and CENP-O/P/Q/R/U) and is assembled directly to the centromeric chromatin when CENP-A is deposited. The outer kinetochore lies onto the inner kinetochore and comprises three complexes of proteins: KNL1, the Mis12 complex, and the Ndc80 complex (KMN). Beyond the outer kinetochore is fibrous corona containing CENP-E and CENP-F. A selection of the dynamic interactors, proteins that localise to the kinetochore without well-established binding sites, are shown on the right (adapted from Cheeseman, 2014).

1.1.5.1. Inner kinetochore

The kinetochore protein structure located proximal to the centromeric chromatin is the constitutive centromere-associated network (CCAN). The 16 CCAN proteins, each also named 'CENP' (**CEN**tromere **P**rotein), are assembled on the centromere. These proteins interact together in inter and intra subcomplexes. Based on genetic and biochemical analyses, they are divided into several subgroups: the CENP-C group, the CENP-T/W group, the CENP-H/I/K(L/M/N) group, the CENP-O/P/Q/R/U group, and the CENP-S/X group (Black, 2017; Perpelescu & Fukagawa, 2011).

The inner kinetochore is responsible for attaching to chromosomes and assembles on a DNA binding the centromere (Black, 2017; McKinley and Cheeseman, 2015). The base of the inner kinetochore is a specific histone H3 variant called CENP-A. The CENP-A nucleosomes form the centromeric chromatin with interspersed canonical H3-containing nucleosomes, all of which additionally include histones H2A, H2B, and H4. The placement of CENP-A determines the site of kinetochore assembly, and the stable CENP-A pool is replenished each cell cycle during G1. Together with CENP-A, the proteins of CCAN assemble near the DNA interface and are stable throughout the cell cycle (Black, 2017; Hori *et al*., 2008). Two particular CCAN components, CENP-C and CENP-T, play a critical role in bridging kinetochore sub-complexes. CENP-C, which also binds CENP-A, reaches outward from the CCAN and contacts the Mis12 complex. CENP-T, which contains a nucleosome-like DNA binding domain, also reaches outward and contacts the Ndc80 complex. The Mis12 and Ndc80 complexes are essential members of the outer kinetochore (Black, 2017).

1.1.5.2. Outer kinetochore

The inner kinetochore components build a platform to assemble the outer kinetochore (Cheeseman & Desai, 2008). The outer kinetochore is responsible for binding to microtubules, holding on to growing and shrinking, and sensing and regulating microtubule attachments. Outer kinetochore proteins can be roughly divided into stable kinetochore members during mitosis and dynamically associated with the kinetochore. The stable kinetochore proteins primarily comprise components of the KNL-1, Mis12 complex, Ndc80

complex (KMN) network (Cheeseman *et al*., 2006). The Ndc80 complex is the conserved microtubule binder of the kinetochore and comprises four proteins: Ndc80 (Hec1), Nuf2, Spc24, and Spc25. The Spc24 and Spc25 subunits form the CENP-T or Mis12 binding base of the Ndc80 complex, and the Nuf2 and Ndc80 subunits contact the microtubule directly. The Mis12 complex is also constituted of four subunits. It acts as a central hub for the kinetochore, as it is positioned between the inner kinetochore and the rest of the outer kinetochore components (Black, 2017). Finally, KNL-1 is a single large protein that plays multiple functions, including a scaffold for many of the dynamic outer kinetochore components. The proteins of the KMN network are present at an estimated number of 15-20 copies per attachment site (number of microtubules in human cells) at the regional centromere (Cheeseman & Desai, 2008).

1.1.5.3. Dynamic kinetochore proteins

The third class of kinetochore components consists of the many proteins that dynamically localise to the kinetochore. Unlike the DNA-binding inner kinetochore proteins that localise throughout the cell cycle or the structural and microtubule-binding proteins of the outer kinetochore that localise for the duration of mitosis, dynamic kinetochore proteins have functions at specific time points. These dynamic proteins have characteristically weaker interactions with the kinetochore that are generally regulated by phosphorylation, competition, or a conformational change. Some of the most studied proteins in this class are the components of the spindle assembly checkpoint (SAC) (*e. g*. Mad2) (Musacchio & Salmon, 2007). These proteins localise to the kinetochore in prophase prior to the formation of stable kinetochore-microtubule attachments. Once these connections are made, checkpoint proteins disappear from the kinetochore. These localisation dynamics are often regulated by phosphorylation. Multiple mitotic kinases and phosphatases are also among the dynamic kinetochore proteins and play roles in regulating kinetochore assembly (*e. g.* CDK1) or establishing the spindle assembly checkpoint (Mpsl), as well as Ska1 complex, Astrin/SKAP complex, among others (Black, 2017).

1.1.5.4. Inner centromere

The chromosome passenger complex (CPC) binds centromeric chromatin, implements a mechanism required for spindle bipolarity, and guarantees that chromosomes are correctly attached to spindle microtubules at metaphase. In addition, the CPC is required for SAC function, mitotic chromosome structure and cytokinesis. The CPC is composed of Aurora B kinase, Survivin, Borealin and **IN**ner **CEN**tromere **P**rotein (INCENP) and is highly conserved within eukaryotes. Its localisation to the inner centromere during mitosis depends on the interaction of Survivin and Borealin with inner centromere protein and phosphorylation of histone H3 by Haspin kinase. Inner centromere protein also binds Aurora B, enabling its activation. Therefore, the activity of Aurora B initiates a feed-forward loop that supports activity and localisation of the CPC during mitosis, which is essential for efficient error correction at kinetochores (Black, 2017).

1.1.6. The mitotic spindle

The cells undergo massive internal reorganisation before and during division. In 1882, Walther Flemming first put name ‘mitosis’ (from Greek for ‘thread’) to the stereotyped process observed in animal cells: the condensation of threadlike chromosomes bound by an array of thinner fibres, their congression at the metaphase plate and eventual segregation to opposite poles of the dividing cell, and the reformation of nuclei in the two daughter cells. The language of threadwork stuck, and the apparatus of chromosome segregation is known as the mitotic spindle (Paweletz, 2001).

The mitotic spindle consists of microtubules nucleated by microtubule organising centres, condensed chromosomes that must be segregated, and kinetochores, which couple microtubule dynamics to chromosome movement. The mitotic spindle also includes numerous regulatory, checkpoint, microtubule-associated, and chromatin-remodelling proteins (Alberts, Johnson *et al*., 2015).

Together with a pair of asters, a mitotic spindle forms the mitotic apparatus. The spindle is a bilaterally symmetric bundle of microtubules and associated proteins with oval shape. It is

divided into opposing halves at the equator of the cell by the metaphase chromosomes. Aster is a radial array of the microtubules at each pole of the spindle (figure I.6) (Lodish *et al*., 2016).

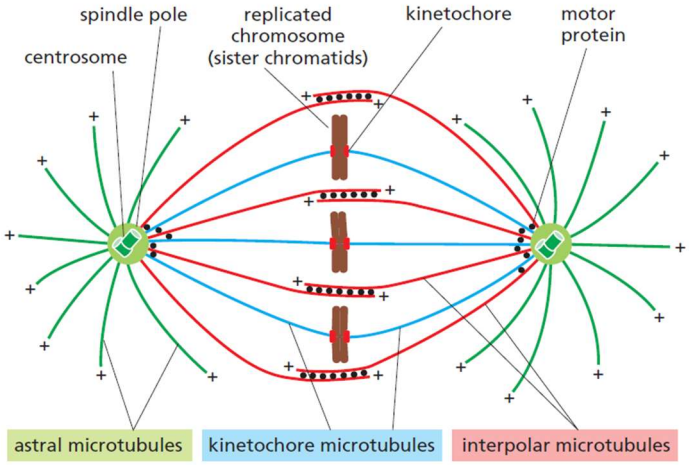

Figure I.6 - The metaphase mitotic spindle.
The plus-ends of the microtubules point toward the cell periphery, while the minus-ends are attached to the spindle poles, designed as centrosomes. K-fibres connect the spindle poles with the kinetochores of sister chromatids, while interpolar microtubules from the two poles interdigitate at the spindle equator. Astral microtubules expand from the poles into the cytoplasm (Alberts, Johnson *et al*., 2015).

A single centrosome at the pole organises three distinct groups of the microtubules whose minus-ends point toward the centrosome in each half of the spindle. The astral microtubules determine the aster; they spread outward from the centrosome toward the cell cortex. The site of cytokinesis is influenced by the positioning of the astral microtubules and by signals from the central spindle. The other two groups of microtubules constitute the spindle. The kinetochore microtubules (also called k-fibres) attach to the chromosomes at the kinetochores. Interpolar microtubules do not interact with chromosomes but instead intersect with interpolar microtubules from the opposite pole. There are two categories of interactions that hold two parts of the spindle together to form the bilaterally symmetric mitotic apparatus: 1) lateral interactions between the overlapping plus-ends of the interpolar microtubules and 2) end-on interactions between the kinetochore microtubules and the kinetochores of sister chromatids (Alberts, Johnson *et al*., 2015; Lodish *et al*., 2016).

1.1.6.1. Building the mitotic spindle

The proper segregation of duplicated chromosomes, crucial for the development and viability of a multicellular organism, requires the formation of a robust microtubule-based spindle apparatus. Entry into mitosis initiates a cascade of signalling events that activate pathways responsible for a dramatic rearrangement of the microtubule cytoskeleton, through changes in the properties of microtubule associated proteins, local concentrations of free tubulin dimer, and through enhanced microtubule nucleation. The latter is considered to be driven by localisation and activation of **γ**-tubulin-containing complexes (γ-TuSC and γ-TuRC) at specific subcellular localisations. For example, upon entering mitosis, animal cells concentrate γ-tubulin at centrosomes to tenfold the average level during interphase, resulting in aster driven search and capture of chromosomes and bipolar mitotic spindle formation (Khodjakov *et al*., 1999). Thus, centrosomes have traditionally been perceived as the primary microtubule organising centre during spindle formation in these cells. However, some previous studies have revealed the existence of complementary mechanisms of spindle formation; mitotic chromatin, kinetochores, the spindle matrix, and existing microtubules can all contribute to a bipolar spindle apparatus (Duncan & Wakefield, 2011).

1.1.6.2. Centrosome-nucleated microtubules

The centrosomes have been established as the primary microtubule organising centres during mitosis. Increased nucleation of microtubules by centrosomes at the onset of mitosis depends on the coordinated action of centriolar and pericentriolar material components. This process is facilitated in human cells, at least in part, by the protein Pericentrin (Zimmerman *et al*., 2004).

Centrosomal Microtubules, once nucleated, are held in the vicinity of the pericentriolar material (Mastronade *et al*., 1993). Nevertheless, the microtubules are not attached to the centrosome, the interaction between microtubules and the pericentriolar material is crucial for centrosome function (Gonzalez *et al*., 1990).

The dramatic increase in centrosome driven microtubule nucleation at the onset of mitosis leads to the astral arrays. Although initially radial, the centrosome derived microtubules begin

to grow with directional bias, such that the density of microtubules between the centrosomes and cell cortex. The assembly of a bipolar spindle is achieved through many additional microtubule associated proteins and microtubule motor proteins, working in concert with one another (Duncan & Wakefield, 2011).

1.1.6.3. Kinetochore-driven microtubules generation

For over 40 years, it has been known that kinetochores can initiate microtubule polymerisation *in vivo* independently of centrosomes (Witt *et al*., 1980). For over 30 years, it has been known that kinetochores can modulate the stability of microtubules that are kinetochore-bound (Hyman & Mitchison, 1990). Live imaging of microtubules has conclusively shown that in normal mitotic cells, these kinetochore-generated microtubules exist, incorporating into the growing, centrosome-driven spindle via their capture by astral microtubules (Khodjakov *et al*., 2003, Maiato *et al*., 2004). Different populations of microtubules are thus incorporated into a single bipolar spindle.

However, the mechanisms underlying kinetochore microtubule generation and their contribution to spindle assembly in normal cells have been challenging to elucidate. In the classical search-capture model of chromosome alignment (Nicklas & Ward, 1994), astral microtubules from opposing centrosomes attach to kinetochores, facilitating chromosome congression. However, if microtubules from the same pole attach to sister kinetochores, the interaction is selectively destabilised such that correct kinetochore microtubule relationships can be established. Thus, kinetochores must contain microtubule binding sites and act as a readout of merely and syntely, in addition to themselves generating microtubules (Duncan & Wakefield, 2011).

1.1.6.4. Chromosome attachment to the spindle

Following nuclear envelope breakdown (NEB), sister chromatids must achieve bioriented attachments to the mitotic spindle to satisfy the Spindle Assembly Checkpoint (SAC). The

kinetochore is integral to chromosome attachment to the mitotic spindle. Ndc80 is a crucial component for generating spindle microtubule attachments. Ndc80 binds to microtubules (Cheeseman *et al*., 2006) and is required for stable kinetochore microtubule attachment and SAC signalling (Etemad *et al*., 2015).

Cells negatively regulate kinetochore microtubule stability depending upon kinetochore attachment status until biorientation is achieved. Aurora B kinase is essential for correcting improper attachments in experimentally induced monopolar spindles (Lampson *et al*., 2004). Aurora B becomes enriched at merotelic attachments where it regulates microtubule depolymerising enzymes such as MCAK to correct these errors (Walczak & Heald, 2008). Moreover, Aurora B negatively regulates improper attachments by phosphorylating the Ndc80 complex, reducing its affinity to microtubules (Cheeseman *et al*., 2006).

1.1.7. Cell cycle regulation and control

The cell-cycle control system is based on an associated order of biochemical switches, each of which initiates a specific cell-cycle event. This order of the cell cycle events depends on many factors (Alberts, Johnson *et al*., 2015). A family of evolutionarily conserved protein kinases called cyclin-dependent kinases (CDKs), which activities are rigorously regulated by protein-protein interaction and phosphorylation. The regulators of CDKs and other proteins are degraded by ubiquitin-mediated proteolysis, which is crucial for cell cycle progression. This process is unidirectional, where the progression is dependent on the correct performance of previous events (Lodish *et al*., 2016; Poon, 2015).

On top of the cell cycle process, surveillance mechanisms designated checkpoints to monitor various events, ceasing the cell cycle to guarantee that each phase is finalized before the next phase is commenced. The important revelation is that the cell cycle is regulated by phosphorylation and proteolysis, like so many other processes in the cell (Poon, 2015).

1.1.7.1. Cyclin dependent kinases (CDKs)

Cell cycle regulation in higher eukaryotes contains a family of CDKs, which regulation is dependent on binding to the cyclins, regulatory subunits of the heterodimeric protein kinases. The catalytic subunits of CDKs have no kinase activity unless they are associated with a cyclin. Throughout the cell cycle, levels of CDKs are comparatively constant, and their activity is regulated by the levels of cyclins and other regulators. The cyclin family proteins can be divided into four classes: G1 (D) cyclins, G1/S (E) cyclins, S (A) cyclins and G2/M cyclins (A and B). The regulation of oscillation of cyclin during the cell cycle is controlled by transcription and protein degradation (Lodish *et al*., 2016; Poon, 2015). The cyclin proteins not only activate their CDK partner but also guide it to specific target proteins. As a result, each cyclin-CDK complex phosphorylates a different set of substrate proteins (figure I.7) (Alberts, Johnson, *et al*., 2015).

When the cell is stimulated to replicate, G1 complexes, CDK4 and CDK6 and their partners, D-type cyclins (D1, D2, and D3), are expressed. A significant target of cyclin D-CDK4/6 is the retinoblastoma gene product pRb. Hyperphosphorylation of pRb by cyclin D-CDK4/6 releases pRb from E2 factor (E2F) (Poon, 2015), allowing E2F to activate transcription of the cyclin A gene, mammalian cells approach for G1 to S phase transition (Cooper & Hausman, 2013; Lodish *et al*., 2016).

The significant regulator of the two phases, G1 and S, is also one of the CDK family of proteins, CDK2. CDK2 associates primarily with cyclin A and cyclin E. The peak level of cyclin E-CDK2 occurs during the G1-S transition, and cyclin A-CDK2 peak occurs in the S-phase. These two complexes also contribute to the hyperphosphorylation of pRb in G1 (Cooper & Hausman, 2013; Poon, 2015).

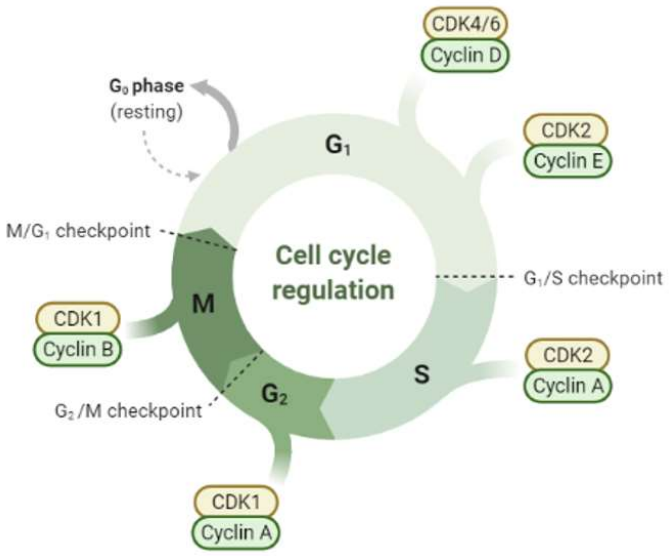

Figure I.7 – A schematic view of the cell cycle.
Each phase in the cell cycle progression is regulated by cyclin-dependent kinases (CDKs) and their regulatory partner proteins, cyclins.

The principal CDK in G2 and mitosis is CDK1, which associates with the mitotic cyclins (cyclin A and cyclin B) and drives cells into mitosis (G2-Mitosis transition). Cyclin B destruction inactivates CDK1 rapidly and permits mitosis exit of the cell (Lodish *et al*., 2016; Poon, 2015).

1.1.7.2. Mitotic entry

Mitotic entry ultimately depends upon the activation of cyclin-dependent kinase 1 (CDK1). In mammalian cells, A- and B-type cyclins, considered mitotic cyclins, are synthesised, and destroyed around mitosis. There are two types of cyclin A (A1 and A2) and three types of cyclin B (B1, B2, and B3). Cyclin A2 is present in all somatic cells, whenever cyclin B1 is predominant in dividing cells. One of the most crucial characteristics of mitotic cyclins is their periodicity. Cyclin A starts to accumulate during the late G1 phase and continue through S-phase and G2 phase. Cyclin B is first synthesised late in the S-phase and increases in concentration as cells proceed through G2, with a peak during metaphase and destruction slightly later than cyclin A, after late anaphase (Poon, 2015).

Cyclin B activates CDK1, which phosphorylates multiple mitotic targets, initiating mitotic spindle assembly via positive feedback loops with downstream effectors – notably Polo and Aurora A kinases. Polo-like kinase 1 (Plk1) is required for correct bipolar spindle assembly via localisation to the centrosome at the onset of mitosis. Here, Plk1 organises centrosomal components such as gamma-tubulin to generate microtubule asters (Dobbelaere *et al*., 2008; Lane *et al*., 1996), contributing to kinetochore-spindle attachment, chromosome segregation, and cytokinesis. Furthermore, Aurora A localisation to the centrosome depends on Plk1 activity – a mechanism that is essential for spindle bipolarity (Cooper & Hausman, 2013; Poon, 2015). Accurate mitotic progression depends upon the regulation of these upstream kinases. Aurora A kinase activity is modulated by reversible phosphorylation. DNA damage at the G2 checkpoint inactivates Cyclin B-CDK1 complexes through the action of Wee1 kinase, in turn, inactivate Aurora A to prevent the onset of mitosis (Marumoto *et al*., 2002).

1.1.7.3. Metaphase-to-anaphase transition

In mitosis, the most crucial task for spindle microtubules is to properly attach to the kinetochores in a bipolar manner, generating driving forces required for faithful chromosome segregation (Black, 2017).

The metaphase-to-anaphase transition is controlled by the activity of a ubiquitin E3 ligase, the Anaphase-Promoting Complex / Cyclosome (APC/C), which ubiquitinates and promotes the degradation of several substrates, particularly cyclin B and securin (Black, 2017).

Prior to anaphase onset, the activity of the APC/C is inhibited by the spindle assembly checkpoint (SAC), which prevents entry into anaphase in the presence of unattached kinetochores. Additionally, under some conditions, for example, when the kinetochore is severely impaired, the attachment will become weak and unstable, and thus the kinetochore is lost from microtubule attachment. The function of the SAC in the cell is to monitor the attachment, block premature chromosome segregation, and correct the improperly attached kinetochores, ultimately ensuring that all chromosomes are correctly bioriented at the cell equator (Black, 2017).

In the presence of unattached kinetochores, the SAC is activated, and SAC proteins catalyse the formation of a signal transducer called Mitotic Checkpoint Complex (MCC) (Black, 2017; Poon, 2015), composed of Mad2, Mad3/BubR1, and Bub3 (Tang *et al*., 2011). The MCC sequestrates Cdc20 and keeps the APC/C inactive, preventing it from targeting Securin and Cyclin B for degradation; this way, sister-chromatid cohesion is maintained, and the cell cycle is arrested, respectively (Alberts & Johnson *et al*., 2015; Cooper & Hausman, 2013).

Other core SAC components include Aurora B and Monopolar spindle 1 (Mps1), which are involved in amplifying SAC signalling, namely the promotion of MCC formation and the error-correction process kinetochore-microtubule attachment. Additionally, SAC function in higher eukaryotes requires the RZZ complex (ROZ-ZW10-ZWILCH); p31comet; protein kinases MAPK, Cyclin B-CDK1 and PLK1; microtubule kinetochore proteins CENP-E (Kinesin-7), dynein and dynactin (Musacchio & Salmon, 2007).

When all kinetochores have aligned, the MCC disassembles, and Cdc20 is released. Cdc20 activates the APC/C that targets two critical mitotic regulators for destruction: securin and cyclin B (Alberts & Johnson *et al*., 2015; Cooper & Hausman, 2013).

1.1.7.4. Anaphase / Cytokinesis

When the SAC is satisfied, activation of the APC/C initiates chromosome segregation in anaphase, characterised by sister chromatids separation and their movement to the opposite poles of the cell performed by the forces of the mitotic spindle. The destruction of Cyclin B regulates the inactivation of CDK1 and causes mitotic exit. Securin is an inhibitor of a protease, separase, that, when activated, cleaves cohesin complexes holding bi-oriented sister chromatids together. This cleavage is the critical step for initiating chromosome segregation in anaphase. A further dramatic reorganisation of spindle Microtubules, regulated by MAPs, accurately coordinates the formation of identical daughter cells (Alberts, Johnson *et al*., 2015).

The initial poleward movement of the chromosomes, accompanied by shortening of the kinetochore microtubules, is designated as anaphase A. Consequently, in anaphase B, the

spindle poles' separation begins after the sister chromatids have separated and the daughter chromosomes have moved some distance apart (Alberts, Johnson *et al*., 2015).

The Central Spindle, composed primarily of Microtubules bundles and MAPs, forms after chromosome segregation and is required for abscission during cytokinesis in several cell types (Wheatley & Wang, 1996). For central spindle assembly, is required the dynamic relocalisation of the Chromosomal Passenger Complex (CPC) to the spindle mid-zone during anaphase. Phosphorylation of numerous central spindle components occurs at the central spindle to initiate microtubule bunding (Ban *et al*., 2004; Wheatley *et al*., 2001).

1.1.8. Cytokinesis

The completion of mitosis, nuclear division, is usually accompanied by cytokinesis, the process by which one cell physically divides in two. To accomplish this, the mitotic apparatus must communicate with the cell's cortex as the membrane ingresses. As the chromosomes undergo mitosis, the cell must undergo cortical remodelling and cell shape changes to partition itself to ensure each daughter cell is distributed a full genomic complement. This is mediated by a contractile ring of actin and myosin II filaments, positioned by signals from the mitotic spindle (Cooper & Hausman, 2013; Green *et al*., 2012), so the cell is cleaved in a plane, which is perpendicular to the spindle positioning. As the cell undergoes cytokinesis, the shape of the invaginating plasma membrane is generally referred to either as the cleavage furrow or the cytokinetic furrow. Constriction of the contractile ring and abscission on the intercellular bridge has a place, and the plasma membrane is released (Cooper & Hausman, 2013; Guizetti & Gerlich, 2010). After cytokinesis, the cell enters a stable G1 state of low CDK activity, where it awaits signals to enter a new cell cycle (Alberts, Johnson *et al*., 2015).

1.2. Hippo signalling pathway

The Hippo signalling pathway initially discovered in *D. melanogaster* is an evolutionarily conserved regulator of tissue growth in the mammalian system (Boggiano *et al*., 2011; Meng *et al*., 2016). The Hippo pathway was named after Hippo (Hpo), a *Drosophila* kinase gene

independently identified to restrict tissue growth by several groups more than a decade ago (Meng *et al*., 2016).

Recently, there has been increasing interest in studying the Hippo pathway. Together with other signalling pathways, this pathway ensures that the organs achieve the correct size by regulating cell proliferation and cell death. The Hippo pathway consists of several upstream regulators that either independently regulate or indirectly feed into the core kinase cascade of the pathway to regulate the activity of two transcriptional coactivators, Yes-associated protein (YAP) and transcriptional coactivator with PDZ-binding motif (TAZ; two homologs of Yorkie [Yki] in *Drosophila*), the transcriptional coactivator of the pathway. YAP/TAZ binds selectively to its cognate transcription factors, which may be context-dependent or tissue-specific, to regulate specific target genes that exert various effects on processes ranging from organogenesis, compensatory proliferation, regeneration, and tumorigenesis. Besides YAP/TAZ, other upstream regulators participate in a context-dependent manner to regulate these varied processes (Meng *et al*., 2016).

1.2.1. Hippo pathway in *Drosophila melanogaster*

More than a decade ago, several groups demonstrated that regulation of the Hippo pathway is achieved by controlling the activity of its effector Yorkie (Yki) (Huang *et al*., 2005; Wei *et al*., 2007). Yki activity is controlled by phosphorylation-dependent or phosphorylation-independent mechanisms that control the Yki's localisation, which eventually affects the regulation of cell proliferation and cell death, the primary output of the Hippo pathway (Huang *et al*., 2005 Meng *et al*., 2016).

The core kinase of the pathway consists of the two S-T (Serine-Threonine) kinases: Hippo (Hpo), a Ste20-like kinase, and Warts (Wts), a nuclear Dbf2-related (NDR) family kinase. Hippo and Warts, together with their adapter proteins, Salvador (Sav) and MOB as a tumour suppressor (Mats), control the activity of the transcriptional coactivator Yorkie (Yki), which is the heart of the Hippo signalling pathway (figure I.8) (Meng *et al*., 2016).

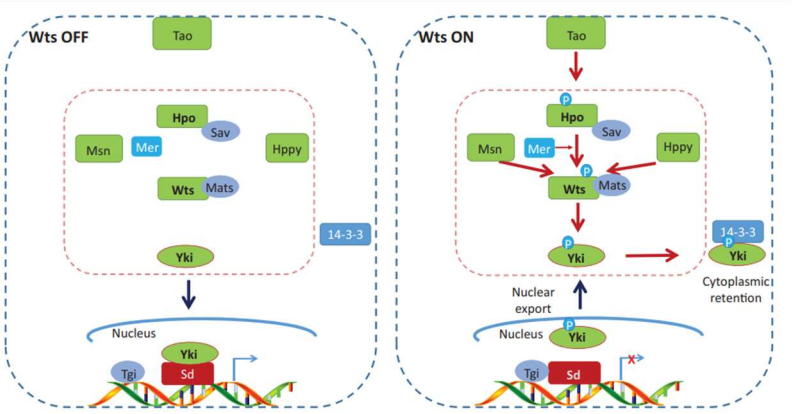

Figure I.8 - The *Drosophila* Hippo pathway.
Active Yki competes with Tgi to interact with Sd in the nucleus and activates the transcription of Sd target genes. When Hpo is activated by Tao kinase or dimerization, it phosphorylates and activates Wts with the assistance of the scaffold proteins Sav and Mats as well as Mer. It is unclear whether Msn and Hppy require Mer and Sav to phosphorylate and activate Wts. Active Wts phosphorylates and inactivates Yki, leading to 14-3-3-mediated Yki cytoplasmic retention (Meng et al., 2016).

Hpo kinase is phosphorylated through the pathway hyperactivation, which activates Wts by phosphorylating it (Dong *et al*., 2007; Wei *et al*., 2007). Mats can now bind to Wts to act as a coactivator for the kinase activity of Wts. Wts phosphorylates Yki at S168 and sequesters it in the cytoplasm. Phosphorylated Yki binds to 14-3-3 protein and is degraded. Yki has several phosphorylation sites that affect its activity, for example, S111 and S250 (Dong *et al*., 2007; Zhang *et al*., 2011). Yki can also be inhibited from entering the nucleus by phosphorylation independent mechanisms (Oh & Irvine, 2008, 2010; Ren *et al*., 2010). Yki can interact with proteins like Expanded (Ex), Hpo, WW domain-binding protein 2 (Wbp2) and Myopic (Mop) in a phosphorylation independent manner. The binding of Yki to these proteins sequesters Yki containing protein complexes in the cytoplasm, thus preventing its degradation. This makes it unavailable for phosphorylation by Wts or other upstream regulators and blocks the transcriptional coactivator activity of Yki (Meng *et al*., 2016).

Yorkie is a non-DNA binding transcriptional coactivator, which binds to several cognate transcription factors in the nucleus to control the expression of target genes. Scalloped (Sd), a TEAD (Transcriptional enhancer factor TEF-1) family protein, is a binding partner of Yki for the regulation of cell proliferation and apoptosis. One co-repressor of Sd, Tondu domain-containing growth inhibitor (Tgi), has been known to compete with Yki to bind on the Sd. Yki

acts as a de-repressor by displacing Tgi from Sd to drive the expression of the target genes (Meng *et al*., 2016). Yki regulates the expression of several target genes like cyclins, Myc (growth-promoting gene), diap1 (drosophila inhibitor of apoptosis 1), between other genes that promote cell proliferation and survival (Huang *et al*., 2005; Meng *et al*., 2016). Several upstream regulators of the pathway are also the transcriptional targets of the pathway, merlin (mer) is one of them, an adaptor protein that contributes to Wts phosphorylation. On the side, some studies show that two other kinases, Misshapen (Msn) and Happyhour (Hppy), can activate Wts and repress Yki independently of Hpo (Meng *et al*., 2016).

1.2.2. Hippo pathway in mammalians

Several components of the mammalian Hippo pathway were known even before the Hippo pathway was formally discovered. For instance, before MOB1 was recognised as a tumour suppressor in the eukaryotes, MOB1 was known in yeast to be essential for mitosis and maintenance of the ploidy (Luca & Winey, 1998). Similarly, before identifying MST1 (mammalian sterile kinase) as a tumour suppressor, MST1 in yeast was known to be activated by caspases and mediate cell death. MST1 codes for the mammalian Ste20 kinase and its interaction with MAPK, p38 were also studied (Duhart & Raftery, 2020). MST1 (also known as STK4) and MST2 (also known as STK3) are two kinases, components of germinal centre kinase II (GCKII) subfamily (Shi *et al*., 2016). Soon after the Hippo pathway was discovered in Drosophila, studies in mammas led to the identification of homologs of the fly Hippo pathway components leading to the discovery of the mammalian Hippo pathway (Meng *et al*., 2016).

The central core kinase comprises MST1/2 (Hpo homologs), SAV1, LATS1/2 (Wts homologs), Mob1 (MOBKL1A and MOBKL1B; Mats homologs), which regulates the activity of transcriptional co-activators YAP/TAZ (Yki homologs). YAP/TAZ (YAP – Yes-associated protein 1; TAZ – Transcriptional co-activator with PDZ-binding motif) interact with TEAD1-4 (four members of the family of transcriptional factors, Sd homolog) in the nucleus to regulate pathway target gene expression (figure I.9) (Pan, 2010; Yu & Guan, 2013).

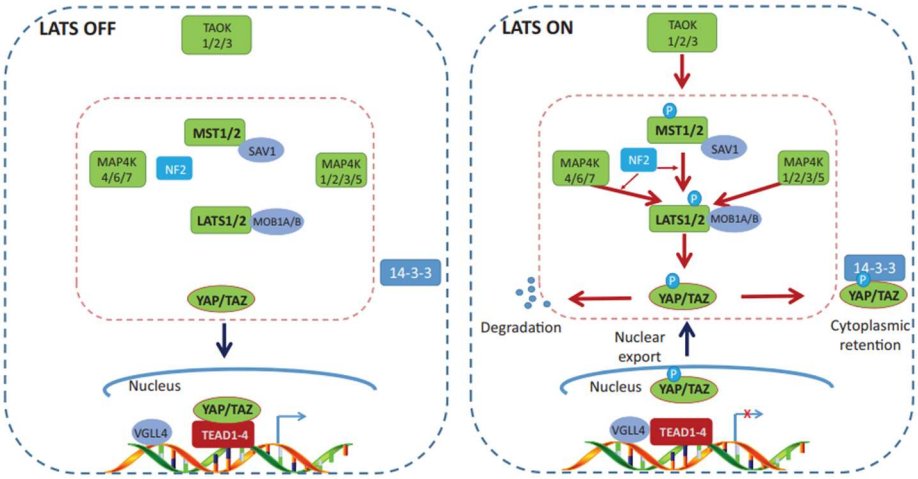

Figure I.9 - The mammalian Hippo pathway.
When the Hippo pathway is inactive, YAP and TAZ are unphosphorylated and localized in the nucleus to compete with VGLL4 for TEAD binding and activation of gene transcription. The Hippo pathway can be activated by TAO kinases, which phosphorylate MST1/2 at its activation loop. MST1/2, in turn, phosphorylate LATS1/2, facilitated by scaffold proteins SAV1, MOB1A/B, and NF2. MAP4K4/6/7 and MAP4K1/2/3/5 also phosphorylate and activate LATS1/2. Phosphorylation of LATS1/2 by MAP4K4/6/7 requires NF2 (also known as Mer). Activated LATS1/2 phosphorylate YAP and TAZ, leading to 14-3-3-mediated YAP and TAZ cytoplasmic retention and SCF-mediated YAP and TAZ degradation (Meng *et al*., 2016).

The STE20 protein kinases MST1/2 phosphorylates SAV1, MOB1, LATS1/2 upon pathway activation (Meng *et al*., 2016; Praskova *et al*., 2008). The Hippo kinase cascade can be initiated by Thousand and one (TAO) amino acid kinase or TAOK1-3 (Tao in *Drosophila*) (Meng *et al*., 2016; Zhao *et al*., 2011), which phosphorylate the activation loop of MST1/2 (Thr183 for MST1 and Thr180 for MST2) and thereby lead to MST1/2 activation (Dong *et al*., 2007).

The physical interaction of MST1/2 and SAV1 is required for enhancing the phosphorylation activity of MST1/2. MST1/2 interact through the SARAH (Sav / Rassf / Hpo) domain that is also shared by SAV1 and Ras association domain containing protein (RASSF) 1-6 (Meng *et al*., 2016). The SARAH domain mediates homo- or heretodimerisation of MST1/2, SAV1 and RASSFs (Shi *et al*., 2016). Activated MST1/2 phosphorylates and activates LATS1/2. Additionally, like *Drosophila* Hippo kinase, MST1/2 can also activate LATS1/2 by direct phosphorylation of LATS1/2 in the activation loop (S909) and the hydrophobic domain (Thr1079). LATS1 is also able to autophosphorylate at S909 (Yu & Guan, 2013). MST1/2 also phosphorylates Mob1. Mob1 is required for potentiating the kinase activity of LATS1/2.

Phosphorylated Mob1 interacts with the auto-inhibitory motif of LATS1/2, which results in the phosphorylation of the auto-activation loop of LATS1/2 (Meng *et al*., 2016; Praskova *et al*., 2008). Apart from regulating LATS1/2 via phosphorylation, its protein levels are regulated by the E3 ubiquitin ligase. LATS1/2 phosphorylates YAP at S127 and TAZ at S89. When mammalian YAP and TAZ are phosphorylated at these sites, they bind to 14-3-3 proteins, which sequester them in the cytoplasm, just like *Drosophila* 14-3-3 sequester S168 phosphorylated Yki in the cytoplasm (Meng *et al*., 2016). Phosphorylation of YAP by LATS1/2 at S381 and TAZ at S311 sensitises YAP and TAZ for the subsequent phosphorylation by Casein kinase 1 (CK1δ/ε). This sequential phosphorylation recruits β-transducin repeat-containing protein (βTRCP), a subunit of the SCF E3 ubiquitin ligase leading to the degradation of YAP and TAZ. When the core kinase is inactive, YAP/TAZ is hypo-phosphorylated. The hypo-phosphorylated YAP/TAZ can enter the nucleus to bind cognate transcription factors to regulate target gene expression (Meng *et al*., 2016; Yu & Guan, 2013).

YAP/TAZ does not contain intrinsic DNA-binding domains but instead bind to the promotes of target genes by interacting with DNA-binding transcription factors. YAP/TAZ primarily bind to the transcription factors TEAD1-4 to control genes required in cell proliferation and cell death (Yu & Guan, 2013).

Similar to *Drosophila*, multiple upstream regulators of YAP/TAZ have been identified. Neurofibromatosis-2 (NF-2) protein is a homolog of Merlin. NF-2 over-expression in mammalian cells results in activation of LATS, resulting in inhibition of YAP. Several junctional proteins can affect YAP and TAZ activity (Yu & Guan, 2013).

YAP/TAZ activity is sensitive to the extra-cellular matrix (ECM), neighbouring cells, and surrounding biological fluids. Actin filaments (F-actin) have been considered essential regulators of cell proliferation, and the microtubules' dynamics are essential for cell division. F-actin interacts with MST1/2 and LATS1/2 and, in turn, affects YAP activity (Meng *et al*., 2016; Yu & Guan, 2013).

The core kinase cascade of the Hippo pathway is well conserved between *D. melanogaster* and humans. Besides, there are a few differences. The mammalian RASSF positively regulates the pathway, whereas the *Drosophila* RASSF negatively regulates the pathway (Yu & Guan, 2013).

Hippo core, with its linear model, served well for initial studies of the Hippo pathway, however recent studies uncovered additional kinases, NDR1/2 (also known as STK38/STK38L), as novel members of the core cassette of Hippo signalling. MST1/2 are responsible for activating phosphorylation of LATS1/2 and NDR1/2 protein kinases for further YAP activation (Hergovich, 2016).

1.3. STRIPAK complex

The **STR**iatin-**I**nteracting **P**hosphatase **A**nd **K**inase (STRIPAK) is a highly conserved complex consisting of 18 proteins. A minimal stable core of STRIPAK complex contains the scaffolding subunit PPP2R1A (also known as PP2Aa), catalytic subunit PPP2CA (also known as PP2Ac), and regulatory subunit striatins (STRNs) containing STRN, STRN3, and STRN4 (Gourdeault *et al*., 2009). Striatins recruit STRiatin-Interacting Protein 1/2 (STRIP1/2), Mps one binder 4 (MOB4) protein, Cerebral cavernous malformation 3 (CCM3, also known as PDCD10). CCM3 interacts with and stabilises the germinal centre kinase III (GCK III) family, which consists of three genes, Sterile-20-like kinase 24 (STK24, also known as Mammalian sterile-20-like kinase 3, MST3), STK25 (also known as Yeast sps1 / sterile-like-20-related kinase 1, YSK1), and STK26 (also known as MST4). The researchers predicted that STRIPAK could form two mutually exclusive complexes with STRNs via STRIP1/2. The interaction with cortactin-binding protein 2 (CTTNBP2) and CTTNBP2 N-terminal-like protein (CTTNBP2NL) is complex I. Complex II contains sarcolemmal membrane-associated protein (SLMAP), tumour necrosis factor receptor-associated factor 3 (TRAF3)-interacting protein 3 (TRAF3IP3), the coiled-coil protein suppressor of IκB kinase-ε 1 (IKKε), designated SIKE1 and fibroblast growth factor receptor 1 (FGFR1) oncogene partner 2 (FGFR1OP2) (figure I.10) (Goudreault *et al*., 2009; Shi *et al*., 2016; Xie *et al*., 2020). The dynamic assembly of STRIPAK complexes controls the downstream effectors. Apart from CCM3 and MOB4, all other components of STRIPAK are represented in mammals by at least two paralogous proteins that can assemble into STRIPAK. Many of the members of STRIPAK components have been conserved throughout evolution (Goudreault *et al*., 2009).

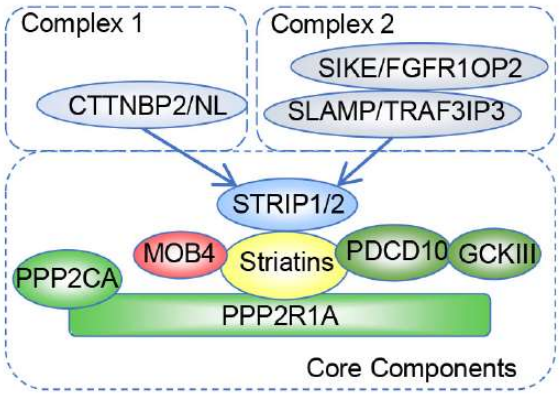

Figure I.10 - Model of STRIPAK complex.
The core components of the STRIPAK complex include STRIP1/2, striatins (STRN, STRN3, STRN4), PPP2R1A, PPP2CA, MOB4, PDCD10, AND GCKIII (STK24, STK25, STK26). The core complex may interact with CTTNBP2 family proteins to form complex one or interact with SLMAP and SIKE family to form complex two (adapted from Xie *et al*., 2020).

The importance of STRIPAK is highlighted in physiological processes, such as apoptosis, Golgi assembly, and embryo, vascular and neural development. For example, knockdown of the strip in *D. melanogaster* presented disturbance in early endosome organisation. Other regulators in the STRIPAK complex, STK24, promotes the development of spine synapse via TAOK1 and TAOK2 associated with the Myosin Va axis. The conserved STRIPAK complex regulates the reactivation of *Drosophila* neural stem cells through functioning as a switch to the Hippo pathway and InR&PI3K/Akt signalling. Moreover, STRIPAK plays an important role in human diseases (Xie *et al*., 2020).

The STRIPAK components show to be localised in different parts of the cell, which suggests that STRIPAK bridges different organelles, such as the nuclear membrane, the centrosome, and Golgi. Furthermore, STRIPAK is the node of active signalling that contributes to broad implications (Xie *et al*., 2020). The coordination of cytoskeletal organisation and cellular development through the actin network regulation and microtubule reorganisation, stability, and morphology are also linked to the STRIPAK complex activity (Li *et al*., 2018).

Scientists summarised that STRIPAK complexes play a crucial role in cancer by regulating actomyosin cytoskeleton, determining their role in migrate mode. Besides the migration ability, different groups reported that the STRIPAK complex regulates the Hippo pathway in various processes. MST1/2 and MAP4Ks, which belong to the STE20 kinase family, interact with STRIPAK via core components in *D. melanogaster* and mammalian cells (Xie *et al*.,

2020). A short description of some of the STRIPAK components and their evolutionarily conserved segments and the role of some of these proteins throughout evolution are summarised below.

1.3.1. Striatins and PP2A

The mammalian striatin family of proteins consists of three members, striatin-1 (STRN), S/G2 nuclear autoantigen (SG2NA, also known as STRN3), and zinedin (also known as STRN4). Striatin family members have no intrinsic catalytic activity but rather function as scaffolding proteins harbouring various protein-protein interaction domains (Moreno *et al*., 2001). In general, striatins are involved in cellular signalling, motor function, and vesicular trafficking (Shi *et al*., 2016). Striatins were also previously shown to interact with the STRIPAK protein MOB4 (Moreno *et al*., 2001).

PP2A is a ubiquitously expressed serine/threonine phosphatase, which is connected to cancer, regulates cell cycle and microtubule dynamics, and plays a role in apoptosis. In mammals, PP2A is a heterotrimeric complex composed of a catalytic subunit (PP2Ac with two known isoforms, PP2Acα and PP2Acβ), a scaffold subunit (PP2Aa which consists of two isoforms, PP2Aα and PP2Aβ), and a regulatory subunit. The PP2Aa subunit mediates the interaction between PP2Ac and various regulatory subunits that determine substrate specificity (Shi *et al*., 2016). Of the regulatory subunits, four types exist (B, B', B'', and B'''), which are required to recruit substrates and determine the subcellular localisation of proteins associated with PP2A (Goudreault *et al*., 2009). Where STRNs were determined to be regulatory B''' subunits and interacting with PP2Aa and PP2Ac without the presence of other B subunits (Shi *et al*., 2016). Also, STRN and STRN3 seem to be targets of PP2A because inhibition of PP2A with Okadaic acid resulted in increased phosphorylation of STRN and STRN3 (Moreno *et al*., 2000). The STRNs contain a CCM3-binding region, which can directly interact with CCM3, a binding partner of GCKIII (Shi *et al*., 2016). Striatins are multi-domain proteins that contain a coiled-coil motif at their N-terminus and a WD40-repeat region at their C-terminus; the coiled-coil (CC) domain has been shown to be essential for homo- and hetero-oligomerisation of the striatin proteins (Gourgreault *et al*., 2009). The CC domain of striatin is contiguous with a basic amphiphilic calmodulin (CaM)-binding site. Elimination of the CaM-binding domain in human striatin results in increased binding of the GCKIII kinases MST3 and MST4

to striatin (Gordon *et al*., 2011). The WD-40 repeat domain of STRNs contains seven WD-40 repeats, which mediate protein-protein interactions, which is one of the potential binding partners for the WD-40-repeat domain is MOB4 (Shi *et al*., 2016). A more detailed description of MOB4 is in subchapter 1.4.

The C-terminal region of striatins is composed of a WD repeat, whereas W represents tryptophan and D represents aspartic acid. A variable region characterises the N-terminal region of the WD-repeat with 6-96 amino acids, followed by a conserved repeat region, about 40 amino acids. The specific structure of WD repeats brings proteins together and serves as a basis for protein-protein interactions (Hwang & Pallas, 2014). Deletion of striatin WD repeats reduces MOB4 binding to striatin (Gordon *et al*., 2011).

1.3.2. GCKIII and CCM3

The members of the GCKIII family share conserved N-terminal kinase domain and C-terminal dimerization domain with a linker region in between. The STRIPAK complex in mammals contains three serine/threonine kinases, MST4, MST3 and STK25, which belong to the GCKIII family. Several biological processes include the participation of GCKIII kinases, like cell growth, proliferation, polarity, and apoptosis (Shi *et al*., 2016).

MST3 contains a nuclear export and localization signal. Cleavage of MST3 by caspase activates the kinase, which translocate to the nucleus and induces apoptosis. Four striatin point mutations were unable to bind PP2A, which resulted in hyperphosphorylated and active MST3. Hence, PP2A was demonstrated to be a negative regulator of MST3 (Gordon *et al*., 2011). In *D. melanogaster*, knockdown of GCKIII or Cka (homolog of STRNs) partially suppresses ectopic wing veins caused by the EGFR gain-of-function (Shi *et al*., 2016).

CCM3 comprises an N-terminal dimerization domain similar to that of GCKIII and a C-terminal focal adhesion targeting homology domain. As a result, CCM3 can form a homodimer or heterodimer with GCKIII kinases. The primary function of CCM3 in STRIPAK complexes is to act as a molecular bridge recruiting GCKIII kinases to STRNs. A trimeric complex formed by MST4, STRN3 and CCM3, recruits MST4 to the STRIPAK (Shi *et al*., 2016).

1.3.3. STRIP1/2

STRiatin Interacting Protein 1 and 2 (STRIP1/2), also named FAM40A/FAM40B, were characterised as regulators of cell morphology and cytoskeletal organisation (Hwang & Pallas, 2014). STRIP1 localises to the Golgi Complex, and depletion of STRIP1 in HeLa cells results in increased DNA content and abnormally shaped or fragmented nuclei. Also, SLMAP, which was localised to the nuclear envelope and membranous material around the mitotic spindle, interacts with STRIP1. Frost *et al*. (2012) suggested that STRIP1 connects the Golgi and centrosomes and is required for centrosome duplication and spindle assembly (Frost *et al*., 2012). In prostate carcinoma cells, depletion of STRIP2 was characterised by an elongated phenotype with very long thin protrusions containing microtubules. In comparison, loss of STRIP2 in HeLa cells leads to reduced cell-cell adhesion (Bai *et al*., 2011).

The STRIP1/2 interacts with striatin and with either CTTNBP2/NL or SIKE/SLMAP in a mutually exclusive manner. However, some recent views of the STRIPAK complex suggest that STRIP1/2 could also interact with PP2A (Shi *et al*., 2016).

1.3.4. Crosslinking between STRIPAK complex and Hippo pathway

As it was mentioned previously, the Hippo pathway was described firstly in *D. melanogaster*. Mutant screening in *D. melanogaster* identified a GCK which acts as a negative control of tissue growth. Loss of function of this kinase resulted in increased tissue growth and reduced apoptosis. In humans, the Hippo pathway core consists of GCKII kinase MST1/2 (also known as STK4/3, Hpo in *Drosophila*) associated with the WW-domain-containing scaffold protein SAV1 (Sav in *Drosophila*) and the NDR kinase LATS1/2 (Wts in *Drosophila*), which is associated with the kinase activator MOB1 (Mats in *Drosophila*). Deregulation of the Hippo pathway may result in developmental defects and cancer. MST1/2 kinases are the central kinase of the Hippo pathway and are the critical components of certain types of STRIPAK complexes (figure I.11) (Shi *et al*., 2016).

Recent data from different groups compelling evidence of GCKs being one of the significant links between Hippo and STRIPAK. The members of various GCKs subfamilies were shown

to functionally interact with either the Hippo pathway, the STRIPAK complex, or both. Hippo subunit Mob1 was described as an interacting partner and a substrate of PP2A (Emami *et al*., 2020; Kuck *et al*., 2019).

SAV1 can directly interact with the catalytic domain of PP2A in STRIPAK and suppress phosphatase activity. This inhibits phosphatase activity of PP2A via binding to the STRIPAK core, thereby counteracting dephosphorylation of the CGKII activation loop. This mechanism is responsible for the mutual downregulation of STRIPAK and Hippo. Taken together, it is possible to suggest that the PP2A-STRIPAK complex activates YAP by suppressing MAP4K/MST-LATS1/2 or enhancing MST1/2 dephosphorylation (Emami *et al*., 2020; Kuck *et al*., 2019).

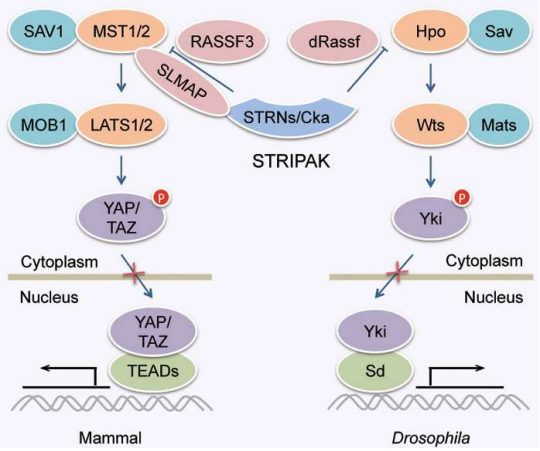

Figure I.11 - STRIPAK complexes and Hippo signalling.
Hippo signalling is negatively regulated by STRIPAK complexes through reducing phosphorylation of MST1/2 or Hpo, consequently producing the activation of YAP/TAZ-TEA domain family members (TEADs) or Yki-Scalloped (Sd) and supporting cell proliferation (Shi *et al*., 2016).

In *D. melanogaster*, Hpo and dRassf associate with *Drosophila* STRIPAK components Cka (homolog of striatins in *Drosophila*), Mts (homolog of PP2Ac in *Drosophila*), Fgfr1op2 and MOB4. The interaction between Hpo and STRIPAK complex may be mediated by dRassf. dRassf, Cka and Mts can inhibit Hpo activation and therefore promote Yki phosphorylation. The mechanism suggests that dRassf antagonises Hpo function, possibly by competing with Sav for binding Hpo (Shi *et al*., 2016).

Structural and biochemical studies discovered that SLMAP contains a forkhead-associated (FHA) domain in the N-terminal region. SLMAP, together with RASSF3, might link MST1/2 kinases to the scaffold STRNs. It is reported that SLMAP and MST1/2 interact in a phosphorylation-dependent manner (Shi *et al*., 2016). Moreover, the SLMAP-MST1/2 interaction connects the STRIPAK to Hippo signalling (Emami *et al.,* 2020; Kwon *et al*., 2021).

On the other side, Chen *et al*. (2018) proposed a different model about how STRIPAK components can inhibit Hippo pathway. Given the structural similarity and the alternative pairing of MST4-MOB4/MOB1 and MOB4-MST4/MST, they suggest that the MST4-MOB4 complex might dynamically assemble and disassemble to interfere the MST1/MOB1 complex, leading to YAP activation (figure I.12) (Chen *et al*., 2018).

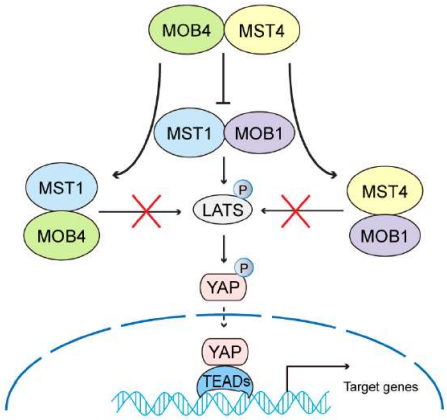

Figure I.12 - Proposed model for MST4-MOB4 mediated YAP activation (Chen et al., 2018).

1.4. Mps one binder (MOB) family proteins

Mps one binder (MOB) is an evolutionarily conserved gene with homologs in all major kingdoms ranging from protists to humans. The first identified protein of the family was described as a binder of Mps1 protein (Mob1p) in the budding yeast *Saccharomyces cerevisiae* (Luca & Winey, 1998). Mob1p was shown to regulate mitotic exit network by

binding to and activating Dbf2/Dbf20 kinases (Chow *et al*., 2010). Moreover, Luca & Winey also identified another MOB protein, Mob2p, that, contrary to the Mob1p, is not essential for yeast survival (Luca & Winey, 1998). The Mob2p acts as regulator subunit of catalytic activity of kinases and interacts with Cbk1 in *S. cerevisiae* (Chow *et al*., 2010).

In *Schizosaccharomyces pombe*, Mob1p regulates septation initiation network and Sid2 kinase. The Mob2p acts as regulator subunit of catalytic activity of kinases and interacts with Orb6, an essential gene in maintaining cell polarity and regulation of gene expression (Chow *et al*., 2010). However, early studies of Mobs characterised them as activators of a different group of serine-threonine kinases highly conserved: yeast Dumbbell former 2 (Dbf2) and Warts/LATS in fruit flies and mammals (Duhart & Raftery, 2020).

In 2005, four *MOB* genes, *dMOB1/Mats* (MOB as a tumour suppressor), *dMOB2*, *dMOB3*, and *dMOB4*, were identified in *D. melanogaster*. dMOB1 protein binds to and activates a *Drosophila* homolog of yeast Dbf2/Sid2/Cbk1/Orb6 protein kinase, Large Tumour Suppressor (Lats)/Warts, which has also been identified as a tumour suppressor (He *et al*., 2005). Deficiency of dMOB1 has been shown to increase cell proliferation and cause defective apoptosis in addition to the initiation of tumorigenesis due to an excessive amount of cell cycle activator Cyclin E and antiapoptotic protein dIAP (Drosophila inhibitor of apoptosis) (Lai *et al*., 2005). Surprisingly, the supplementation of the human dMOB homolog, hMOB1B, into the dMOB1-deficient cells rescued the phenotypes in the mutant flies, indicating that the function of MOB protein is evolutionally conserved. Moreover, dMOB1 also regulates the cytoskeletons by interacting with *Drosophila* Trc, a member of the NDR family (He *et al*., 2005).

dMOB1, *dMOB2* and *dMOB4* are essential genes because their depletion is lethal (Chow *et al*., 2010). Some recent studies suggest that dMOB2 can play a role in wing hair morphogenesis, possibly by forming a complex with a Trc. However, the action mechanism is not defined yet. dMOB3 can also interact with Trc, but, once again, direct partners of dMOB3 are still to be elucidated. dMOB4 has been linked to neurological function (Gundogdu & Hergovich, 2019).

One of the most recent studies indicated that depletion of dMOB4 in fly cells results in defective focusing of kinetochore fibres in mitosis (Trammel *et al*., 2008). Possibly, this role

could be linked to dMOB4 being a part of the STRIPAK complex (Gundogdu & Hergovich, 2019).

The human genome encodes seven MOB genes, namely *hMOB1A, hMOB1B*, *hMOB2*, *hMOB3A, hMOB3B, hMOB3C* and *hMOB4*/*Phocein* (Florindo & Tavares, Human Genome Data Base, direct submission, 2003). Products of these genes are characterised by the 180-200 amino acid long MOB domain (Chow *et al*., 2010; Goudreault *et al*., 2009; Luca & Winey, 1998; Vitulo *et al*., 2007). A phylogenetic tree analysis of the dMOBs and hMOBs demonstrated that hMOB1A, hMOB1B and dMOB1 cluster together into one subgroup. Likewise, hMOB2 and dMOB2, as well as hMOB3A, hMOB3B, hMOB3C and dMOB3 form separate subgroups, respectively. It is noteworthy that hMOB4 and dMOB4 also form a subgroup of their own, representing the most distant subgroup of MOBs (figure I.13) (Gundogdu & Herogvich, 2019).

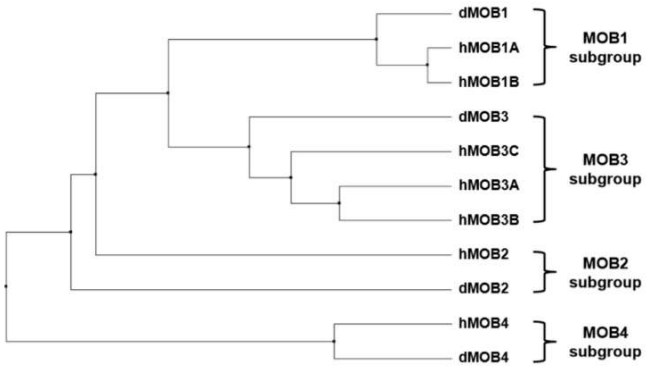

	vs. hMOB1A	vs. hMOB2	vs. hMOB3A	vs. hMOB4
hMOB1A	100 %			
hMOB1B	96 %			
hMOB2	37 %	100 %		
hMOB3A	51 %	29 %	100 %	
hMOB3B	51 %	29 %	80 %	
hMOB3C	48 %	28 %	72 %	
hMOB4	22 %	17 %	20 %	100 %

Figure I.13 – The UniProtKB nomenclature for the analysed proteins is defined.
Top: Phylogenetic relationship within the fruit fly and human MOB family protein. **Bottom**: Primary sequence identities within the human MOB protein family (adapted form Gundogdu & Herogvich, 2019).

Interestingly, whereas hMOB1A/B physically interact and activate all four human NDR/LATS kinases (Bichsel *et al*., 2004; Hergovich, 2011), hMOB2 is a negative regulator of NDR kinase activity by competing for the binding of NDR kinase to hMOB1 (Figure I.14) (Kohler *et al.*, 2010). Although hMOB3A/B/C show higher sequence similarity to hMOB1 than hMOB2, hMOB3A/B/C proteins do not interact with or (de)activate all four NDR/LATS kinases (Hergovich, 2011; Kohler *et al*., 2010). hMOB4, also known as Phocein, do not appear to interact with NDR kinases. hMOB4 is described as a STRIPAK complex component, which can bind two distinct regions of STRN (Gundogdu & Hergovich, 2019).

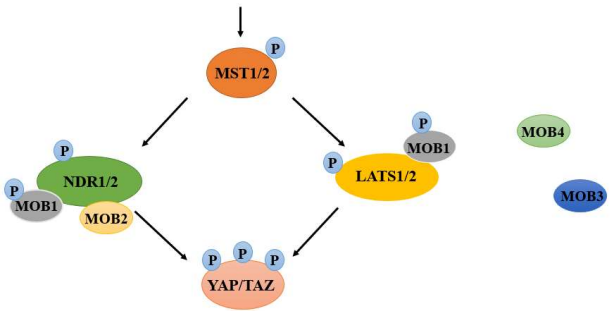

Figure I.14 - The MST/hMOB/NDR complex.
hMOB1 bonds to both LATS and NDR. hMOB1 is phosphorylated by MST1/2, resulting in the efficient ternary complex formation ofhMOB1/MST/NDR. hMOB2 specifically interacts with un-phosphorylated NDR kinases, which competes for the binding of hMOB1 to NDR. hMOB3 and hMOB4 do not interact with or (re)activate NDR/LATS. Phosphorylation is indicated by 'P' in blue.

The roles of hMOB1 have been extensively characterised in tissue-cultured systems. A recent study demonstrated that hMOB1A and hMOB1B regulate abscission during cytokinesis. The study demonstrated that knockdown of hMOB1A and hMOB1B causes hyper-stabilisation of microtubules, as well as prolonged centriole separation in G1 phase. This indicates that MOB proteins may be involved in regulating microtubule stability as well as centriole re-joining after telophase and cytokinesis (Florindo *et al*., 2012).

hMOB1A/B physically interact and activate all four human NDR/LATS kinases through one unique and highly conserved domain in NDR/LATS kinases (Gundogdu & Hergovich, 2019). hMOB1A/B proteins are essential for the functions of human NDR1/2 in apoptosis and centrosome duplication in a NDR binding dependent manner (Hergovich *et al*., 2009;

Vichalkovski *et al*., 2008). In addition to the association with NDR kinases, hMOB1A/B proteins also interact with human MST1/2, bridging NDR/LATS to the upstream MST kinases. Moreover, human MST1/2 kinases and the *Drosophila* Hippo kinase phosphorylate hMOB1A/B and Mats, respectively, and increase MOB1/Mats protein affinity towards NDR/LATS or Wts kinase (Praskova *et al*., 2008). Furthermore, the binding of NDR kinases to hMOB1A/B is reported to release the kinase from the auto-inhibitory status by the autoinhibitory segment (AIS) (Bichsel *et al*., 2004).

Moreover, spatial relocalisation seems to be another critical aspect of NDR kinase activation. Artificial targeting of hMOB1 or Mats proteins to the plasma membrane leads to rapid and robust activation of NDR/LATS kinase or Wts, respectively. Direct membrane targeting of Trc kinase itself could also rescue the effect of T*rc* mutant flies (Gundogdu & Hergovich, 2019). These observations indicate that the cellular membrane might be an essential place for activating NDR/LATS kinases. However, the mechanisms of NDR kinases being recruited to and activated at the plasma membrane by MOB1 remain to be elucidated, hMOB1 indicates to be a critical tumour-suppressive adaptor by regulating downstream NDR/LATS activity (Gundogdu & Hergovich, 2019).

hMOB2 protein shares approximately 37% sequence identity with hMOB1 (Figure I.13) (Gundogdu & Hergovich, 2019). While hMOB1 proteins bind to both NDR and LATS kinases, hMOB2 only interacts with NDR kinases (Figure I.14). hMOB2 associates with NDR kinase through the N terminal region of the hMOB1 binding motif. Therefore, it is reasonable to observe the competing binding between hMOB1 and hMOB2 towards NDR kinases. Interestingly, while hMOB1 was found to associate with activated NDR kinases, hMOB2 forms a complex with intact un-phosphorylated NDR kinases (Kohler *et al*., 2010). This affinity preference indicates that hMOB2 restricts the hMOB1 induced activation process of NDR kinases. However, the mechanism of interplay between hMOB2 and hMOB1 towards NDR activation remains to be depicted. One possible explanation is the subcellular location of hMOB2. hMOB1 proteins predominantly locate at cytoplasm, but hMOB2 is found to be accumulated in the nucleus. This alternation of subcellular localisation of hMOB2 might block the membrane location and activation of NDR kinase by hMOB1. Nevertheless, the functions of hMOB2 merit further investigation (Gundogdu & Hergovich, 2019).

hMOB3A/B/C proteins are three distinct protein products from three different genes. hMOB3 group proteins share about 50% amino acid identity with hMOB1 (Figure I.13) (Hergovich,

2011). However, hMOB3A/B/C do not interact with or (de)activate NDR/LATS kinases. The biochemical roles and potential physiopathological roles of uncharacterised hMOB3 need to be deciphered (Gundogdu & Hergovich, 2019).

hMOB4, also known as Phocein, do not appear to interact with NDR and LATS kinases. hMOB4 is described as a STRIPAK complex component, which can bind two distinct regions of STRN. However, the role of hMOB4 in the STRIPAK complex remain speculative. In regard, hMOB4 has been reported to form the complex with MST4 (Chen *et al*., 2018).

Taken together, MOB proteins are essential regulators of NDR/LATS kinases. While MOB1 proteins function as activators, the role of human MOB2 protein is a specific negative regulator for human NDR kinases. The function of the hMOB3A/B/C and hMOB4 proteins must be defined. Notably, it is possible that MOB complexes do not signal in isolation but rather may be interlinked. It is conceivable that hMOB2, hMOB3, and hMOB4 are interconnected with hMOB1-regulated Hippo signalling to some degree.

1.4.1. MOB4 in *Homo sapiens*

The monopolar spindle one binder 4 (MOB4) protein, also known as phocein, with a size of 225 amino acids in canonical form (~26 kDa) (Baillat *et al*., 2001) is located to chromosome 2 (q33.1) (figure I.15) (GeneCards).

In HeLa cells, MOB4 was localised to the cytoplasm, membrane, and complex Golgi, supporting the role in vesicle transport (Baillat *et al*., 2001). MOB4 was localised to somatodendritic compartments of neurons (Baillat *et al*., 2002). Later, it was shown to be located, together with SG2NA, in the dendritic spines of cerebellar Purkinje cells and hippocampal pyramidal neurons (Haeberlé *et al*., 2006). However, it is expressed in many types of tissue (Baillat *et al*., 2001). Nevertheless, the Golgi localisation of MOB4 protein was not observed in polarised cells, such as neurons (Haeberlé *et al*., 2006).

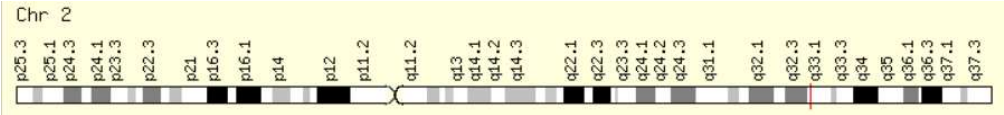

Figure I.15 - MOB4 gene localisation at chromosome 2 (q33.1) (GeneCards)

MOB4 was shown to interact with all members of the striatin family: striatin/STRN, SG2NA/STRN3 and zinedin/STRN4 (Baillat *et al*., 2001). MOB4 is a component of the STRIPAK complex, and it was found to be a part of the PP2A/STRN/MST3 complex (Goudreault *et al*., 2009). Structural parts of the MOB domain, shared with other MOB family members, are partially conserved in MOB4. However, MOB4 is the most divergent clade within the MOB family, and it was assumed that MOB4 has another function than the other MOB proteins (Vitulo *et al*., 2007).

MOB4 contains a region homologous to the small chain signature of σ subunit of clathrin adaptor protein (AP) complexes (Baillat *et al*., 2001). The AP complexes consist of two large subunits, one medium subunit and one small subunit, where the small σ subunit stabilises the AP complex mediating the formation of vesicles and selective packing of cargoes (Park & Guo, 2014). The adaptor complexes AP-1, AP-2, and AP-3 are involved in clathrin-mediated vesicular traffic and endocytosis. Clathrin-mediated endocytosis is required not only for nutrient uptake but also to remove receptors, integral proteins or lipids from the plasma membrane. The AP-1 complex is required for trans-Golgi coated vesicles, whereas the AP-2 complex associates with plasma membrane coated vesicles (Park & Guo, 2014). In comparison, the AP-3 complex is involved in transport from trans-Golgi to lysosomes (Gu *et al*., 2001).

MOB4 was also shown to interact with epidermal growth factor receptor substrate 15 (EPS15) and nucleoside-diphosphate kinase (NDPK) (Baillat *et al*., 2002). EPS15 interacts with AP-2 and is involved in clathrin-mediated endocytosis (Benmerah *et al*., 1996). NDPK interacts with dynamin I by mediating the abscission of vesicles from the plasma membrane (Baillat *et al*., 2002).

The secretion blocking agent brefeldin A (BFA) inhibits small G proteins of the ADP-ribosylation factor (Arf) family, which organise vesicular trafficking (Donaldson *et al*., 1992).

Localisation of MOB4 and SG2NA in rat neurons was altered upon exposure to BFA. Thus, the interaction of MOB4 with EPS15 or NDPK and altered localisation of MOB4 upon BFA treatment suggests that MOB4 is involved in vesicular traffic (Baillat *et al*., 2002).

The deregulation of the hMOB4-containing STRIPAK complex correlates with a broad range of human diseases including, diabetes, autism, cardiac disease, cerebral cavernous malformation (CCM), and, last but not least, cancer (Gundogdu & Hergovich, 2019).

In an analysis of the database, The Protein Atlas, it was possible to find expression levels of MOB4 in cancer compared to the normal tissue. It is possible to observe that levels of MOB4 are highly expressed in cancer and have no specific tissue association. The table shows a medium value of MOB4 expression in each cancer type. Colorectal cancer shows high expression levels whenever cervical and renal cancers show low levels of expression (figure I.16). These data suggest that MOB4 is an oncogene (The Protein Atlas).

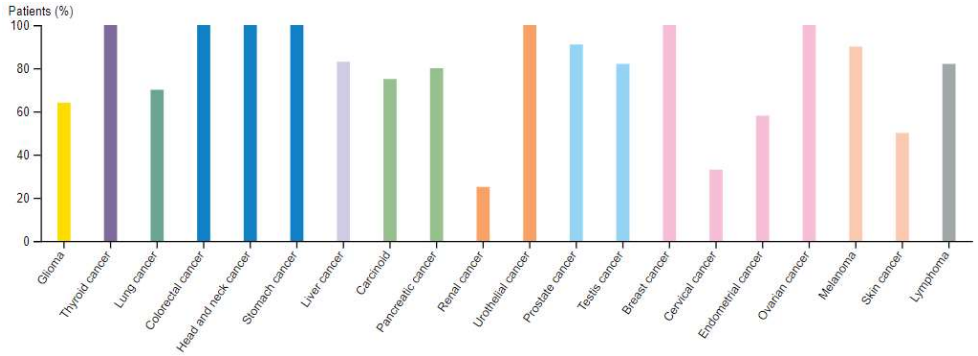

Figure I.16 - Medium values of MOB4 expression through the different types of cancer. Most cancers present moderate to intense granular cytoplasmic staining, with additional nuclear positivity in several cases (The Protein Atlas).

Chen *et al*. (2018) suggested a scheme that in pancreatic cancer cases that involved MOB4 and MST4 in deregulation of the MST1/MOB1-LATS1/2 pathway that sequesters MST1 and MOB1, respectively, and, consequently, have translocation of YAP1/TAZ to the nucleus (figure I.12), thus contribute with an oncogenic function. The same authors mentioned that high mRNA expression of MST4 and MOB4 correlates with the growth and migration of PANC-1 cells, making them associated with a low survival prognosis (Chen *et al*., 2018).

Nevertheless, the authors did not identify if this dysregulation would be transmitted to other types of tumours.

Our laboratory focuses on the study of the cell cycle and the mechanisms involved in this process. Given this, the MOB family raises interest, and a preliminary study was carried out on this family's proteins. Regarding the MOB4 protein, exciting results were obtained. It was observed that when the levels of protein MOB4 were decreased (using the RNAi technique), the cells failed to align the chromosomes in the metaphase plate and that the γ-tubulin was found scattered at the spindle poles and not concentrated (figure I.17) (Florindo, unpublished).

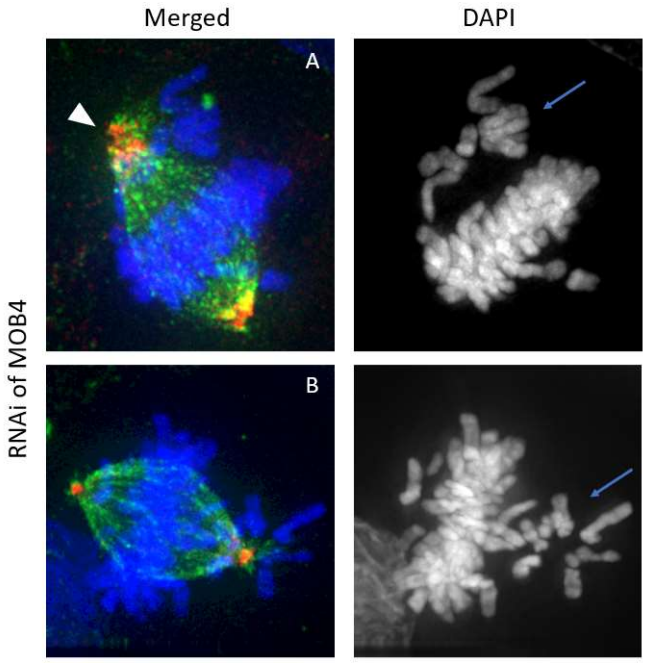

Figure I.17 - MOB4 protein RNAi in HeLa cells result in misaligned chromosomes.
In green is represented α-tubulin (located to the microtubules), in red is the γ-tubulin (located to the centrosomes) and DAPI staining for DNA. **A** – a cell represents scattered γ-tubulin across the spindle pole (white arrowhead), and blue arrows point for misaligned chromosomes. **B** – a cell with misaligned chromosomes at metaphase (blue arrow) (Florindo, unpublished).

Live-cell imaging was performed to better analysis of what happened when the levels of MOB4 were reduced. It was observed that cells downregulated of MOB4 had a delay in prometaphase. Control cells took an average of ~66 minutes to go through prometaphase,

while cells submitted to the RNAi took an average of ~303 minutes, suggesting that the checkpoint was activated (figure I.18). Five died in prometaphase from seven initial cells that were followed since the beginning of mitosis (Florindo, unpublished).

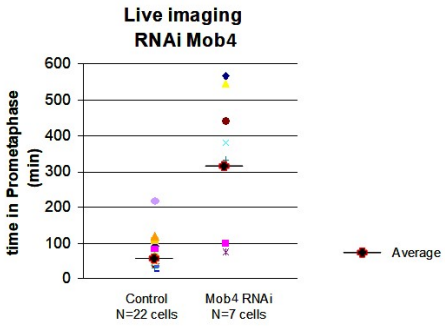

Figure I.18 – Average time cells spend in prometaphase in control and submitted to RNAi of MOB4.

Cells submitted to RNAi of MOB4 suffer a prometaphase arrest, and death rate is high in mitosis. Cells take an average of ~303 minutes, whenever in control, this time is ~66 minutes (Florindo, unpublished).

When analysed which other proteins can have similar phenotypes when subjected to RNAi. It has been published that when CENP-E protein levels are reduced, it results in the same phenotype, misaligned chromosomes.

Given this, it was analysed if MOB4 downregulation alters CENP-E localisation and used CENP-A protein as a reference for the study. Interestingly, the CENP-E localisation was not altered, and it was not possible to affirm the same about CENP-A (figure I.19). Previously in the introduction, it was described that CENP-A protein is a vital protein of a functional centromere.

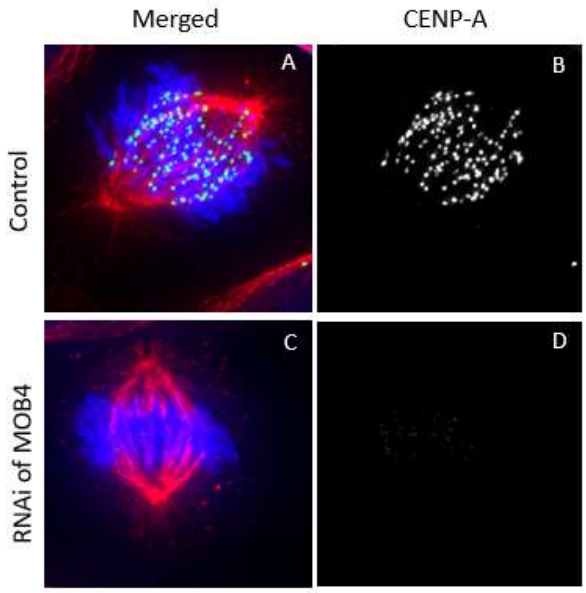

Figure I.19 - Cells submitted to RNAi of MOB4 lost CENP-A form centromeres.
A - Regular mitotic spindle, α-tubulin is represented in red (located to microtubules), CENP-A is represented in green (localised to centromeres), and DNA is stained blue. **A, B** – CENP-A localisation to the centromeres in control cells; **C, D** – CENP-A is lost from centromeres in cells submitted to RNAi of MOB4 (Florindo, unpublished).

Together, previous data from our laboratory suggest that MOB4 is an essential gene required for metaphase-to-anaphase transition: MOB4 downregulation causes strong defects in chromosome congression and alignment and a mitotic block. It was found that MOB4 accumulates on mitotic spindle, MOB4 was localised at centrosomes. In MOB4 depleted cells, CENP-A is lost from mitotic kinetochores, yet the outer kinetochore protein CENP-E remains unaffected (Florindo, unpublished). MOB4 might be required for proper kinetochore-microtubule attachment, but the exact function of MOB4 is still unknown.

1.4.2. MOB4 in *Drosophila melanogaster*

Very little is known about *Drosophila* MOB4 until the moment. In *Drosophila* embryonic cells (Schneider 2 cells, S2), dMOB4 was shown to have a role in mitotic spindle assembly, specifically in fibre spindle focusing (Trammel *et al*., 2008). This phenotype resembles that observed after the protein depletion encoded by an abnormal spindle (Asp), a microtubule

organising protein (Carmo Avides & Glover, 1999). Trammel *et al*. demonstrated that dMOB4 is not required for Asp's localisation. Moreover, they indicated that dMOB4 localises to the centrosomes and kinetochores (Trammel *et al*., 2008).

In addition to studies in cultures cells, studies were carried out in organisms, namely in *D. melanogaster*. A null mutant was created, and it was observed that adults were smaller in both males and females and that the mutants had smaller chest bristles than wild type *Drosophila* (figure I.20). The male mutants were also observed to be sterile. This result is exciting since dMOB4 is essential for male meiosis but not for female meiosis (Wainman, 2003).

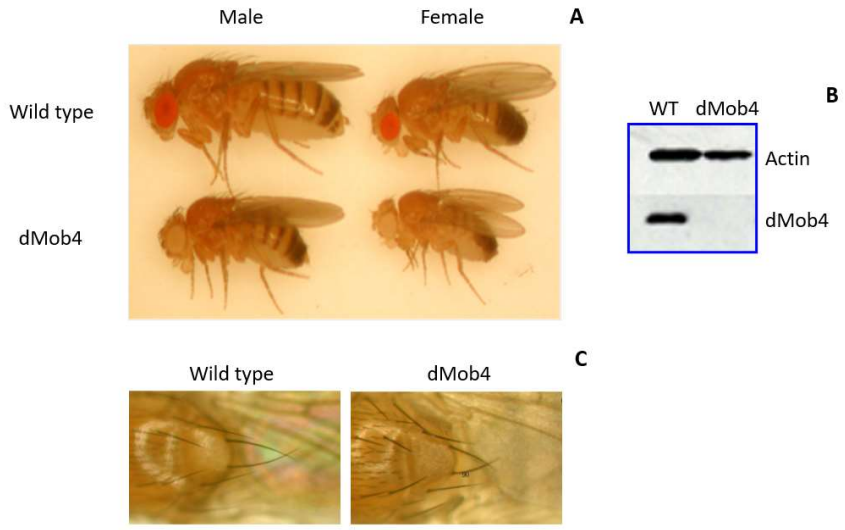

Figure I.20 - Wild type and Null mutants of Drosophila melanogaster.
A - Wild type males and females are larger than mutants; **B** - Western blot showing that levels of dMOB4 protein in mutants are null or below detectable levels; **C** - The thorax bristles in mutants are smaller compared to Wild type flies (Wainman, 2003).

In another study in vivo of *Drosophila* MOB4 null mutants presented abnormal synaptic development with a supernumerary bouton phenotype, disrupted axonal transport, disorganised microtubules, and larval lethality. Interestingly, the lethality observed was rescued by ubiquitous expression of the human orthologue of dMOB4, hMOB4, which is over 80% identical at the amino acid level, highlighting functional evolutionary conservation among the molecules (Schulte *et al*., 2010).

1.5. Objectives

The main objective of this work was to determine the mitotic function of human protein MOB4, with the biologic question of understanding the manner by which it contributes to and helps control mitosis.

Preliminary results suggest that MOB4 is involved in chromosome alignment and centrosome structure. Live-cell imaging results indicate that RNAi of MOB4 in cells resulted in the mitotic block and a high rate of cell death. Additionally, it was observed that MOB4 is essential for CENP-A localisation at kinetochores and the concentration of γ-tubulin at centrosomes. These data provided the beginning to this thesis, and the main objective can be divided into specific aims that will help elucidate the MOB4 function:

- Understand if MOB4 localisation in mitosis is dependent on microtubules.
- Identify what other mitotic spindle components can present MOB4 specific localisation: kinetochores or microtubules.
- Determine if MOB4 accumulation in interphase cells is dependent on microtubules.
- Identify if MOB4 levels are variable during the cell cycle.

CHAPTER II

MATERIALS AND METHODS

2. Materials and methods

2.1. Cell culture

2.1.1. Cell lines

For this study, two different cell lines were used: HeLa cell line, uterine cervix adenocarcinoma, was obtained from American Type Culture Collection (ATCC® CCL-2™); HeLa mCherry-Histone H2B EGFP-Alpha Tubulin Cell Line was obtained from Ximbio; human near-diploid colorectal carcinoma cells HCT116 conditionally expressing OsTIR1 under the control of the Tet promoter was obtained from Riken Cell Bank. CRAL1 cell line is conditional AID (auxin-inducible degron) mutant (figure II.1), generated by Álvaro Tavares and Inês Santos, generated in HCT116 Tet OsTIR1. All cell lines were maintained at 37ºC in a humidified incubator (Hera Cell, Heraeus) with 5% CO_2.

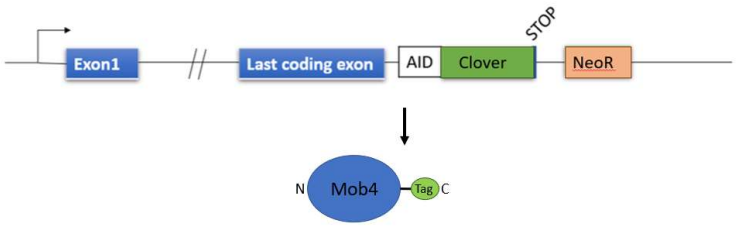

Figure II.1 - Schematic representation of CRAL1 cell line.
A double-strand break after the last stop codon of the gene of interest, generated by CRISPR-Cas9, created a site for insertion of a donor harbouring a tag (AID and Clover) and a marker (Neomycin resistance gene). Fusion protein is expressed, MOB4 and a tag (AID and Clover) at the C terminus.

2.1.2. Subculture and cellular conditions

HeLa cells were grown in BenchStable™ Dulbecco´s Modified Eagle Medium (1X) + GlutaMAX™-I (Gibco™), supplemented with 10% heat-inactivated Fetal Bovine Serum (FBS, Gibco™) and 1% Antibiotic-Antimycotic (100 unit/mL penicillin and 100 ug streptomycin, Gibco™).

HCT-116 Tet OsTIR1 and CRAL1 were grown in McCoy´s 5A Medium (1X) (Modified) (Gibco™), supplemented with 5% heat-inactivated FBS (Gibco™) and 1% Antibiotic-Antimycotic (Gibco™).

All experiments were carried out in Laminar Flow Hood (LFH) (Hera Safe, Heraeus), which was turned on 15 minutes before, and the culture medium, Trypsin, and PBS 1X were preheated in 37ºC water bath (Precisterm). All the material must be sterile or autoclaved and decontaminated by ethanol 70% before using in LFH. Cell lines were grown in 60 mm or 100 mm tissue culture dishes (VWR®).

All four cell lines used were subcultured at least twice a week, using a set of dilutions ranging from 1:5 to 1:10, according to the specific doubling time for each cell line, and to avoid metabolic stress due to space (70-90% optical confluency) and nutrient restrictions. Also, the medium was changed every time the pH indicator, phenol red, present in the culture medium required. During the cell growth, the colour of the medium changes, from red to orange/yellow, as pH changes due to the metabolites released by cells. In this process, the medium was aspirated. The adherent cells were washed with approximately 5 ml of Phosphate Buffered Saline 1X (PBS pH 7,4, Gibco™), isosmotic saline obtained through diluted sterile PBS 10X (Gibco™). Then, 500 µL (1 ml for 100 mm dish) of 0,05% trypsin-EDTA (Ethylenediamine tetraacetic acid) 1X (Gibco™) was added to the tissue dish with attached cells and left for approximately 3-5 minutes incubated at 37°C to promote cell detachment. After this time, the complete detachment of the cells was verified under an inverted microscope. A fresh medium was added to the dish to neutralize the trypsin, and cells were resuspended by gentle pipetting and transferred to the new tissue culture dish with determined dilution. The dish was completed with fresh medium to reach the final volume of 5 ml for 60 mm dishes or 10 ml for 100 mm dishes. Cells were observed through an inverted microscope and incubated at 37°C. Cells were observed every day to check the confluency and viability.

Whenever cell number was required, cells were counted through the Neubauer chamber 0,0025 mm^2 (figure II.2). After resuspending the cells, 10 ul of suspension with cells were pipetted and released into the counting room and absorbed by capillarity. Under the microscope, all cells in four big corner squares (figure II.2D) were counted. Cells were seeded in new dishes with the required concentration. The following formula was used for counting cells in big squares in the Neubauer chamber:

$$\text{Concentration (cells / ml)} = (\text{Number of cells} \times 10\,000) / \text{Number of squares}$$

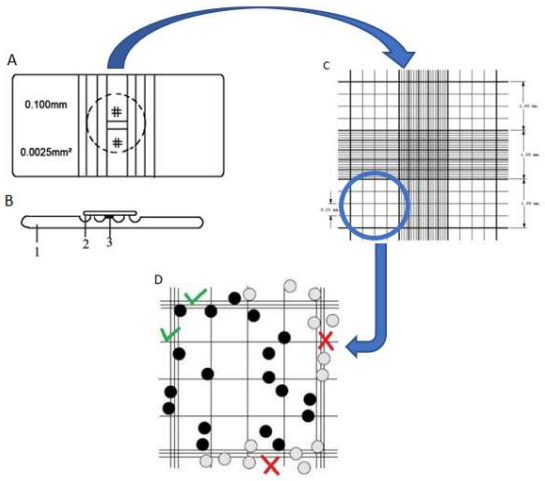

Figure II.2 - Neubauer chamber.
A – Front map, **B** – Longitudinal section (1 – cell count plate, 2 – cover slide, 3 – counting room), **C** – 9 squares of the chamber, **D** – one of four big corner squares used for cell counting (when cell touch limits, only two sides should be counted, top and left, per example) (adapted from https://laboratoryinfo.com/manual-cell-counting-neubauer-chamber/).

2.1.3. Freezing and thawing the cell line

Cells were grown in 100 mm dishes, and, once the optical confluency reached 90 %, cells were washed once with PBS 1X, detached by trypsinization, resuspended in a new medium, and transferred to the 50 ml falcon (VWR®). The cell suspension was centrifuged at 1 000 rpm for 5 minutes (Laboratory centrifuge Sigma 2-7) at room temperature. The supernatant was removed, and the precipitate containing the cells was resuspended in a freezing medium and finally collected in the cryotubes (VWR®). The freezing medium was prepared with 80% FBS, 10% culture medium, and 10% Dimethyl Sulfoxide (DMSO, Sigma-Aldrich®). The cryotubes were placed immediately in ice, and before being placed at -80°C (ThermoFisher Scientific).

Thawing cells was carried out by heating cryotubes within 1-2 minutes in a 37°C water bath. The thawed cell suspension was transferred to the 50 ml falcon with 5 ml of preheated culture medium, followed by centrifugation at 1 000 rpm for 5 minutes to remove the DMSO cryopreservation agent toxic to cells. The supernatant was discarded, and the pellet was resuspended in 5 mL of preheated fresh culture medium and finally placed in a 60 mm culture

dish and kept at 37°C and 5% CO_2. One day after, the medium was changed to remove dead cells.

2.2. RNA interference

In a six-well plate, 2 x 10^5 HeLa cells were seeded per well in 2 ml antibiotic-free standard growth medium supplemented with Fetal Bovine Serum (FBS). The cells were incubated at 37ºC in a 5% CO2 incubator for 24 hours.

For the transfection were prepared two solutions: 1) 50 ul of Opti-MEM™ Reduced Serum Medium (Gibco™) + 3 ul Oligo19 (table II.1); 2) 50 ul of Opti-MEM™ Reduced Serum Medium + 2 ul Lipofectamine™ 2000 Transfection Reagent (Invitrogen™). The siRNA duplex solution (Tube 1) was directly added to the Transfection Reagent solution (Tube 2). The final solution was incubated for 20 minutes at room temperature. At the same time, supplemented growth medium was changed to Opti-MEM™. Past 20 minutes, the solution with Oligo19 and Transfection Reagent was added to the cells drop by drop. Cells were then returned to the incubator for 2 hours, and then transfection solution was changed to DMEM supplemented with FBS. Cells were then incubated for 48 hours before being processed as required.

Table II.1 - Oli19 sequence for targeting hMOB4 RNA

	Sequence	Target RNA
Oli19	GCAGGGUUAGCAUAAAGGAdTdT	hMOB4

2.3. Cold depolymerisation and recovery of microtubules

At the cellular level, many processes are temperature regulated. For instance, incubating cells on ice for a specific time (depending on cell type) is sufficient to induce microtubule depolymerisation.

For cold assay of microtubules in Hela cells expressing mCherry-Histone H2B EGFP-Alpha Tubulin, “trypsinised cells” were seeded onto coverslips in 1 mL media per well in a 24-well plate. To allow disassembly of the microtubule cytoskeleton, 24-well plate containing cells adhered to coverslips were placed directly onto the ice and incubated for different time points with a purpose to identify the complete microtubule depolymerisation.

Once all microtubules are disassembled, ice recovery can be achieved through the recovery at 37ºC. To recover microtubule nucleation after ice treatment, the 24-well plate was quickly lifted from the ice bucket on ice and placed at 37ºC (figure II.3). The cold media was changed to the one at 37ºC. At different times, the DMEM media was substituted by pre-warmed buffer for 2 minutes, followed by 2-minutes fixation in Methanol / Acetone (1:1) at -20ºC. Coverslips were mounted in Mowiol on glass slides. Microtubule recovery was quantified by visual array index (VAI). Images of randomly selected cells were scored.

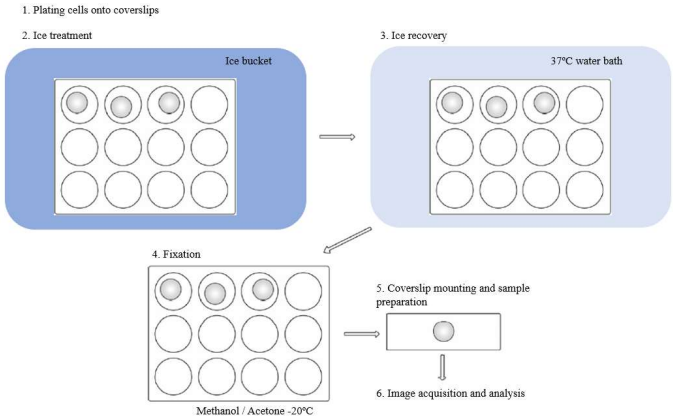

Figure II.3 - Steps of ice recovery assay.
The sequence of the main steps during ice recovery assay. 1 – Plating cells into coverslips; 2 – Ice treatment; 3 – Ice recovery at 37ºC; 4 – Fixation; 5 – Coverslip mounting and sample preparation; 6 – Image acquisition and analysis. Small grey circles represent coverslips and white arrows indicate the transition from one step in the procedure to the next (adapted from Grimaldi *et al*., 2013).

2.4. MG132 proteasome inhibitor assay

To increase the number of mitotic cells, cells were divided into two groups under the same experimental conditions, whereinto one group was added 10 uM of the proteasome inhibitor MG132 for 6 hours in order to stop the cells at the metaphase-anaphase limit, and in the other group, they were maintained without the addition of MG132. Then, immunofluorescence was

performed with an anti-α-tubulin mouse antibody. With the immunofluorescence result, a count was performed in random fields of each experimental condition of the number of metaphase cells and mitotic index.

Following formula was used to calculate mitotic index:

$$\text{Mitotic index} = \frac{\text{Number of dividing cells}}{\text{Total number of counted cells}}$$

2.5. Indirect immunofluorescence

The immunofluorescence technique relies on using the specificity of antibodies labelled with fluorochromes to target specific biomolecules within a cell, allowing their visualization in the sample (Oliver and Jamur, 2010).

Immunofluorescence was performed using sequentially two antibodies: a primary antibody that recognized and bonded to the target molecule and a secondary antibody, which carried the fluorophore and recognized and bonded to the primary antibody.

Cells were grown on 12 mm microscope coverslips (VWR®) in 24-well plates for two days for HCT116 cells and one day for HeLa cells. Before fixation, cells were washed with PEM buffer (0,1 M PIPES pH 6,95, 2 mM EGTA, 1 mM $MgSO_4$) + 30% Glycerol (Sigma-Aldrich®) preheated to 37ºC for 2 minutes. Cells were fixed in methanol/acetone (1:1) at -20ºC for 2 minutes, washed three times with PBS and permeabilized with 0.5% (v/v) Triton X-100 diluted in PBS for 10 minutes, washed three times with PBS and blocked with 2 % (v/v) FBS, 2% Bovine Serum Albumin (BSA) in PBST (0,05% Tween20 (v/v) in PBS) for 30 minutes at room temperature, and incubated with primary antibody in 1% (v/v) Fetal Calf Serum (FCS) in PBST diluted for a specific concentration for 1 hour at room temperature. After rinsing three times, 5 minutes, with PBS 1X, and one time with PBST, cells were incubated with the secondary antibodies in 1% (v/v) Fetal Calf Serum (FCS) in PBST diluted to a specific concentration for 30 minutes. Fluorochrome conjugated to secondary antibody emits light; due to this reason, this incubation was done in a dark, humid chamber. The cover glasses were rinsed, once again, three times with PBS and one time with PBST. Cover glasses were incubated with 0,25 µg/mL of DAPI (4'-6-diamidino-2-phenylindole) for 10 minutes at

room temperature in the dark prior to being mounted in microscope slides in Mowiol mounting medium [0,1 M Tris-HCl pH 8,5, 25% (w/v) glycerol, 2,4% (w/v) DABCO (1,4-Diazabicyclo[2.2.2]-octane), 10% Mowiol 4-88]. After drying, the coverslips were sealed with varnish and stored at 4˚C.

Cells were examined with a magnification of 100x and numerical aperture (NA) of 1,4 by standard fluorescence microscopy. Image stacks with Z-step of 0,4 um were acquired by Zeiss Axio Imager Z2 microscope (Zeiss) using Zeiss AxioVision software.

2.6. Transfection, colony formation and genomic detection

The conditional depletion of a protein is a powerful approach to analysing its function in vivo, especially for essential proteins for cell viability (Natsume *et al*., 2016). However, it is crucial to be concerned about the genetic, epigenetic, and phenotypic heterogeneity that may be present inside a population of cells before single-cell isolation. Creating a cell line from a single cell represents a considerable genetic bottleneck, and experiments may be perplexed if a single cell-derived clone captures only a limited number of characteristics of the variety present in the starting cell population. Indeed, some established cell lines are known to exhibit significant interclonal heterogeneity. Due to the possibility of parental heterogeneity, it is crucial to analyse multiple independent knock-in/knock-out cell lines in order to confirm that some unforeseen result is not a clonal artefact (Giuliano *et al*., 2019; Tang, 2019).

Additionally, stimulating a single cell to proliferate to develop a clonal population of millions of cells represents a considerable selective pressure. This pressure could enhance specific genetic and epigenetic alterations within the growing clone that encourage proliferation. To account for this selective force, it is essential to compare the experimental knock-out/knock-in with the clonal “control” cell line derived under similar conditions (Giuliano *et al*., 2019).

The AID system helps investigate the physiological functions of essential proteins. In the presence of auxin, cells expressing TIR1 can rapidly and conditionally deplete proteins tagged with an AID. The AID system has been used in various organisms, including human cells (Nishiruma *et al*., 2009). Two components need to be introduced into the cells to achieve an inducible loss of protein function with the AID system. The first is establishing a TIR1-expressing cell line (figure II.4.A), and the second is to tag endogenous gene of interest and

replace it with the one with AID-tagged protein encoded (figure II.4.B) (Lambrus *et al*., 2018; Natsume *et al*., 2016).

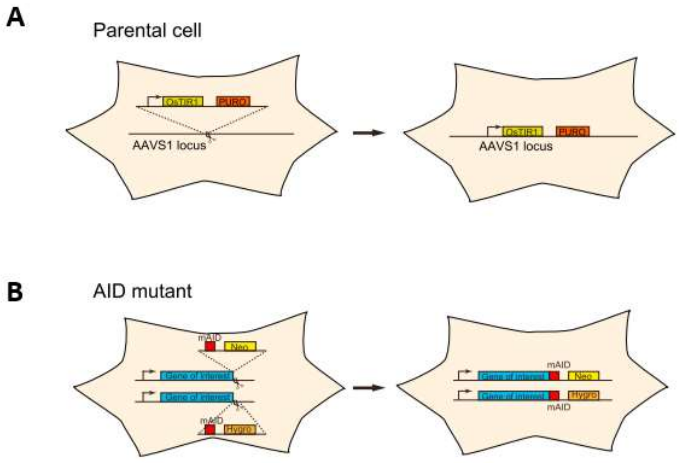

Figure II.4 - Construction of human conditional AID mutants.
A schematic illustration showing the strategy of construction of human conditional AID mutants. **A** - primarily, parental cells must be generated by introducing a transgene encoding OsTIR1 at the safe-harbour AAVS1 locus. **B** - by tagging both alleles of a target gene of interest with mAID in the parental cells, conditional AID mutants can be generated. One resistance gene or two different can be used, targeting both alleles (Natsume *et al*., 2016).

The HCT116 parental cell line that expressed OsTIR1 under the control of the conditional tetracycline responsive promoter (Tet-OsTIR1) was used to construct a conditional AID mutant, the same as for CRAL1. An inducible expression system is introduced at the safe harbour AVSS1 locus (Natsume *et al*., 2016).

The pMK292 (mAID-mCherry2-NeoR) system (Addgene plasmid #72830), for C-terminal targeting, was inserted between homology arms of the gene MOB4. All-in-One plasmid vector that contains dual U6 promoter-driven sgRNA cassettes and encodes Cas9D10A nickase, coupled via a "ribosomal-skipping" 2A peptide-linker30, to the fluorescent marker protein mCherry2 (Chiang *et al*., 2016).

A method to generate conditional human HCT116 mutants by homology-directed repair (HDR)-mediated gene tagging using CRISPR-Cas9 is represented in figure II.5.

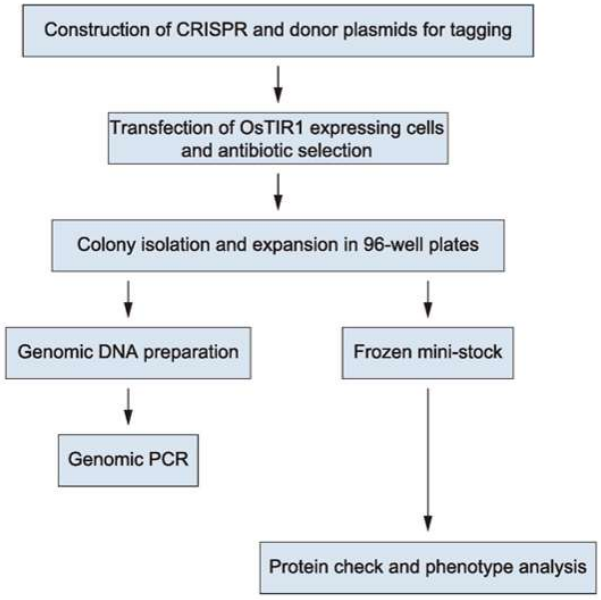

Figure II.5 - The strategy used for generating conditional AID cells by tagging an endogenous protein of interest (Yesbolatova *et al*., 2019).

2.6.1. Transfection

Parental cell line HCT116 Tet-OsTIR1 was used for the transfection. Sub-confluent culture (approximately 70%) of low-passage-number HCT116 Tet-OsTIR1 cells was prepared. Cells were collected by trypsinization to prepare a cell suspension. Cells were collected and counted to 2 × 10^5 cells/ml. 1 mL of the diluted cells was seeded per well in a 6-well plate and completed to 2 ml of culture medium per well and cultured at 37ºC for two days. To prepare the transfection mixture in one microcentrifuge tube (tube A) were mixed 100 µL of Opti-MEM® I Reduced Serum Medium (Gibco™), 1000 ng of plasmid CRISPR construct 'pRN3P with MOB4Hom1-AID-Cherry-neo-MOB4Hom2' with the first PAM sequence mutated for hMOB4 and 1000 ng of guide RNA1 + guide RNA2for hMOB4 cloned in all-in-one (AIO) Cherry. Another microcentrifuge tube (tube B) was mixed 100 ul of Opti-MEM I and 4 uL of Lipofectamine® 2000 Transfection Reagent (Invitrogen™). Both tubes were incubated at room temperature for 3 min. After, the mixture of tube A was added slowly, drop by drop, to tube B (Oligonucleotide to Transfection reagent) and incubated for 20 min at room temperature. The culture medium in the 6-well plate was changed to preheated to 37ºC 800 ul Opti-MEM® before the transfection mixture was applied to the cells. Cells were mixed gently

by rocking the plate back and forth and incubated at 37ºC for an additional 2 hours to permit complex internalization. Following this incubation, more 1 ml of OptiMEM® I was added to the cells and were incubated at 37ºC for 24 hours.

One day after transfection, cells were collected in 2 ml of the medium after trypsinization and seeded by splitting into two 100 mm dishes containing 10 ml of culture medium.

Non-transfected cells were plated in parallel, seeded in a 6-well plate, then transferred to the 100 mm dish. They suffered the same antibiotic selection as transfected cells did to control the antibiotic selection.

2.6.2. Antibiotic selection and colony formation

The final concentration of antibiotics was 500 ug/ml of Geneticindisulfat (G418) Lösung (Carl Roth®). As soon as cells were attached to the bottom of the Petri dish, antibiotic selection started. Culture medium was replaced with a fresh one containing an appropriate antibiotic concentration every two days until colonies had become visible (12 days after plating colonies were visible). Non-transfected cells were all dead until this moment.

Twelve days after antibiotic selection, formed colonies were visible to the naked eye and confirmed by an inverted microscope.

2.6.3. Single-cell isolation and expansion in 96-well plates

After introducing CRISPR-Cas9 and gRNA by transfection, single cells must be isolated to generate clonal lines that can be verified as complete knock-ins.

The polyclonal cell culture in a 100 mm dish was harvested by trypsinisation, counted in Neubauer chamber, and processed to isolate monoclones by limiting dilution. Cell suspension, diluted to a concentration of 10 cells/ml, was placed in a multichannel pipette reservoir. By using a multichannel pipette, 100 ul/well of the diluted cells were pipetted into each row of a 96-well plate.

Due to the low proportion of single-cell isolated with dilution method, 20 96-well plates were used to isolate clones.

Twenty-four hours followed the dilution after the cells had settled. It was possible to check by microscopy for wells that contained a single cell, no cells or more than one. Cell expansion was verified under the inverted microscope every 2-3 days.

Cells were cultured in 96-well plates until the well reached high confluency. The medium containing the antibiotic was changed every two days. Due to a need for secreted factors from neighbouring cells during the first eight days, a conditioned medium was used to increase cell attachment and survival. Conditioned medium was prepared by mixing four parts of new supplemented McCoy´s 5A medium and one part of the filtered medium. The filtered medium was obtained by collecting medium from culture dishes with parental cell line plated every two days. The filtration of this medium with a syringe and 0,22 um filter was performed to eliminate dead cells.

Once that well was near confluence, cells were transferred to a well of a 24-well plate. Between 2 and 4 days, the line continued expanding until a sufficient number of cells could be harvested for the validation assays.

To collect each cell line, this was trypsinised and resuspended with 500 ul of the medium. A part of this suspension was used to prepare a frozen stock, and the other was used to prepare genomic DNA for PCR genotyping.

2.6.4. Genomic DNA preparation

The tube containing 100 ul of medium with collected cells was centrifuged at 2 000 g for 10 minutes at 4ºC (VWR® by Hitachi Koki Co, Ltd). The supernatant was discarded, and the pellet was washed with 1 ml of cold PBS 1X and centrifuged one more time with the same conditions, and the supernatant was discarded. At this step, the pellet was frozen at -20ºC (between a few minutes and one day) or proceeded with protocol immediately. Lysis buffer (10 mM Tris-HCl pH 8, 10 mM EDTA, 10% SDS and 10 mM NaCl) was added to pellet, followed by addition of Proteinase K with final concentration 0,25 mg/ml. The tube was incubated at 55ºC for 1 hour, at 95ºC for 20 minutes (to inactivate Proteinase K), and finally at room temperature for 10 minutes. For DNA precipitation, one volume of Isopropanol and

10% of Sodium Acetate (3 M) was added to the tube and was incubated on ice for 10 minutes. The tube was centrifuged at 15 000 g for 20 minutes at 4ºC. After discarded the supernatant, the pellet was washed with 1 ml 70% Ethanol and centrifuged at 15 000 g for 10 minutes at 4ºC. Ethanol was discarded and pellet dried at room temperature before adding TE buffer (10 mM Tris-HCl pH8 and 1 mM EDTA). DNA concentration was measured on NanoDrop™ (ThermoScientific™).

2.6.5. Genotyping by polymerase chain reaction (PCR)

One of the most critical developments in gene technology has been the Polymerase Chain Reaction (PCR), which can amplify regions of DNA, genes, or whole plasmids.

Double-stranded DNA is dissociated by heating. Then, it is cooled until optimal melting temperature for nucleotide primers present in excess, one of which is complementary to a region of one strand and the other to a region of the other strand. The primers bind to the DNA strands, which bind faster than the strands reassociate because of the higher concentrations of the primers and the second-order kinetics of association. In the presence of Deoxyribonucleotide triphosphates (dNTPs) and a thermostable DNA polymerase, *Thermus aquaticus (Taq*-Polymerase*)*, the strands are replicated from the 3'-OH ends of the primers. This procedure is then repeated, with the number of strands of DNA doubling at each cycle, 2(n+1), where *n* is a number of cycles of heating, cooling, and replication (Lorenz, 2012).

In a 1,5 ml microcentrifuge tube, the MasterMix solution was prepared with reagents required for PCR reaction to happen. The reagents were added in following order: 4,97 ul ddH20 (di-distilled water), 1 ul 10X DreamTaq™ Buffer (includes 20 mM MgCl2) (Thermo Scientific™), 1 ul dNTPs (2 mM, Invitrogen®), 1 ul Forward primer (10 uM), 1 ul Reverse primer (10 uM) and 0,03 ul of DreamTaq DNA Polymerase (5 U/ul) (Thermo Scientific™). In separate 0,2 ml thin-walled PCR tubes were added 9 ul of MasterMix solution and respective DNA template to be analysed to the final volume of 10 ul. The tubes were shaken to mix well all reagents before being placed into the Thermocycler (S1000™ Thermal Cycler, Bio-Rad).

Table II.2 - The Thermocycler programme used for PCR reaction

Step	Temperature	Time	# of cycles
Initial denaturation	95ºC	5 min	
Denaturation	95ºC	30 sec	39
Primer annealing	58ºC	30 sec	
Extension	72ºC	2 min	
Final extension	72ºC	10 min	
Cooling	4 ºC	∞	

When the program has been finished, the 0.2 ml thin-walled PCR tubes were removed and stored at 4°C. PCR products were detected by electrophoresis in an agarose gel.

Table II.3 - Primer sequences

Name	Direction	Sequence
PriAL20	Forward	cgttggctacccgtgatatt
PriAL22	Reverse	ttggtcaccttcagcttgg
PriAL44	Forward	tgaattcctgcagcccggggatc
PriAL47	Reverse	cgctctagaactagtggatc

2.6.6. Electrophoresis agarose gel

Gel electrophoresis is the standard laboratory procedure for separating DNA by size for visualization and purification. Electrophoresis uses an electrical field to move the negatively charged DNA toward a positive electrode through an agarose gel matrix. Shorter DNA fragments migrate through the gel more quickly than longer ones. To determine the approximate length of a DNA fragment by running it on an agarose gel alongside molecular weight marker is added. The DNA bands on agarose are invisible unless the DNA is labelled or stained somehow. The staining DNA method used was to expose it to the dye, which

fluoresces under ultraviolet (UV) light when bound to DNA (/www.addgene.org/protocols/pcr/).

To prepare agarose gel solution, Tris-Acetate-EDTA 1X (TAE) buffer was mixed with agarose powder to obtain 0,8% gel. The solution was warmed up until the powder was completely dissolved. The agarose solution was left to cool down until 50ºC, and GelRed® Nucleic Acid Gel Stain (Biotium) was added.

The agarose was placed into a gel tray with the well comb in place. It was set at room temperature for 30 mins until it was completely solidified. Loading buffer 6x (30% glycerol, 0,25% Bromophenol Blue in dH2O) was added to each DNA sample. Once solidified, the agarose gel was placed into the gel box (electrophoresis unit) and filled with 1x TAE until the gel was covered. A molecular weight DNA ladder (GeneRuler 1 kb Plus Ladder) was loaded into the gel. The gel was running out at 50 V for about 1 hour. The staining pattern was observed under UV light in a bioimaging system (GeneCards).

2.7. Protein extract preparation

Cells were washed and incubated with cell detachment solution (50 mM Tris-HCl, 140 mM NaCl, 10 mM EDTA, and 10 mM β-Mercaptoethanol). The cells were allowed to detach for 5-10 min at room temperature. The detachment was monitored by a brightfield microscope. Cells were centrifuged at 3 000 g for 5 minutes at 4ºC. The debris was removed, and the pellet, washed with PBS at 4ºC, was centrifuged one more time with identical conditions, and the pellet was frozen at -20ºC.

Before being used, Laemmli loading buffer 2x (100 mM Tris-HCl pH 6,8, 20% glycerol, 5% SDS, 0,2% Bromophenol blue, and 200 mM β-Mercaptoethanol) was added to samples, and they were denatured by boiling for 10 minutes. When not used, it was kept at -20ºC.

2.8. Sodium Dodecyl Sulphate Polyacrylamide Gel Electrophoresis (SDS-PAGE) and Western blot

The most popular method for estimating the size of a polypeptide chain is by its mobility in polyacrylamide gel electrophoresis (PAGE) in the presence of the detergent sodium dodecyl

sulphate (SDS). In this method, the size of a protein is estimated by its migration through the tiny pores of a gel matrix. The gel matrix is continuous rather than particulate, so smaller proteins migrate more rapidly than large proteins (Walker, 1996).

Crosslinked polyacrylamide gels are formed from the polymerization of acrylamide monomer in the presence of smaller amounts of N, N'-methylene-*bis*-acrylamide (30% acrylamide/*bis*-acrylamide, Bio-Rad®). The addition of ammonium persulfate initiates the polymerization (provides the free radicals that drive polymerization) and the base N, N, N', N'-tetramethylenediamine (catalysator of the reaction) (TEMED, Sigma-Aldrich®). The anionic detergent SDS is used to give a negative charge to samples, and the amount of SDS bound is almost always proportional to the molecular weight of the polypeptide. SDS-polypeptide complexes migrate through polyacrylamide gels in accordance with the size of the polypeptide (Walker, 2002).

In a discontinuous system, a non-restrictive large pore gel, called a stacking gel, is layered on top of a separating gel called a resolving gel. Each gel is made with a different buffer, and the tank buffers are different from the gel buffers. The sample and the stacking gel contain Tris-HCl (pH 6,8), the buffer reservoir contains Tris-glycine (pH 8.3), and the resolving gel contains Tris-HCl (pH 8,8). The short stacking gel on the top of the resolving gel aims to concentrate the protein sample into a sharp band before it enters the leading resolving gel, thus giving sharper protein bands in the resolving gel. The stacking gel, with high porosity, allows deposition of the complexes in a stack on the surface of the resolving gel. The higher pH of the resolving gel helps the ionization of glycine. The resulting glycine ions migrate through the stacked polypeptides and travel through the resolving gel immediately behind the chloride ions. The SDS-polypeptide complexes move through the resolving gel in a constant voltage and pH zone and are separated according to size by the filter (Sambrook *et al*., 1989).

Samples were boiled for 3 minutes and then loaded onto a 10% polyacrylamide gel (recipes of gels are represented in Annex 1). The relationship between mobility and size is determined by relating the observed mobility to that of standard proteins of known size (Precision Plus Protein™ Standards Dual Color, Bio-Rad) loaded onto the gel. The electrophoresis in a running buffer (25 mM Tris, 190 mM glycine, 0,1% SDS) was carried out by a PowerPac™ 300 Electrophoresis System (Bio-Rad) at 12 mA per gel for the run in the stacking gel and then increased to 25 mA per gel in resolving gel (figure II.6).

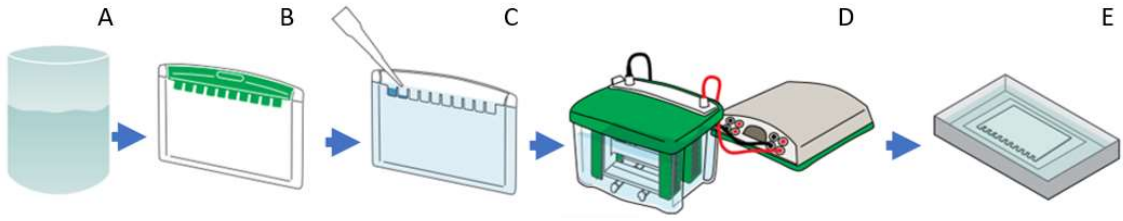

Figure II.6 - Representative diagram of SDS-PAGE protocol.
A – Running buffer preparation; **B** – Running gels preparation; **C** – Sample loading; **D** – Electrophoresis performing; **E** – Place the gel into the water (adapted from www.bio-rad.com).

Proteins in sample separated by electrophoresis in polyacrylamide gels were transferred electrophoretically, sandwiched between two chromatography paper sheets on each side soaked in transfer buffer, in a way that retains the electrophoretic pattern, to a 0,2 um PVDF membrane (Amersham^{TM} Hybond^{TM}) to which the proteins stick tightly. The transfer was carried out in Transfer buffer (25 mM Tris, 190 mM Glycine) and by a PowerPac^{TM} 300 Electrophoresis System (Bio-Rad) at 275 mA for 1 hour (figure II.7).

Specific proteins were identified immunochemically by a procedure known as Western blotting. Blocking of non-specific binding was achieved by placing the membrane in a 10 % (w/v) solution of non-fat milk in Tris-buffered saline (TBS) 0.1% Tween®20 (TBST) for 1 hour in gentle agitation at room temperature.

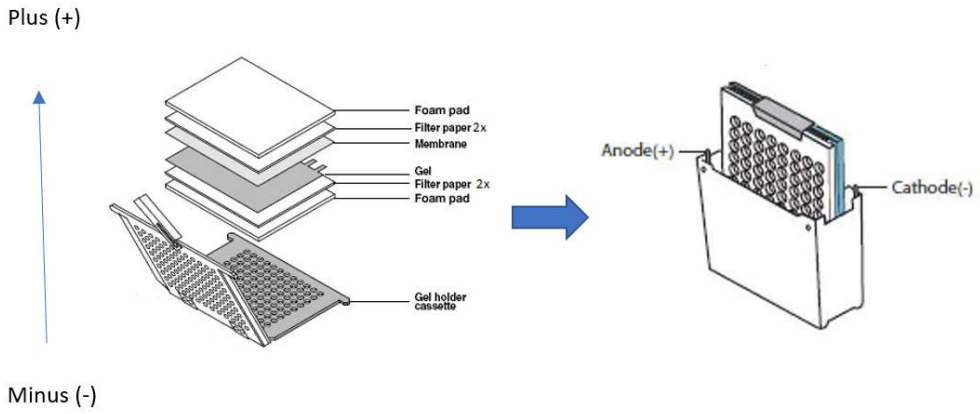

Figure II.7 - Representative diagram of the transfer sandwich setup for tank transfer (adapted from www.bio-rad.com).

For protein detection, the membrane was incubated with the primary antibody in 1% non-fat milk in TBST, for 1 hour at room temperature, with gentle agitation. After rinsing the membrane three times, with 1% non-fat milk in TBST, to remove the unbound primary antibody, the membrane was incubated with the secondary antibody conjugated with horseradish peroxidase (HRP) and diluted at a specific concentration in 1% non-fat milk in TBST. The incubation lasted for 1 hour, at room temperature, with gentle agitation.

After rinsing the membrane, the reactivity of HRP was developed by Enhanced Chemiluminescence (ECL). Solution 1 [1 M Tris-HCl pH 8,5, 250 mM Luminol (5-amino-2,3-dihydro-1,4-Phthalazinedione), 90 mM p-Coumaric acid (4-Gydroxycinnamic acid)] and Solution 2 (1 M Tris-HCl pH 8,5, 30 % H_2O_2) were prepared previously, and Working Solution was prepared by mixing equal parts of detection agents 1 and 2.

The membrane was incubated in the Working Solution for 1 minute at room temperature. The absorbent paper was used to remove any excess of the Working Solution from the membrane. The membrane was placed in a plastic page protector and exposed to the X-ray cassette film. The exposure time could vary between 5 and 30 minutes. The X-ray film was developed by using appropriate developing and fixing solutions.

Table II.4 Primary antibodies used for Western blotting and indirect immunofluorescence

Designation	Anti-	Generated in	Reference	Company
DM1A	A-Tubulin	Monoclonal mouse	#T-9026	Sigma
GTU-88	Y-Tubulin	Monoclonal mouse	#T-6557	Sigma
Anti-Mob3, clone 16E2	MOB4 / Phocein	Monoclonal mouse	#MABS22	Millipore
GNS-1	Cyclin B1	Monoclonal mouse	#554176	Pharmingen

Table II.5 – Secondary antibodies used for Western blotting and indirect immunofluorescence

Designation	Anti-	Generated in	Reference	Company
AlexaFluor 594	Mouse	Goat	#A11005	Molecular Probes
IgG HRP-conjugated	Mouse	Rabbit	#AB_2340061	Jackson ImmunoResearch

2.9. Stripping and rebloting Western Blot

Stripping and reprobing a western blot is a method in which the primary and secondary antibodies are removed from a western blot so the blot can be reprobed. A blot may be stripped and reprobed several times to visualize other proteins (*www.thermofischer.com*). The membrane was rinsed in water to remove excess chemiluminescent substrate on the membrane. The Harsh-stripping solution (1% SDS, 62,5 mM Tris HCl pH 6,8, 0,8% β-mercaptoethanol) was added to a small plastic box with a tight lid to incubate the membrane with gentle agitation for 30 minutes at 60°C in a linear shaking bath (Grant GLS Aqua 12 Plus). The stripping buffer volume must be enough to cover the membrane fully. Then, the membrane was washed two times with agitation for 10 minutes each at room temperature in a wash buffer (TBST). The membrane proceeded to reblock prior to reprobing.

2.10. Genome editing

Genetic perturbation is a potent approach to the analysis of protein function in vivo. Recent progress in genome-editing technology provides precise, targeted genomic changes, including whole-gene insertion or deletion, stacking, or pyramiding of genes, and precise modification of genetic elements that permit scientists to introduce, change or optimise genetic traits interest. Various classes of edit-enabling technologies have been developed in the past decades, including Zinc Finger Nucleases (ZFNs) and Transcription activator-like Effector Nucleases (TALENs) (Weeks *et al*., 2015). Although these approaches can generate a DSB at a specific locus, both ZFNs and TALENs require complicated re-engineering of the DNA-

binding domains to target different DNA sequences. Thus, their versatility and utility are minimal. The development of the Clustered Regularly Interspaced Short Palindromic Repeats (CRISPR)/CRISPR-associated proteins (CRISPR/Cas) system as a programmable genome-editing tool was built on a firm foundation of earlier research (Giuliano *et al*., 2019).

2.10.1. Creation of DNA double-strand breaks to allow genome editing

Genomes and their constituent genes are made of double-stranded DNA; this DNA can be broken accidentally (*e.g*., by radiation) or purposefully, using proteins called endonucleases (often called nucleases) that can generate double-strand breaks (DSBs) ion DNA. Cells have mechanisms to repair DSBs in DNA, and these mechanisms can be used to generate alterations in the DNA sequence. Groundbreaking work in bacteria, yeast, and mammalian systems shows that DSBs dramatically stimulate the rate of DNA repair by nonhomologous end-joining (NHEJ). The broken ends are reattached (figure I.21). Such NHEJ repair often results in the deletion or insertion of DNA sequences of varying lengths, disrupting gene function (National Academies of Sciences, Engineering, and Medicine, 2017).

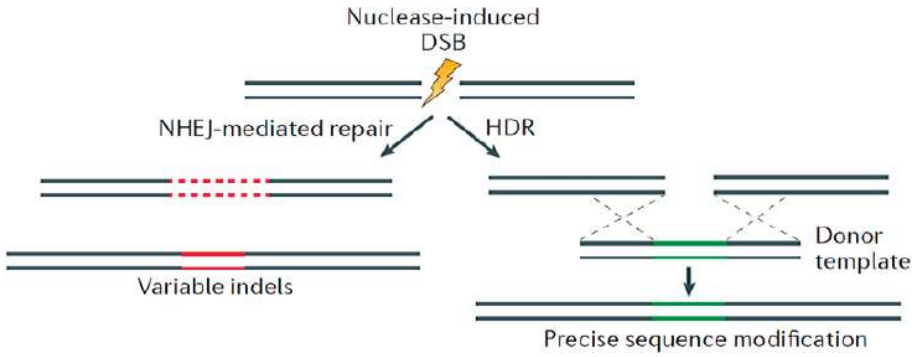

Figure II.8 - Genome-editing outcomes are mediated by repair of nuclease-induced double-strand DNA breaks by NHEJ or HDR.
DSB - double-strand break; HDR - homology-directed repair; NHEJ - nonhomologous end-joining (National Academies of Sciences, Engineering, and Medicine, 2017).

Nevertheless, if a homologous stretch of DNA is introduced into the cell as a donor template, homology-directed repair (HDR) can guide more accurate repair. If specific alterations are involved in the homologous stretch, it can introduce precise changes to the recipient genomic

DNA. These cellular DNA repair mechanisms have been used to develop several methods that allow genes or the genome to be edited precisely (National Academies of Sciences, Engineering, and Medicine, 2017).

2.10.2. CRISPR/Cas9

The CRISPR system provides several advantages for perturbing mammalian gene function compared to FokI-nuclease- or RNAi-mediated approaches. Unlike ZFNs and TALENs, CRISPR is highly versatile. CRISPR has the potential to generate complete loss-of-function perturbations, bypassing the problems inherent in studying a partial-loss-of-function phenotype (Giuliano *et al*., 2019).

CRISPR/Cas9 is an adaptive immune system widespread in bacteria and archaea and is used to protect hosts from infection by invading viruses, phages, and plasmids (Giuliano *et al*., 2019). The CRISPR locus was first identified and reported as an array of 29-base pair (bp) tandem repeats interspaced with 32 bp spacer sequences of DNA in *Escherichia coli* (*E. coli*) in 1987 (Ishino *et al*., 1987). Several studies were performed about CRISPR until, in 2012, the most significant breakthrough in CRISPR research came with the work by Jinek *et al*. This work demonstrates in vitro DNA cleavage activity using recombinant Cas9 coupled with a single guide RNA (sgRNA) derived from the fusion of CRISPR RNA (crRNA) and trans-activating crRNA (tracrRNA) (figure I.22) (Jinek *et al*., 2012).

CRISPR/Cas9 is a ribonucleoprotein complex consisting of two key molecules that introduce a mutation into the DNA: 1) single effector protein, Cas9, that acts as a pair of ‘molecular scissors’ that can cut the two strands of DNA at a target location in the genome; 2) guide RNA (gRNA), which consists of a small pre-designed RNA sequence (about 20-nucleotide) located within a gRNA scaffold (Giuliano *et al*., 2019). Site-specific cleavage occurs at locations determined by both base-pairing complementarity between the crRNA and the target protospacer DNA and a short motif [referred to as the protospacer adjacent motif (PAM)] juxtaposed to the complementary region in the target DNA (Jinek *et al*., 2012).

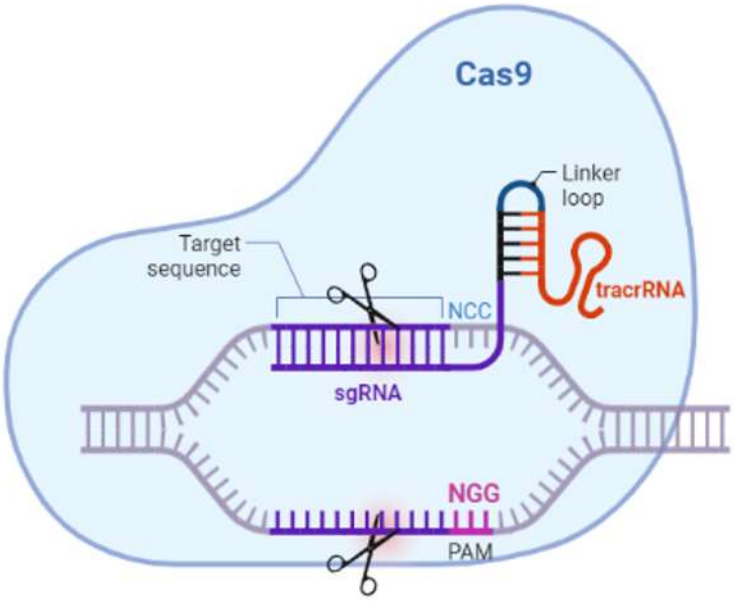

Figure II.9 - Schematic outline of Cas9-gRNA-mediated genomic targeting.
gRNA guides Cas9 to the target genome region to induce a blunt DSB 3-bp upstream of the PAM sequence. In Streptococcus pyogenes, NGG is PAM sequence, where "N" can be any of nucleotide bases.

The gRNA is designed to find and bind to a genomic target. The gRNA has nucleotides that are complementary to those of the target DNA sequence in the genome. On the side of Cas9 and gRNA, one more molecular component is required for the cleavage reaction. Critically, Cas9 requires a 3-nucleotide Protospacer adjacent motif (PAM) (NGG) on the non-complementary DNA strand proximal to the cleavage site. This PAM serves as an anchor for Cas9 to initialise contact with the target nucleic acid and allows it to discriminate between self versus non-self DNA. Following PAM contact and DNA melting, the complementary strand base pairs with the gRNA, resulting in cleavage of both strands. At this stage, the cell recognises DNA damage and tries to repair it (Yang *et al*., 2014).

One of the approaches available via CRISPR is to generate CRISPR-modified clones derived from single cells, which allows the construction of cell lines in which every individual cell harbours the same set of total loss-of-function (or null) mutations in a gene of interest. Moreover, challenging a cell line to repopulate itself from a single progenitor cell represents a significant genetic bottleneck and may also select specific genetic alterations. It is essential to be aware of these potential genetic compensatory mutations, especially when knocking out an essential protein (Giuliano *et al*., 2019).

2.10.3. Conditional knockout

The CRISPR/Cas system gene-editing has revolutionised the generation of gene knockouts in human cells (Cong *et al*., 2013; Mali *et al*., 2013). However, some genes are essential for cellular viability, and a big part of them is essential for proliferation (Wang *et al*., 2015). Since these genes cannot be perturbed constitutively, conditional knockout or depletion of encoding proteins is helpful for functional analysis (Giuliano *et al*., 2019). Recently, conditional approaches using a degron have been drawing increased attention. A degron-fused protein can be rapidly and efficiently degraded when needed. The primary defect arising from the depletion can be observed before the phenotype is complicated or compromised by the secondary defects (Natsume *et al*., 2016).

Recently, a highly efficient method for inducible protein degradation has been developed. This approach relies on the evolutionarily conserved Skp1–Cul1–F-box (SCF) degradation pathway and uses additional target-specific components derived from plants. In plants, the hormone auxin (AUX) mediates the interaction of the protein transport inhibitor response 1 protein (TIR1) with the auxin / indole-3-acetic-acid (AUX/IAA) family of transcriptional repressors, leading to AUX/IAA degradation. TIR1 is a part of the E3 ubiquitin ligase SCF-TIR1 that recruits an E2 ubiquitin-conjugating enzyme. Together, they polyubiquitinate and target AUX/IAA proteins via a specific amino acid degron sequence for proteasome-dependent degradation (figure I.23). TIR1 from *Oryza sativa* (OsTIR1) is used for a more efficient process and is fused with a mini-Auxin-inducible-degron (mAID), with 7 kDa of molecular weight and protein of interest. In the presence of auxin, proteasomal degradation of the mAID-tagged protein has a place. The depletion of the degron-tagged protein is rapid and efficient, such that within 30 to 60 minutes, the protein of interest is depleted to <10% that of wild-type levels. The AID system is reversible and tuneable (Giuliano *et al*., 2019; Natsume *et al*., 2016).

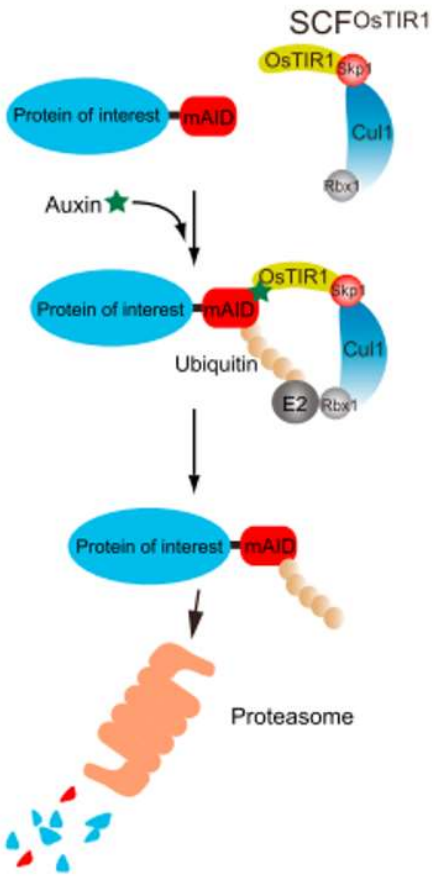

Figure II.10 – Depletion of protein by the auxin-inducible degron (AID) system.

The protein of interest is fused to an AID tag in human cells that express the TIR1 protein. The addition of auxin promotes the interaction between TIR1-containing Skp1-Cul1-F-box E3 ubiquitin ligase, which recruits E2 ubiquitin-conjugating enzyme. Together they polyubiquitinate (poly Ub) the AID tag, thereby targeting the AID-tagged protein for degradation by the proteasome (Natsume *et al*., 2016).

CHAPTER III

RESULTS

3. Results

3.1. Lack of MOB4 causes mitotic defects

Recently, some areas of biology have been changed. RNA molecular biology is one of them, with the discovery of small (20-30 nucleotide) non-coding RNAs that regulate genes and genomes, RNA interference (RNAi), the biological mechanism by which double-stranded RNA (dsRNA) causes gene silencing by targeting complementary mRNA for degradation. RNAi's first step involves processing and cleaving longer double-stranded RNA into siRNAs, generally bearing a 2-nucleotide overhang on the 3' end of each strand. The enzyme responsible for this processing is an RNase III-like enzyme termed Dicer. When formed, siRNAs are bound by a multiprotein component complex called RISC (RNA-induced silencing complex). Within the RISC complex, siRNA strands are separated, and the strand with the more stable 5'-end is typically combined into the active RISC complex. The antisense single-stranded siRNA component then guides and aligns the RISC complex on the target mRNA. Through the action of catalytic RISC protein, a member of the argonaut family (Ago2), mRNA is cleaved (figure III.1), eliminating the protein expression (Dana *et al*., 2017).

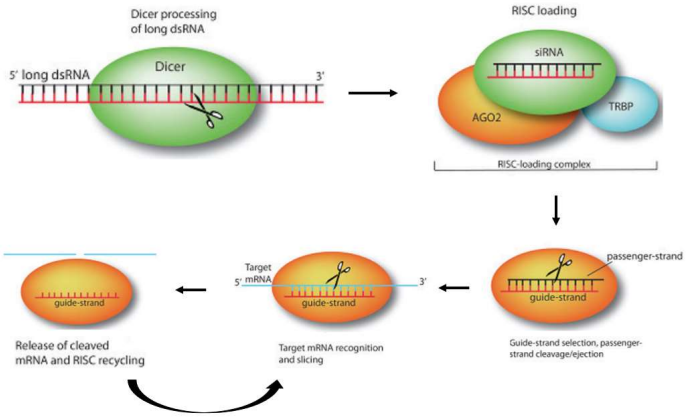

Figure III.1 – siRNA mediated silencing of target genes by guiding sequence-dependent slicing of their target mRNAs.

After entry into the cytoplasm, siRNA is loaded onto RISC directly or utilise a Dicer mediated process. After RISC loading, the passenger strand departs, initiating the RNA interference process via target mRNA cleavage and degradation (adapted from Dana *et al*., 2017).

Preliminary results from our laboratory indicate that MOB4 is an essential gene required for metaphase-to-anaphase transition. Depletion of MOB4 causes multiple mitotic defects in HeLa cells (multipolar spindle, mitotic spindle collapse, chromosome misalignment) and, consequently, mitotic bock. (Florindo, unpublished).

The project's first objective was to continue our work in MOB4, study the loss of function of MOB4 in HeLa cells. To continue the study, I performed RNAi assays of MOB4. I used HeLa cells expressing mCherry-Histone H2B and EGFP-Alpha Tubulin for RNAi protocol and transfected them with Oligo19 (Oli19), complementary to a specific region of mRNA of MOB4. The Oli19 was used previously in our laboratory. It was allowed to the mechanism of RNAi act on cells for 96 hours, after which, cells were fixed and analysed by fluorescent microscopy. MOB4 RNAi leads to several mitotic defects in HeLa cells (figure III.2).

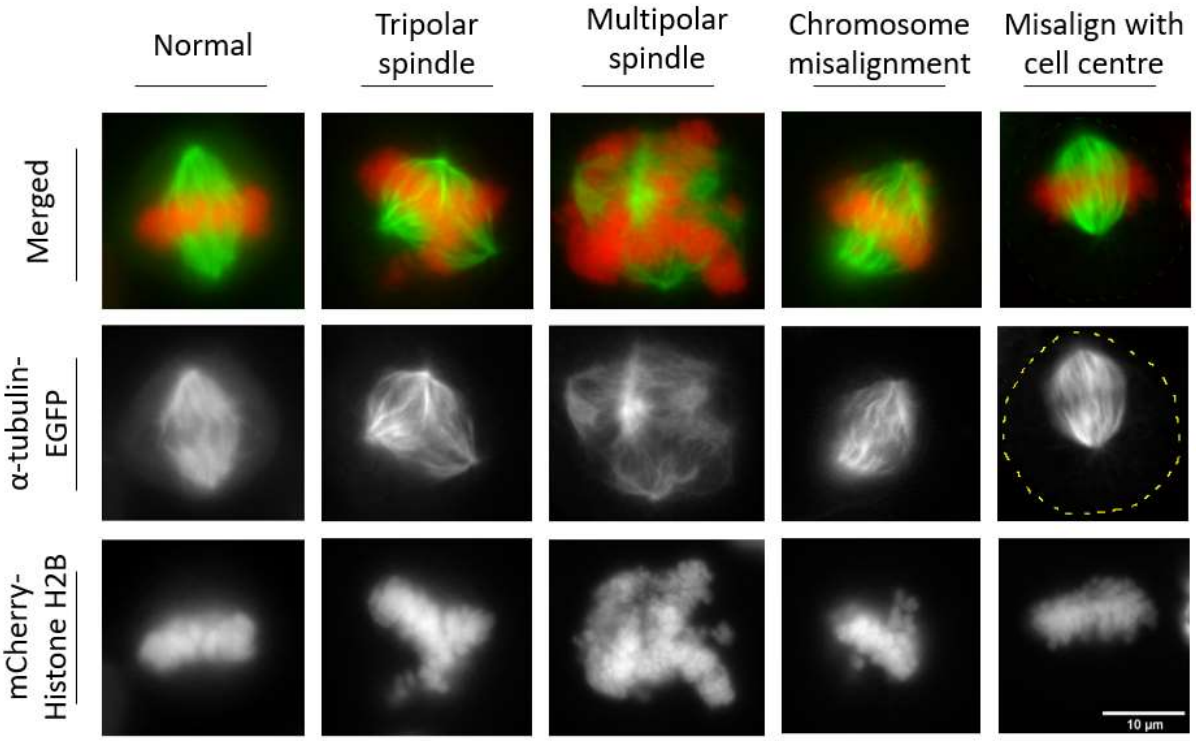

Figure III.2 - Representative images of transfected HeLa cells constitutively expressing EGFP-α-tubulin and mCherry-Histone H2B.

Each set of images represent different mitotic cells, which were considered normal or abnormal and in what way. Yellow dashed line shows cell size in 'Misalign with cell centre'. Images acquired on Microscope Zeiss Axio Imager 2, lens 100x.

3.2. Microtubule stability in HeLa cells expressing mCherry-Histone H2B EGFP-Alpha tubulin

The mitotic defects observed in cells depleted of MOB4 (Florindo, unpublished) are similar to defects observed in cells with kinetochore malfunction (Zhou *et al*., 2002; Vigneron *et al*., 2004). This phenotype can result from two possible scenarios: the kinetochore-microtubule attachment is not stable, or the microtubules cannot attach to the kinetochores at all. We hypothesise that MOB4 could be required for proper kinetochore-microtubule attachment. The cold assay was used to characterise the microtubule dynamics in mitotic cells. Cold treatment can prompt microtubule depolymerisation depending on cell type and subpopulations of microtubules inside a given cell type. Some examples of cold-stable subpopulations of microtubules in mammals have been found in epithelia, flagella (centrioles), axons, and mitotic spindles (Bane *et al.*, 2002). Unstable spindle microtubules disassemble when exposed to cold temperatures (Brinkley & Cartwright, 1975; Rieder, 1981). If MOB4 affects kinetochore-microtubule attachment, then spindle microtubule depolymerisation should be faster and following recovery should be slower in cells downregulated of MOB4.

HeLa cells expressing mCherry-Histone H2B EGFP-Alpha Tubulin were used to perform an assay. Since HeLa cells do not possess cold-stable microtubules, all microtubules are depolymerised at 4ºC. A time point for complete disassembly needed to be determined. After, cells were allowed to recover different time points at 37ºC before being fixed, and the extent of recovery was quantified.

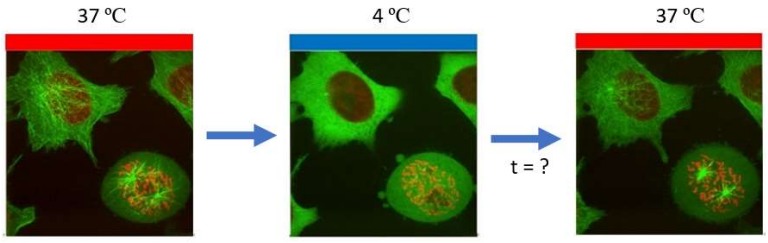

Figure III.3 – Images of the microtubule dynamics in interphase and mitotic cell at 37ºC and 4ºC.

Regular microtubule network in interphase and mitotic cell at 37ºC (left), disassembled tubulin throughout the cytoplasm (middle) after incubation at 4ºC, and microtubule nucleation when cells are placed at 37ºC. A question to be answered is what time is necessary to start repolymerisation of microtubules after complete disassembly at 4ºC (adapted from www.cherrybiotech.com).

A left panel of figure III.3 represents the microscopy images of extended microtubules in interphase cells and spindle formation in a mitotic cell at 37ºC. The middle panel shows labelled tubulin in the cytoplasm after complete depolymerisation at 4ºC and microtubule nucleation de novo when cells are placed at 37ºC. This experiment aims to determine a regular pattern for microtubule dynamics in HeLa cells and compare them to the values in cells downregulated of MOB4 protein.

3.2.1. Microtubule recovery is extremely fast

To determine the time necessary for microtubule depolymerisation, cells were placed on ice, and the medium was changed to the one at 4ºC. At a steady-state, the dense microtubule network obscures microtubule nucleation events at centrosomes (figure III.4E) and spindle poles (figure III.4G). Upon ice treatment, the entire microtubule network undergoes depolymerisation. No microtubules in interphase cells could be observed after 30 minutes of ice exposure (figure III.4F) and 35 minutes for mitotic cells (figure III.4H).

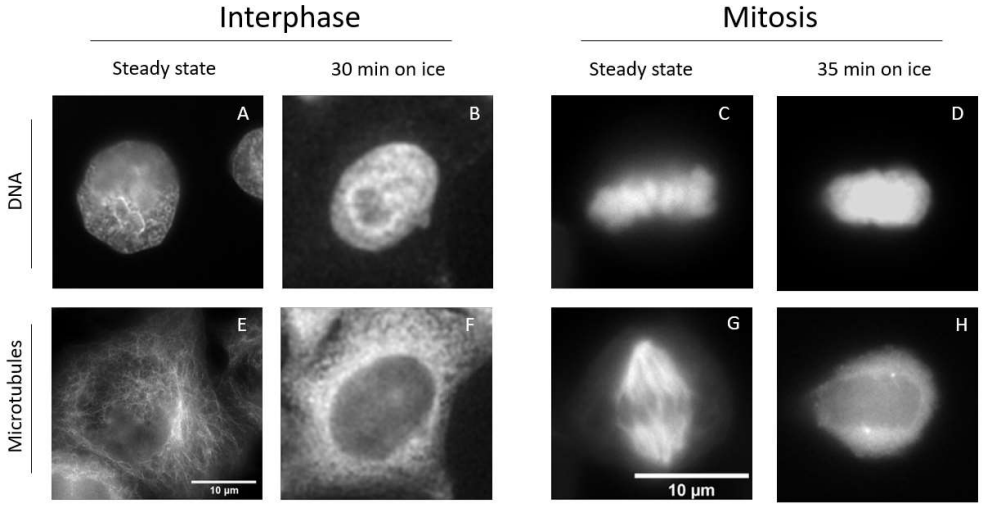

Figure III.4 - Estimated microtubule depolymerisation (EGFP-Alpha Tubulin) by determining a Visual Array Index in HeLa cells expressing mCherry-Histone H2B EGFP-Alpha Tubulin.

A, B, E, F – interphase cells; **C, D, G, H** – mitotic cells. **F** – at 30 min, complete depolymerisation is visible in interphase, **H** – after 35 min on ice, only the centrosomes were visible in mitotic cells. Images acquired on Microscope Zeiss Axio Imager 2, lens 100x.

During the protocol's realisation, gradual depolymerisation was observed, and relative quantification is represented in figure III.5.

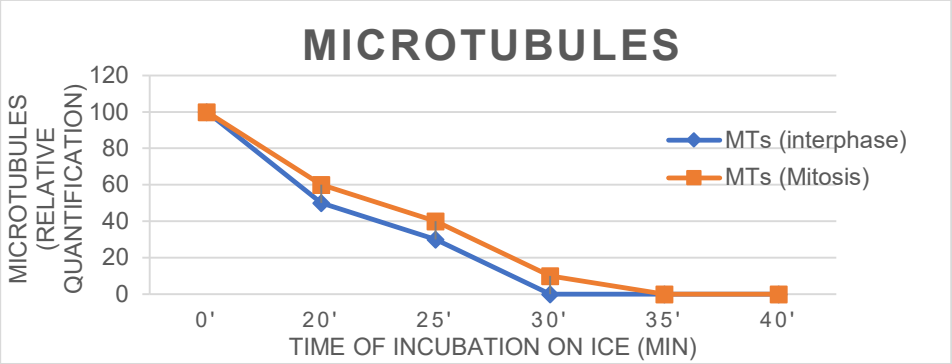

Figure III.5 - Relative quantification of microtubules at different time points during cold treatment.

100 is for intact microtubules, and zero is for complete depolymerisation. Full depolymerisation was reached at 30 minutes in interphase cells and 35 minutes in mitotic cells.

For recovery, cells were placed at 37ºC, and the cold medium was changed to the new at 37ºC. Different time points were used to establish the repolymerization point. After 2 minutes (minor time point could not be efforted) at 37ºC was possible to visualise microtubules (figure III.6C, D). From these results, I could conclude that microtubule repolymerisation is extremely fast.

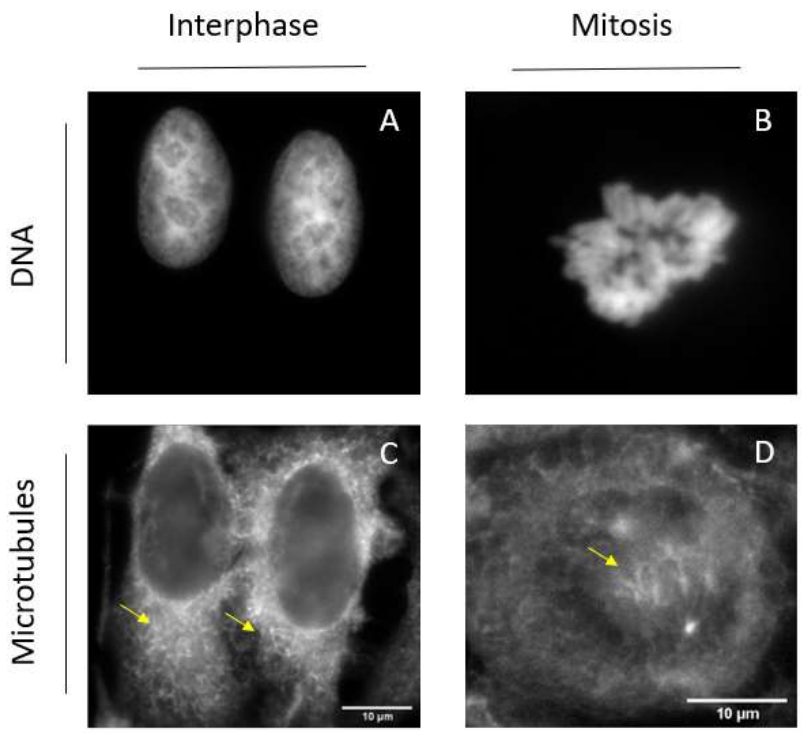

Figure III.6 - Detection of microtubules using the recovery assay in HeLa cells.
A, B – mCherry-H2B Histone; **C** - Interphase and **D** – mitotic microtubules (EGFP-Alpha Tubulin) after 2 min at 37ºC. The yellow arrow indicates nucleated microtubules. Images acquired on Microscope Zeiss Axio Imager 2, lens 100x.

3.2.2. Cold and nocodazole assay for microtubule depolymerisation / recovery

Antimitotic agents can cause cell arrest in mitosis. Nocodazole is an antimitotic agent already used in clinical practice that interferes with the dynamics of microtubules, culminating in stopping the cell cycle in mitosis (Jordan *et al*., 1992). The amount of microtubules that remains after cold and nocodazole treatment is an indirect readout for microtubule turnover since not stable microtubules are rapidly depolymerised. At the same time, stable microtubules (k-fibres) persist (Gayek & Ohi, 2014).

In my experiment, I placed cells on ice and added a new cold medium, which contained 1uM nocodazole. The addition of nocodazole will allow the delaying of the microtubules repolymerisation. By using these conditions new time for depolymerisation was established. A cold medium with nocodazole and 45 minutes of cold exposure were necessary to make microtubules disappear. For repolymerisation, cells were placed at 37ºC and quickly rinsed three times with a new medium at 37ºC. This delay allowed us to observe that

repolymerisation starts at 9 minutes in interphase cells (figure III.7F) and 7 minutes in mitotic cells (figure III.8F).

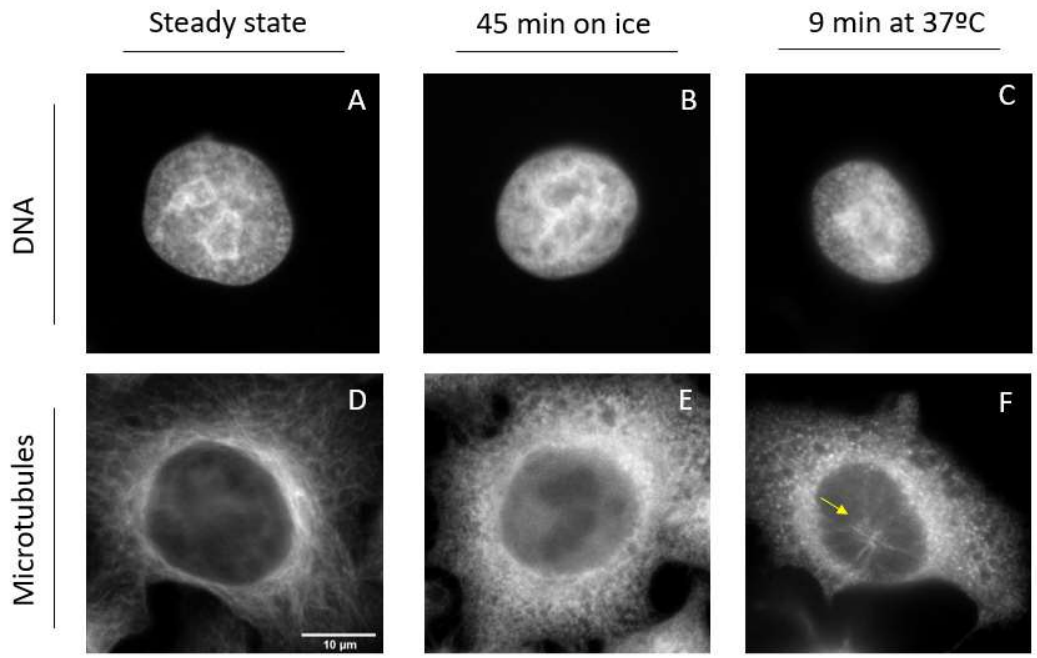

Figure III.7 - Estimated microtubule recovery in interphase Hela cells.
A, B, C – mCherry-H2B Histone; **D, E, F** - EGFP-Alpha Tubulin. **D** – Large population of long microtubules throughout the cell; **E** - No intact microtubules are observed, a random distribution of labelled complexes throughout the cell; **F** - Cell has small asters with few, short microtubules (yellow arrow). Images acquired on Microscope Zeiss Axio Imager 2, lens 100x.

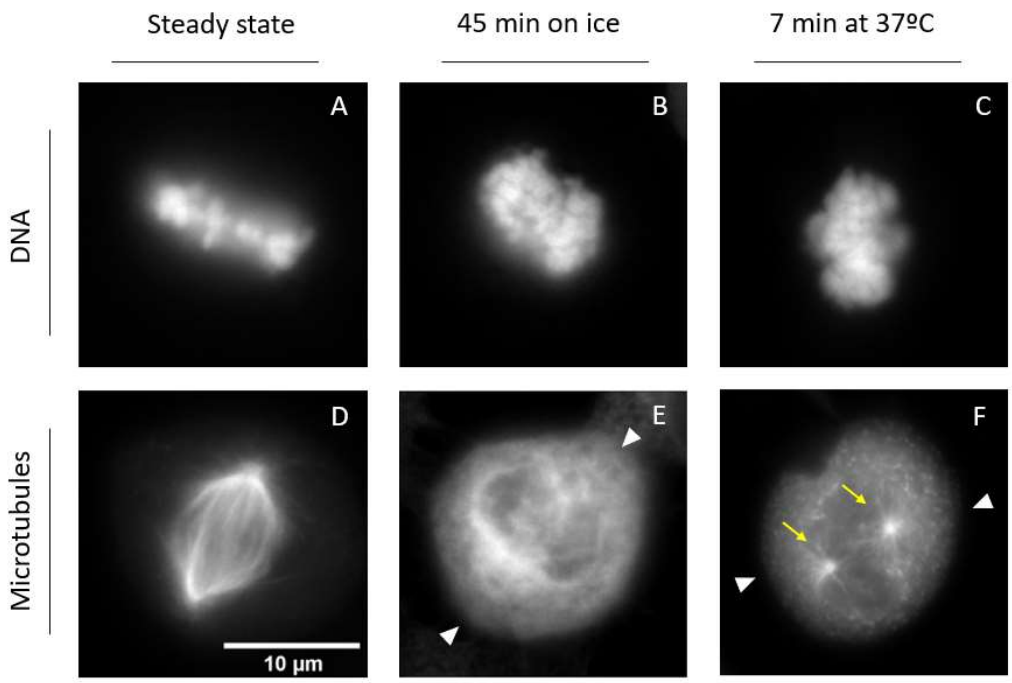

Figure III.8 - Estimated microtubule recovery in mitotic HeLa cells.

A, B, C – mCherry-H2B Histone; **D, E, F** - EGFP-Alpha Tubulin. **D** - standard mitotic spindle morphology; **E** – microtubules are depolymerised; white arrowheads point to possible spindle orientation; **F** - few short microtubules start to repolymerise from two spindle poles (yellow arrows), white arrowheads point possible spindle orientation. Images acquired on Microscope Zeiss Axio Imager 2, lens 100x.

The next step should be transfecting the cells with RNAi of MOB4 and determining if the microtubule dynamics is affected in MOB4 depleted cells.

3.3. Does MOB4 localisation in mitotic CRAL1 cells is dependent on microtubules?

Previous data in our laboratory demonstrated that MOB4 is localised to the centrosomes, microtubules, and kinetochores in mitotic HeLa cells (Florindo & Tavares, unpublished). We wanted to understand if MOB4 mitotic localisation is altered in the absence of microtubules. Since Álvaro Tavares and Inês Santos have generated HCT116 cells stably expressing MOB4 protein tagged to GFP (CRAL1 cells), it is possible to analyse MOB4 localisation without additional immunofluorescence protocol.

The mitotic index is the fraction of mitotic cells in a whole population of cells. The high index of proliferation can reach 10 per cent in some types of cells or can be around 0,1 per cent in low proliferating populations, such as thyroid, liver, or kidney epithelium (Hendry & Scott, 1987). The frequency of cells in mitosis is relatively low, even in a highly proliferating cell population. Nocodazole incubation results in microtubule depolymerisation, misaligned chromosomes, and mitotic arrest due to incapacity to satisfy the SAC, significantly increasing a mitotic index (Teusel *et al*., 2018). I aimed to increase the number of mitotic cells with nocodazole and analyse MOB4 behaviour in cells with no microtubules.

The treatment was performed following the protocol established by Claudia Florindo, 12 hours incubation with 60 ng/ml nocodazole. As a negative control, untreated cells were used, and for solvent control, the vehicle, DMSO, was added to cells.

Coverslips were treated with Poly-D-Lysine to facilitate cell adhesion to tissue culture dishes. I observed that interphase cells acquired rectangular shapes and grew in small groups (figure III.9).

In my experiment conditions, Poly-D-Lysine resulted in a limitation or inhibition of adhesion and the creation of stress fibres. These results suggest that normal cell behaviour was disrupted. Additionally, the mitotic index was not increased.

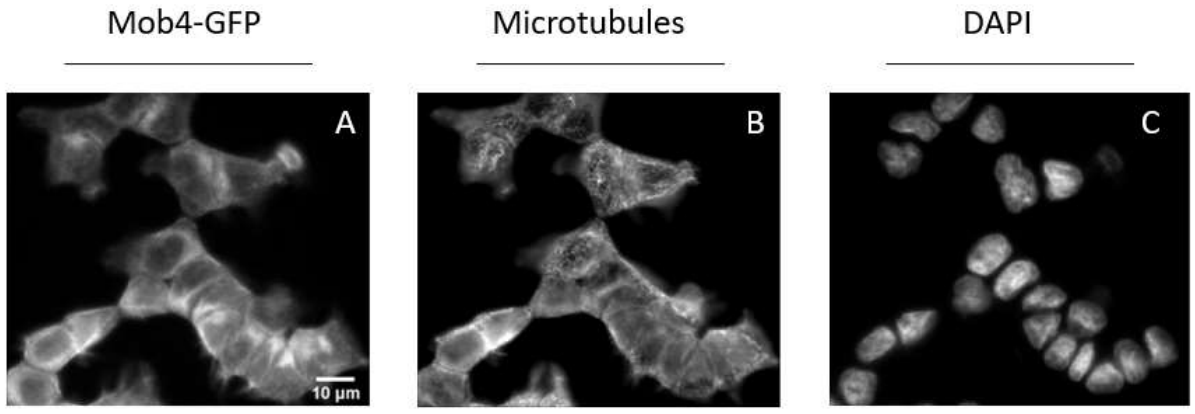

Figure III.9 – Representative images of CRAL1 cells on Poly-D-Lysine treated coverslips.

A – MOB4-GFP, **B** – microtubules, stained with DM1α (antibody against α-tubulin, 1:200) to label tubulin, washed and incubated with secondary antibody linked to Alexa Fluor594 (1:1000), **C** - washed and stained for DNA with 0,1 ug/ml DAPI. Images acquired on Microscope Zeiss Axio Imager 2, lens 40x.

To overpass this problem, I incubated cells with 150 ng/ml nocodazole for 2 hours to depolymerise microtubules and analysed mitotic cells. Non-treated cells were used as a control (figure III.10).

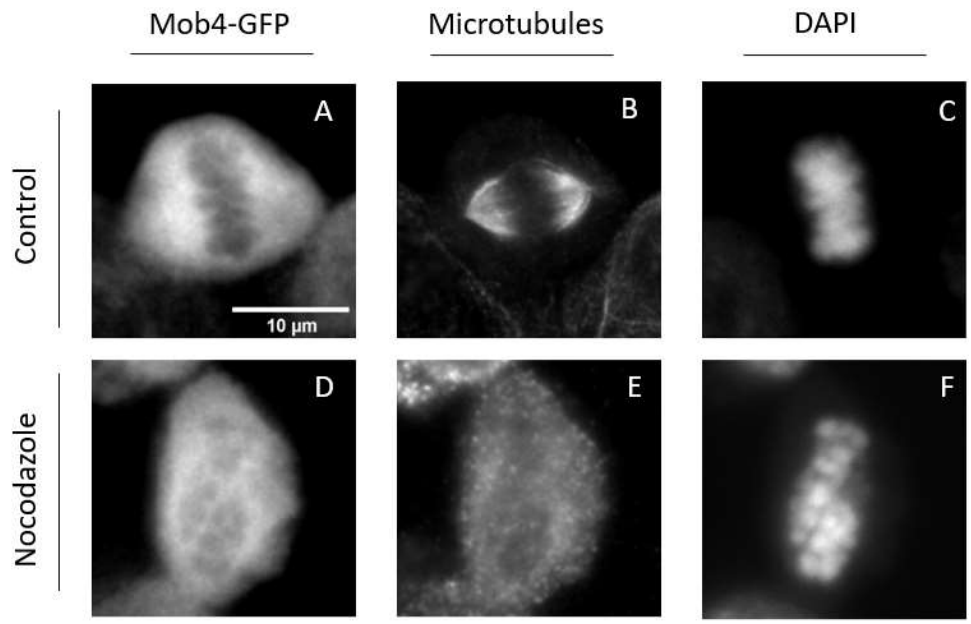

Figure III.10 - Representative images of CRAL1 cells.
B - standard mitotic spindle in non-treated cells (Control); **E** - cell treated with 150 ng/ml Nocodazole for 2 hours with depolymerised microtubules. **A, D** – MOB4-GFP; **B, E** – microtubules stained with DM1α (antibody against α-tubulin, 1:200) to label tubulin, washed and incubated with secondary antibody linked to Alexa Fluor594 (1:1000), **C, F** – staining for DNA with 0,1 ug/ml DAPI. Images acquired on Microscope Zeiss Axio Imager 2, lens 100x.

Mitotic cells were analysed in control (n=20) and nocodazole treatment (n=22). A specific MOB4-GFP localisation that suggests corresponding to one of the centrosomes was observed in both groups (III.1). A number of cells with MOB4-GFP specific localisation was similar with and without microtubules.

Table III.1 - MOB4-GFP localisation at centrosomes in treated and non-treated mitotic cells.

MOB4-GFP specific localisation	Control	Nocodazole treated	Total Number of cells
Yes	6	14	20
No	5	17	22

These results suggest that, in my experiment conditions, MOB4-GFP localisation at centrosomes is not altered with depolymerised microtubules.

3.4. MG132 treatment results in the accumulation of MOB4-GFP in the nucleus periphery in interphase CRAL1 cells

MOB4 might be required for proper kinetochore-microtubule attachment and can be localised at kinetochores in mitotic cells. Mitotic cells compose a low percentage of the entire cell population, and metaphases are a small fraction of all mitotic cells. To obtain more cells blocked at metaphase and analyse MOB4 localisation, I wanted to treat cells with nocodazole, release, and add MG132.

MG132 (carbobenzoxy-Leu-Leu-leucinal) is a peptide aldehyde, a low-molecular-weight proteasome inhibitor, with selective inhibition of this degradative pathway. The ubiquitin-proteasome pathway degrades most proteins in mammalian cells (Lee & Goldberg, 1998). The Anaphase-Promoting Complex/ Cyclosome (APC/C), a multisubunit E3 ubiquitin ligase, promotes anaphase inception by marking securin (Nasmyth *et al*., 2000) and Cyclin B1 (Hagting *et al*., 2002) for degradation by the proteasome (Maiato & Schuh, 2018).

To establish a safe drug concentration for prolonged incubation with MG132, I tested different concentrations, 10-100 uM. The safe concentration was 10 uM. I started with 2 hours for incubation time and mitotic index was similar to non-treated cells. After, I increased the incubation time for 6 hours. The mitotic index observed was 5-6% in MG132 cells and 2-3% in non-treated cells. I repeated the experiment, n=3, and the mitotic index had similar values, 5-6%.

Microscopy analysis of treated and non-treated cells suggests that, in my experiment conditions, MOB4-GFP is not localised at kinetochores. It was possible to observe aggregates of MOB4-GFP protein on the nucleus periphery in interphase cells incubated for 6 hours with 10 uM MG132 (figure III.11C). According to previous data from our laboratory, MOB4-GFP accumulates at the nucleus periphery during G2. This localisation corresponds to Golgi Complex (Santos & Tavares, unpublished).

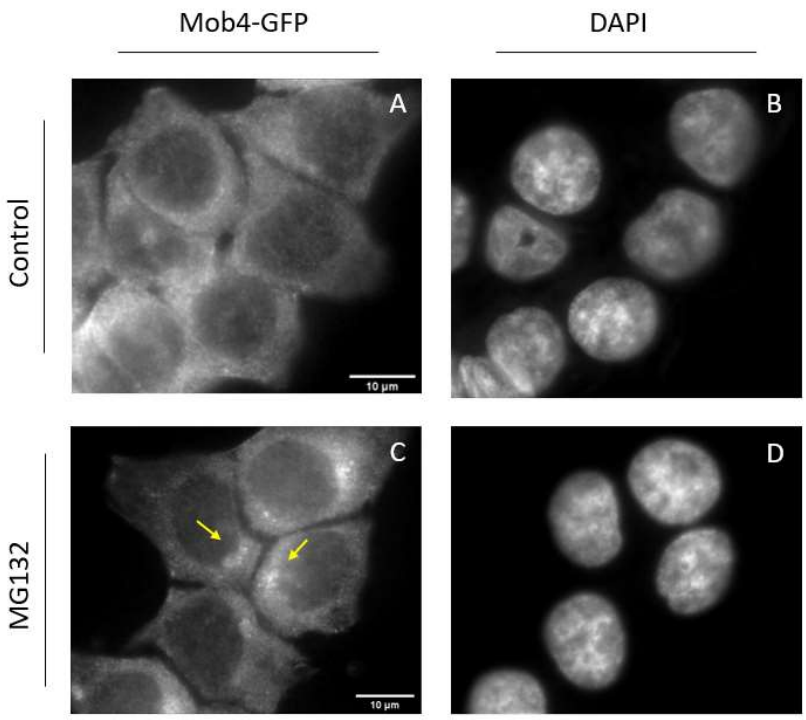

Figure III.11 - CRAL1 cells were incubated with a proteasome inhibitor.
A, B - control; **C, D** - 10 uM MG132 treatment for 6 hours, specific accumulations of MOB4-GFP are pointed with yellow arrows. Images acquired on Microscope Zeiss Axio Imager 2, lens 100x.

Quantitative analysis of interphase cells indicates that more cells with MOB4-GFP aggregates were observed in cells incubated with MG132 (200/500) compared to non-treated cells (25/500).

These results gave place for some new questions: 1) Do these accumulations depend on microtubules? 2) Does MOB4 cell concentration vary during the cell cycle progression?

3.5. Accumulation of MOB4-GFP in interphase is not dependent of microtubules

Microtubules are essential, dynamic, and multitasking proteins that serve as structural elements in most eukaryotic cells. During interphase, microtubules enable directed movement of motor proteins on the microtubule surface, providing tracks for long-distance, motor-driven transport of vesicles and organelles (Gudimchuk & McIntosh, 2021). The STRIPAK complex, between other proteins, is associated with dynein, motor protein, which transports cargoes

along the microtubules towards the microtubule organising centre, the centrosome (Li *et al*., 2018).

MOB4, as a STRIPAK complex component, could interact or be transported by motor proteins, along the microtubules, to the Golgi Complex, where it can interact with striatin and SG2NA (Baillat *et al*., 2001). The presence of the striatins and STRIPs in the Golgi, the presence of SLMAP in the outer nuclear envelope, the association between SLMAP and centrosomes, and the copurification of MOB4 and PP2A with the complex are essential clues to one function of the STRIPAK complex in human cells (Wurzenberger & Gerlich, 2011). In mammals, striatin, MOB4 interactor, is connected to dynein (Goudreualt *et al*., 2009)

To identify if MOB4 aggregates at Golgi are dependent on microtubules, I used different conditions for CRAL1 cells in this experiment, incubation with MG132, in the presence or not of nocodazole (figure III.12). A 6-hour incubation with 10 uM of MG132 caused the accumulation of MOB4-GFP in the nucleus periphery in a significant number of interphase cells (figure III.12, D-F). Likewise, these accumulations are visible in MG132 treatment in the presence of nocodazole (figure III.12, G-I). A low number of cells with MOB4-GFP aggregates was observed in a 2-hour nocodazole incubation (figure III.12, J-L). The same was observed in cells incubated with MG132 for 2 hours.

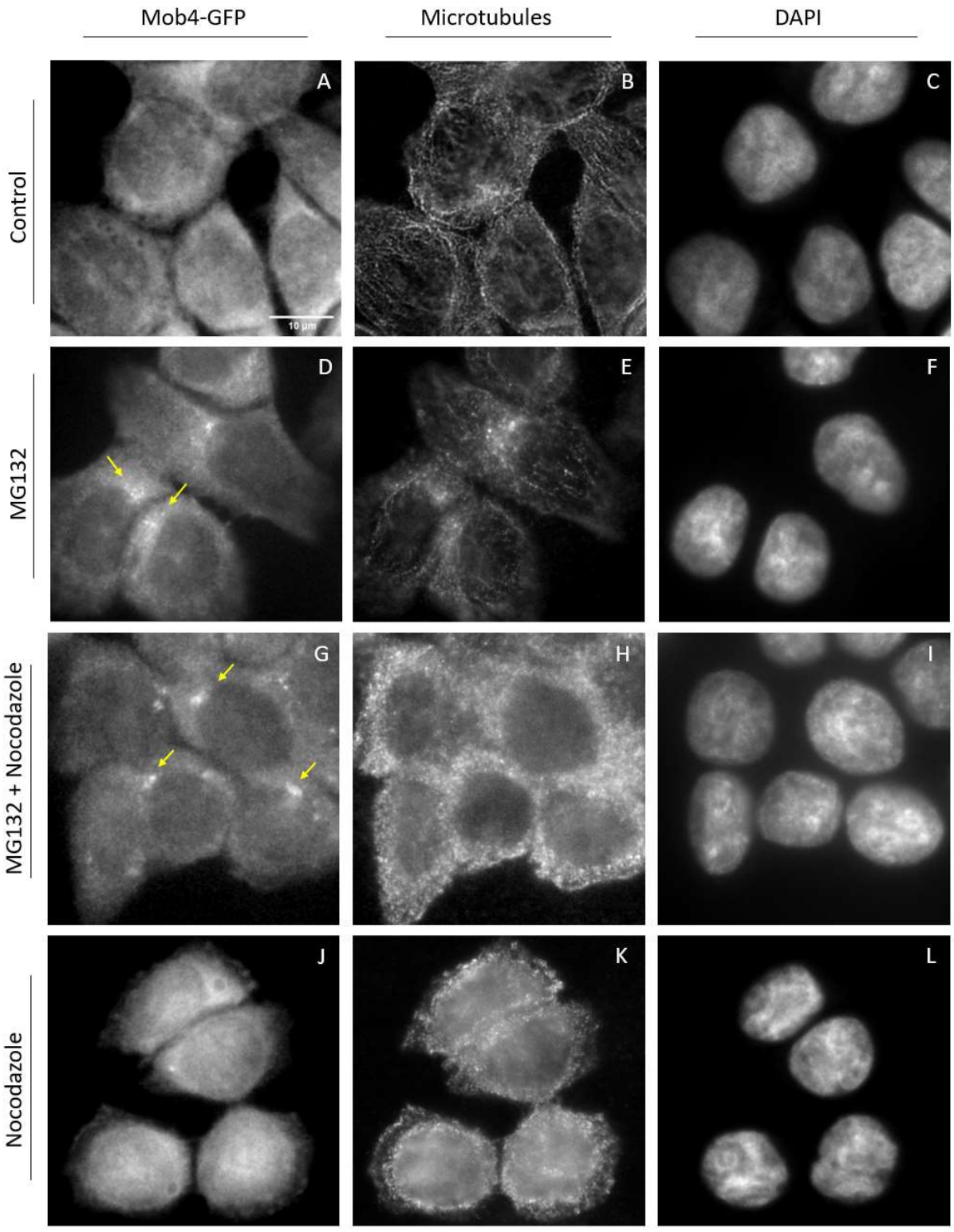

Figure III.12 - Representative images of CRAL1 cells.

A-C – Control, cells treated with drug vehicle, DMSO; **D-F** – 6-hour incubation with 10 uM MG132, yellow arrows point for MOB4 accumulation in the cytoplasm on nucleus periphery; **G-I** – 4-hour incubation with 10 uM MG132 and further 2-hour incubation with 150 ng/ml nocodazole and 10 uM MG132, yellow arrows point for MOB4 accumulation; **J-L** – 2-hours incubation with 150 ng/ml nocodazole, microtubules are depolymerised. Images acquired on Microscope Zeiss Axio Imager 2, lens 100x.

The quantitative analysis of treated cells confirms that increased cells with MOB4-GFP accumulations is visible in MG132 treatment and is similar in both cases, 42 and 41 %, without and with nocodazole, respectively (figure III.13). Nocodazole incubation for 2 hours resulted in 5% of cells with MOB4-GFP aggregates. Two-hour incubation with MG132 originated 5,5% of cells with MOB4-GFP aggregates.

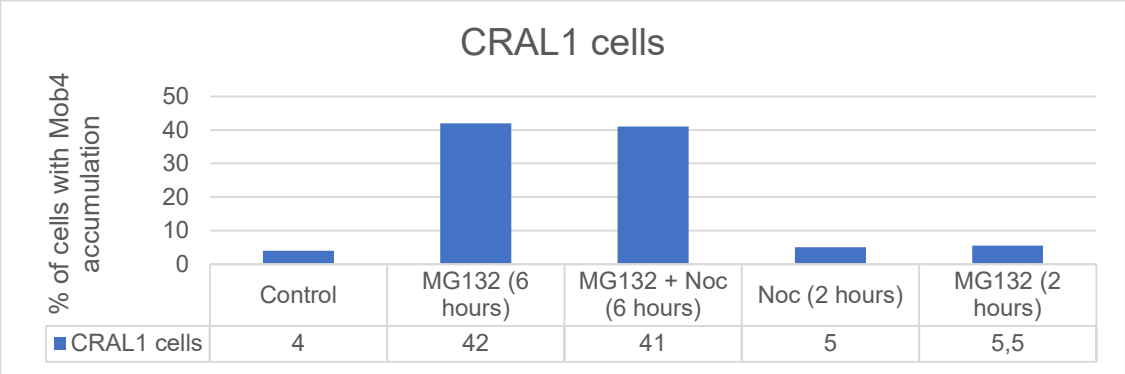

Figure III.13 - Quantitative analysis of cells with MOB4-GFP accumulation in interphase cells (n=500).

As a control, non-treated cells were used. MG132 is for 6-hour incubation with 10 uM MG132. MG132+Noc is for 4-hour incubation with 10 uM MG132 followed by a 2-hour incubation with 10 uM MG132 and 150 ng/ml nocodazole. Noc is for 2-hour incubation with 150 ng/ml nocodazole. MG132 is for 2-hour incubation with 10 uM MG132.

Together these results suggest that MOB4-GFP aggregates on the nucleus periphery are present in the absence of microtubules in interphase CRAL1 cells.

3.6. MOB4-GFP accumulates to the nucleus periphery in absence of microtubules

As shown previously, 6-hour incubation with MG132 originates accumulation of MOB4-GFP in the cytoplasm in interphase cells. When cells are treated with MG132 and nocodazole is added, these aggregates are also present. A question that comes up is: does MOB-GFP starts to accumulate if the microtubules are already depolymerised? To answer this question, I incubated cells with nocodazole, and added MG132.

The concentration of nocodazole I used for 2 hours was 150 ng/ml. For prolonged treatment, cells were incubated with 50 ng/ml nocodazole for 8 hours, and 10 uM MG132 was added for a further 6 hours. That resulted in 14 hours of nocodazole treatment in total.

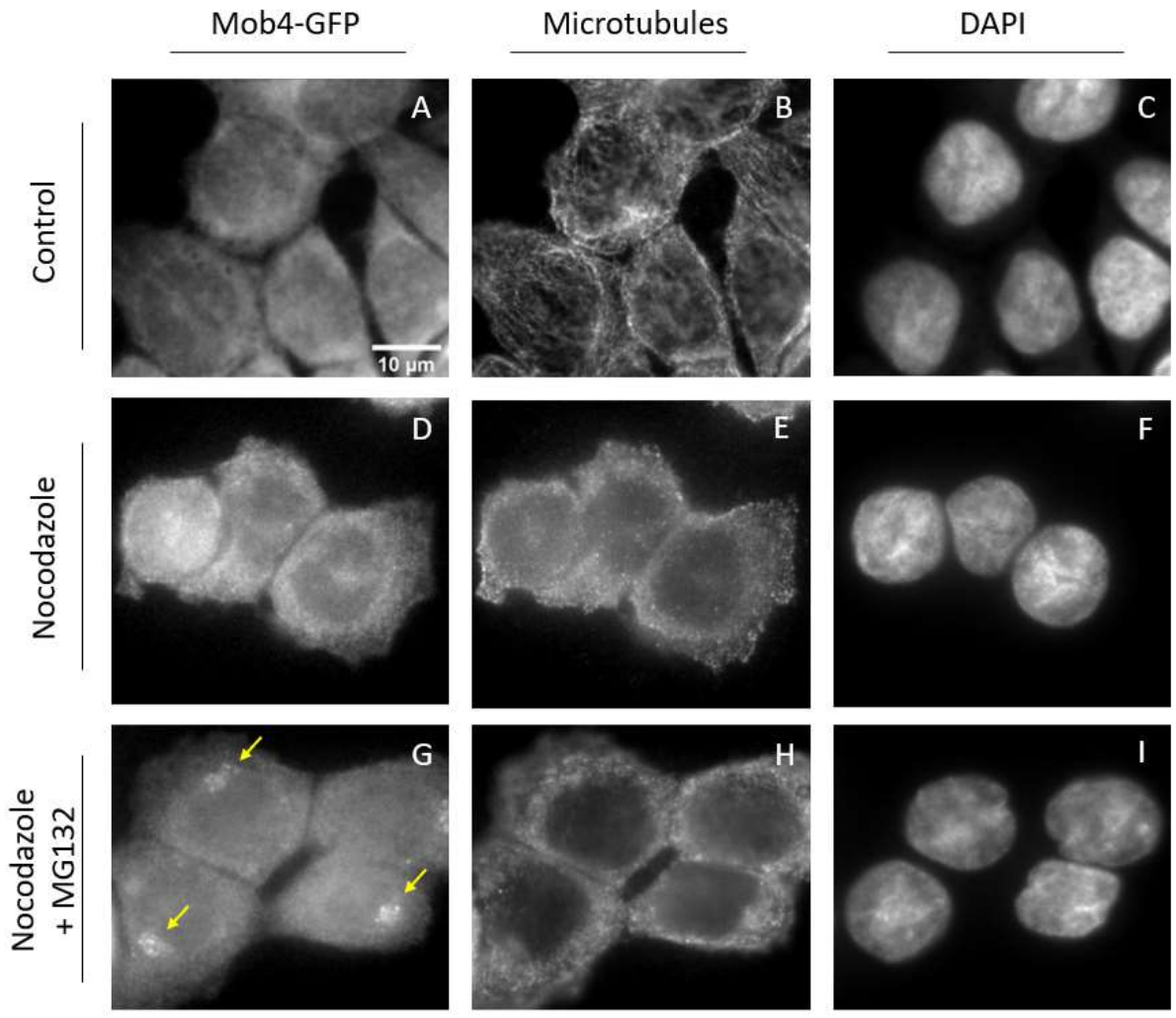

Figure III.14 - Representative images of CRAL1 cells.

A, D, G – MOB4-GFP, **B, E, H** – Alpha-tubulin incubated with DM1α antibody (1:200) and incubated with AlexaFluor594 (1:1000), **C, F, I** – DNA stained with 0,1 ug/ml DAPI. **A-C** – Control cells treated with vehicle drug, DMSO; **D–F** – 14-hour incubation with 50 ng/ml of nocodazole; **G–I** – 8-hour incubation with 50 ng/ml of nocodazole + 6-hour incubation with 50 ng/ml of nocodazole and 10 uM MG132. **G** – Yellow arrows point for aggregates of MOB4-GFP in the cytoplasm. Images acquired on Microscope Zeiss Axio Imager 2, lens 100x.

Microscope analyses indicate that, in the presence of nocodazole, MOB4-GFP aggregates were observable when MG132 was added (figure III.14G).

Quantitative analysis indicates that control and nocodazole incubation have similar numbers of interphase cells with MOB4-GFP, around 5%. Incubation with nocodazole and MG132 has a different pattern. Of 146 observed interphase cells, 99 had MOB4-GFP aggregates present in the cytoplasm, corresponding to 67% of total interphase cells. The value is 1.5-fold of MG132 treatment.

Of 99 cells with MOB4-GFP aggregates, five cells have more than one accumulation, precisely, two separate MOB4-GFP aggregates on the nucleus periphery (figure III.15A). Cells with two aggregates correspond to the 5% of a total number of cells with MOB4 accumulation.

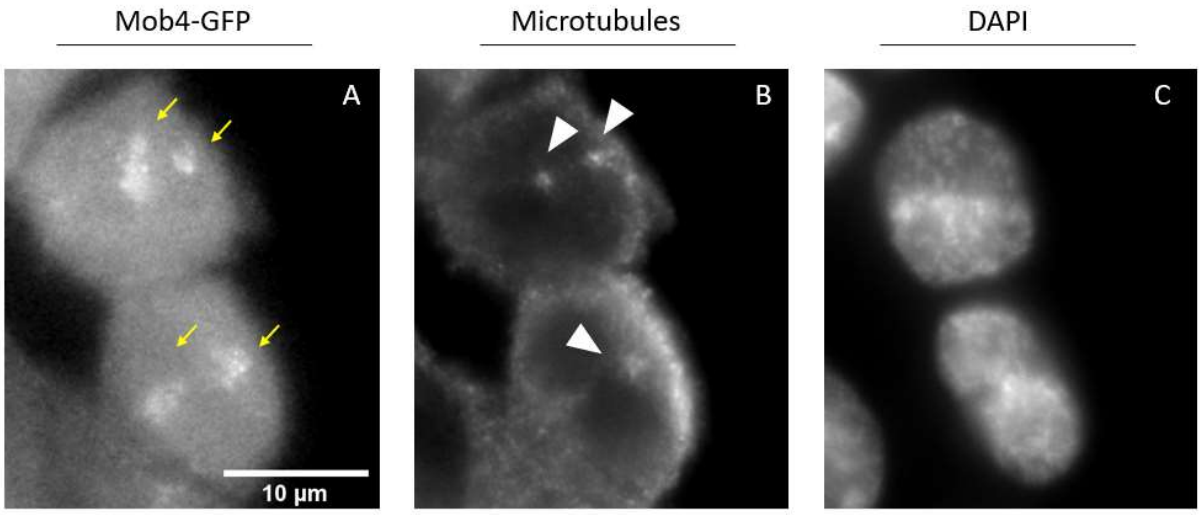

Figure III.15 - CRAL1 cells were treated for 8 hours with nocodazole + 6 hours with nocodazole and MG132.

A – MOB4-GFP, yellow arrows point for two separate aggregates of MOB4 in the interphase cell cytoplasm; **B** – Alpha-tubulin incubated with DM1α antibody (1:200) and incubated with AlexaFluor594 (1:1000), white arrowheads point for possible tubulin aggregates or centrosome; **C** – DNA stained with 0,1 ug/ml DAPI. Images acquired on Microscope Zeiss Axio Imager 2, lens 100x.

These data suggest that prolonged incubation with nocodazole followed by nocodazole and MG132 treatment results in MB4-GFP accumulation in the nucleus periphery. Additionally, a higher number of cells with accumulations were observed in the presence of two drugs.

3.7. MOB4-GFP concentration is stable throughout cell cycle

As mentioned previously, in our laboratory, we start to see the MOB4-GFP aggregates during G2, and its intensity increases closer to the mitosis (Santos, unpublished). We hypothesized that MOB4-GFP protein levels vary during the cell cycle.

To test this hypothesis, cells were incubated with Thymidine (S-phase block), followed by STLC (S-trityl-L-cysteine) incubation. As a negative control, non-treated cells were used (figure III.16). This experiment was performed simultaneously in CRAL1 and HeLa cells. The purpose of using two different cell lines is to understand if MOB4 behaviour is specific to colorectal cancer cells (HCT116) or can be general in human cancer cells.

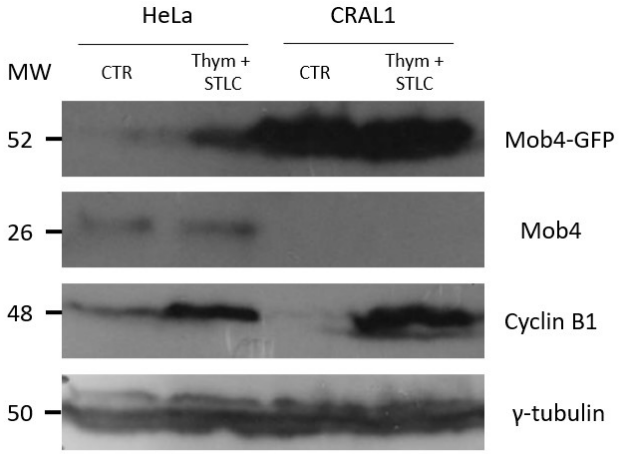

Figure III.16 - Western blot of lysates of HeLa and CRAL1 cells.
CTR is for non-treated cells; **Thym + STLC** is for 16 h Thymidine + 12 h STLC incubation; MW indicates the molecular weight of the proteins in kilodaltons (kDa). 10% gel was used for running the samples. Enhanced Chemiluminescence (ECL) Solution and X-Ray film were used for signal detection.

Cyclin B1 antibody was used as a control to the treatment; shallow levels of this protein are observed in non-treated cells. Higher levels of Cyclin B1 in drug treatment were observed. For loading control, γ-tubulin was used. Similar protein levels of MOB4-GFP were observed in both samples, mitotic block and non-treated. These results suggest that MOB4 protein levels are stable during the cell cycle.

3.8. CRISPR / Construction of conditional AID mutants

Our laboratory's preliminary data show that overexpression of MOB4 in human cells is lethal. A lack of MOB4 is lethal in *D. melanogaster* at the larvae stage. The application of RNAi technology in HeLa cells permitted identifying several mitotic defects that conduce to apoptosis after several hours of the mitotic block (Florindo, unpublished). Though, experiments performed with RNAi are limited in several aspects. First, RNAi exemplifies a partial loss-of-function perturbation of protein, as RNAi constructs decrease protein expression but cannot entirely eliminate the targeted gene. Secondly, it was previously shown that RNAi constructs are highly susceptible to off-target knockdowns that can confuse the characterisation of a gene of interest (Giuliano *et al*., 2019). Thirdly, it usually takes more than two days to downregulate a pre-existent protein within cells once the transcription is turned off (Nishimura *et al*., 2009).

The conditional depletion of a protein of interest is helpful for loss-of-function studies. It is advantageous in terms of specificity, reversibility, and time required for depletion, which can be achieved by fusing the protein of interest with a degron that induces rapid proteolysis of the fusion protein (Natsume *et al*., 2016). Since parental cell populations can have genetic, epigenetic, and phenotypic heterogeneity, it is essential to create several cell lines, to compare the experimental knock-in to the clonal "control" cell line derived in similar conditions (Giuliano *et al*., 2019).

The CRAL1 cell line was generated by introducing the auxin-inducible degron (AID) to induce the degradation of a target protein. Therefore, it was decided to generate more cell lines from the HCT116 cell line to confirm the previously observed results with the CRAL1 cells. An inducible expression system was introduced at the safe harbour AVSS1 locus of HCT116 cells (Natsume *et al*., 2016).

3.9. Nucleic acid amplification

Nucleic acid amplification is a pivotal process in biotechnology and molecular biology and has been widely used in research, medicine, agriculture and forensic. Polymerase chain reaction (PCR) was the first nucleic acid amplification method developed and has been the method of choice since its invention by Mullis. PCR is the preferred method for application-

oriented fields involving nucleic acid amplification for simplicity, more accessible methodology, and an extensively validated standard operating procedure (Fakruddin *et al*., 2013).

3.9.1. Polymerase chain reaction (PCR)

To identify the clonal cell line with the insertion, obtained through the application of CRISPR, the PCR was performed. The PCR method permits the analysis of the genomic region of interest. The CRISPR construct contains the mini auxin-inducible degron (mAID), the gene encodes for mCherry2 and the sequence for resistance to Neomycin, NeoR. Figure III.17 is the schematic representation of the hMOB4 gene with the insertion and the primers for amplification of 3 genomic regions. If the construct is not inserted, the external pair of primers, PriAL44 and PriAL47, amplify the DNA and the final product has approximately 1400 bp (band A). If the construct is inserted, two internal pairs of primers, PriAL44/22 and PriAL20/47, raise band B and C, respectively. The final product of bands B and C is around 1000 bp.

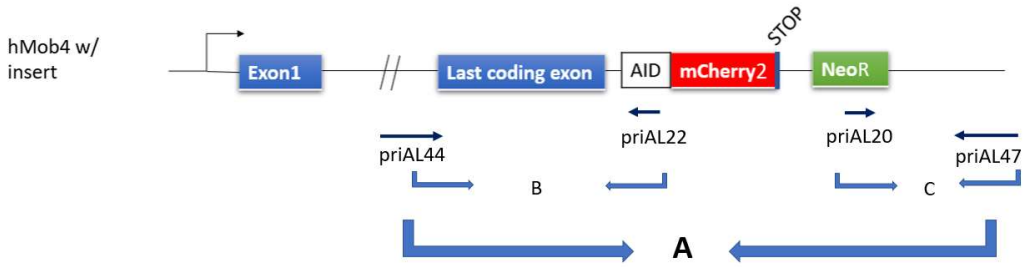

Figure III.17 - Schematic representation of place of construct insertion in hMOB4 and primer hybridisation.

Band **A** - when the insertion has no place, the forward primer, priAL44, and the reverse primer, priAL47, hybridise, and the band at ~1400 bp is present. In case of insertion of construct, pair of primers priAL44 (forward) and priAL22 (reverse) originate the band **B** (~1000 bp), and the pair of primers priAL20 (forward) and priAL47 (reverse) originate the band **C** (~1000 bp).

Due to the high number of samples and to accelerate the DNA screening process, the clones were screened for the external pair of primers (Band A). When the band is present, at least one of the alleles has not inserted the construct. Since we were looking for bi-allelic mutants,

only those that did not present the band at 1 400 bp were screened for three pairs of primers (band A, B, and C) to confirm the insertion. Inês Santos already established the protocol used for this experiment.

The schematic drawing of the predictable agarose gel results from the PCR screening of the clones is shown in figure III.18. One of the following results should be observed when each clone is screened with the three pairs of primers. Only band A was visible in a gel is the signal of no insertion in any of alleles (figure III.18-1), when the A, B, and C bands were visible, insertion in one of the alleles had a place (figure III.18-2); if bands B and C were observed, both alleles of the gene were targeted by the construct (figure III.18-3).

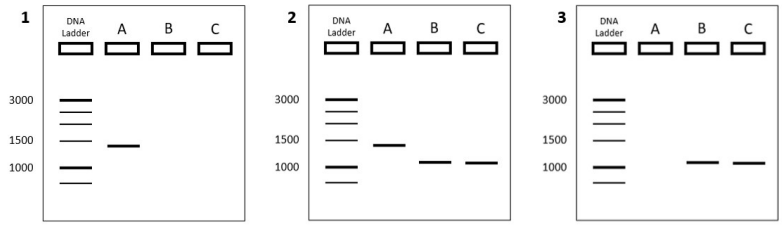

Figure III.18 – Illustration showing the predictable DNA bands separated on a gel.
1 - no insertion, only the band A is present; **2** - insertion in one allele, all three bands are present (A, B, and C); **3** – insertion in both alleles of a gene, two bands are present (B and C).

The PCR results obtained from the first two groups (12 and 14 samples) of isolated clones were screened for band A. The amplified fragment of HCT116 Tet OsTIR1 without insertion is 1400 bp (figure III.20 – '+'). When the construct is inserted into the gene, the final product is not shown because the Thermal Cycler was programmed. The elongation period was not long enough to allow amplification of this product.

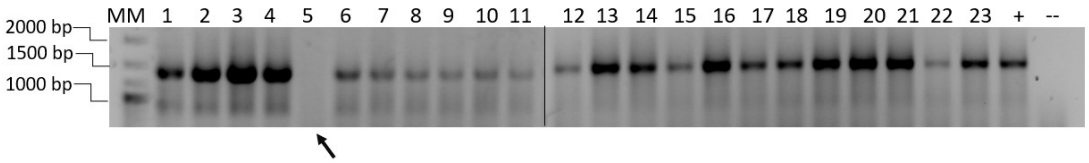

Figure III.19 - PCR product in 0,8 % (w/v) agarose gel stained with SafeRed™ of isolated clones, using the primers PriAL44 and PriAL47.
MM - Molecular marker 1 kb DNA Ladder. Lanes **1-23** represent DNA from the isolated clones; '+' is for the positive control (HCT116 Tet OsTIR1); '**-**' is for the negative control, no template in reaction. The arrow points for the Clone Nº 5, which has no product at 1400 bp.

The results from these PCR reactions show that all the clones, except the clone nº 5, have a band at 1400 bp, which means that the construct was not inserted (figure III.19). The clone nº 5 did not show the band at 1 400 bp, suggesting a biallelic clone. The PCR protocol was repeated for this clone with 3 pairs of primers.

The following PRC reaction included 3 pairs of primers (Band A, B, and C) for clone nº 5 and the external pair of primers (Band A) for other clones to be tested failed. The gel presented several faint bands (*e. g.*, lanes 27, 30, 32, 33), as well as some samples failed the amplification (*e. g.*, lanes 26, 29, 31) with the unused primer on the bottom, and the positive control failed ('+') (figure III.20).

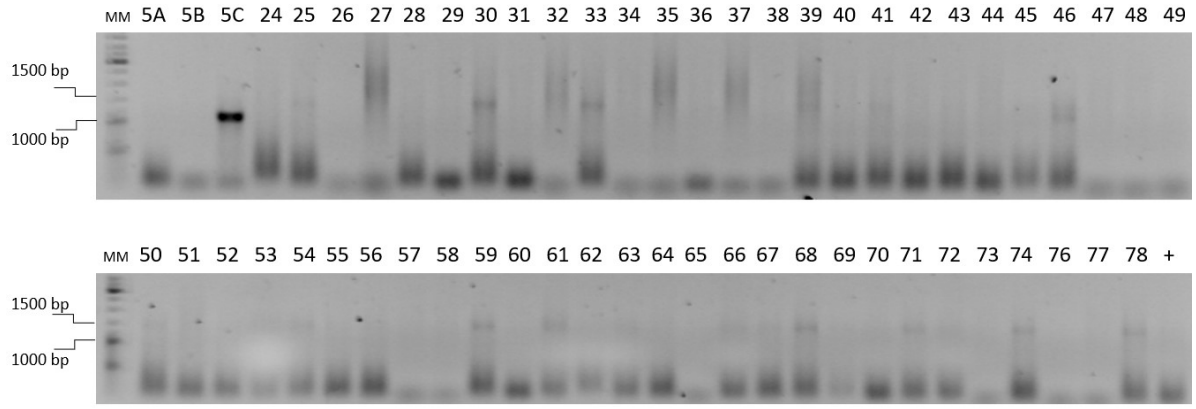

Figure III.20 - PCR product in 0,8 % (w/v) agarose gel stained with SafeRed™ of isolated clones.
5A – clone nº 5 screening with the primers PriAL44 and PriAL47; **5B** - primers PriAL44 and PriAL22; **5C** - primers PriAL20 and PriAL47. **MM** - Molecular marker 1 kb DNA Ladder. Lanes 24 - 78 represent DNA from the isolated clones; '+' is for the positive control (HCT116 Tet OsTIR1).

In order to clarify the reason by which the protocol failed, different settings and solutions were investigated *a posteriori*.

3.9.2. PCR optimisation

During the polymerase chain reaction, DNA is amplified by a series of polymerisation cycles consisting of three temperature-dependent steps: DNA denaturation, primer-template annealing and DNA synthesis by a thermostable DNA polymerase. The purity and yield of the reaction products depend on several parameters: magnesium concentration, buffer

composition, enzyme, primer concentration, amount and quality of the template DNA, and cycle parameters as the annealing temperature. Due to the failed PCR protocols, it was decided to optimise the protocol for amplification of the gene product and test each condition: reagents, annealing temperature, and primer concentrations. Unfortunately, all these conditions failed to produce PCR products.

Since it was impossible to genotype clones resulting from the CRISPR technique, including the confirmation of clone nº 5, it was decided to do the western blot of this clone to identify if the MOB4-mCherry protein is expressed in cells.

3.10. MOB4-mCherry is not expressed by clone Nº5

Western blotting (WB) is one of the gold standard protein analytical techniques. This assay will allow targeting of specific proteins in a complex of biological samples by interacting with the antibodies after separating the proteins by SDS-PAGE and transferring them to a membrane (Li *et al*., 2011).

Cell lysates from clones nº 5 (suspected of being a bi-allelic clone), 74 and 78 (randomly selected to test the expression of the protein of interest), CRAL1 and HCT116 cells were analysed. CRAL1 cells were used as a positive control, with the molecular weight of the fusion protein MOB4-GFP of 52 kDa, as a negative control was used the HCT116 cell line, with the molecular weight of endogenous MOB4 26 kDa. The clones 5, 74, and 78, suspected of being mono or bi-allelic, were used to test the fusion protein expression. The protein expression possible patterns could be: 1) one band at approximately 52 kDa, similar to CRAL1 cells, if a clone has a biallelic insertion, so, both alleles express fusion protein; 2) one band at 52 kDa and one band at 26 kDa, suggesting that a clone had an insertion in one of the alleles, whereby, endogenous and the fusion protein is expressed by cells; 3) one band at 26 kDa, indicating that construct has not been inserted and endogenous protein is expressed, 26 kDa (figure III.21).

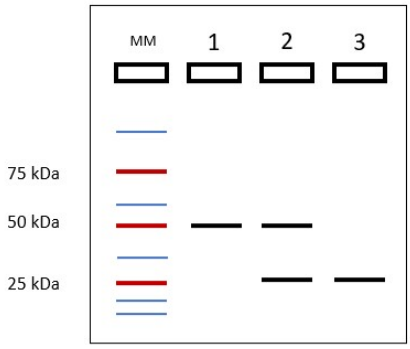

Figure III.21 – Schematic representation of protein expression pattern in isolated clones.
MM – Protein ladder and Band size (kDa). **1** – one band at 52 kDa indicates fusion protein expression only; **2** – one band at 52 kDa and one at 26 kDa indicate endogenous and fusion protein expression; **3** – one band at 26 kDa indicates for only endogenous protein expression.

When I analysed Western Blot results, I did not observe fusion protein expression in any one of the clones. As expected, MOB4-GFP at 52 kDa is expressed by CRAL1, and nothing is observed in these cells at 26 kDa. The negative control HCT116 express only the endogenous MOB4 at 26 kDa. The three clones express only the endogenous MOB4 at 26 kDa (figure III.22).

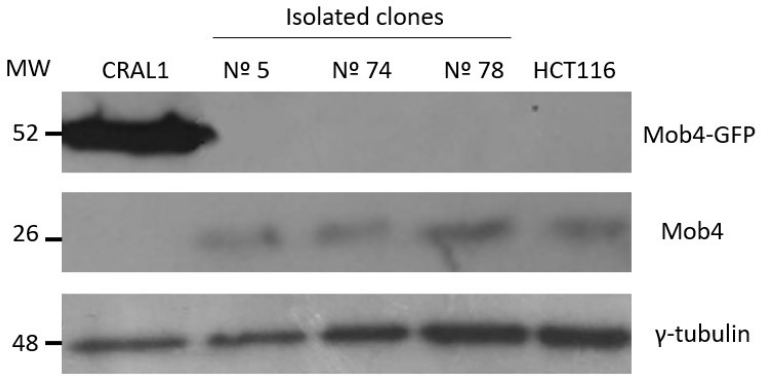

Figure III.22 - Western blotting of cell lysates. MW indicates the molecular weight of proteins in kilodaltons (kDa).
As expected, CRAL1 express the MOB4-GFP protein at 52 kDa, and HCT116 express the endogenous MOB4 at 26 kDa. The isolated clones nº 5, 74, and 78 express only endogenous MOB4 protein, 26 kDa. 10% gel was used for running the samples. Enhanced Chemiluminescence (ECL) Solution and X-Ray film were used for signal detection.

The experiment was repeated, n=3, and only the endogenous expression of MOB4 protein was observed. These results suggest that none of these clones expresses the MOB4-mCherry2.

CHAPTER IV

DISCUSSION

4. Discussion

Mob1p, the first MOB protein, was discovered in *S. cerevisiae* as a part of a signalling cascade known as the mitotic-exit network (MEN). Mob1p and proteins Dbf2 and Cdc15 (human orthologs of NDR/LATS kinases and MST1/2 kinases, respectively) were shown to be required for cytokinesis and mitotic exit (Luca *et al*., 2001).

A second yeast MOB protein, Mob2p, was shown to be a part of a separate signalling network called RAM to regulate Ace2p activity and morphogenesis. Mob2p was shown to function with a second yeast NDR/LATS kinase called Cbk1p and the yeast ortholog of human the GCK-III kinases called Kic1 to control cell polarity. The two yeast MOB complexes are mutually exclusive, and the members are non-interchangeable, thus demonstrating two different biological functions controlled by these MOB-kinase complexes (Hergovich, 2011).

This apparent separation between the cell cycle and cell polarity functions of MOB-NDR/LATS is not conserved in mammalians. The number of NDR/LATS kinases and MOB proteins and thus of potential MOB-kinase interactions has grown with the increasing complexity of the organism. Studies in D. melanogaster and human have identified MOB1A and MOB1B (dMOB1 in *D. melanogaster*) as core components of the Hippo tumour suppressor signalling pathway. Loss of dMOB1 results in tissue overgrowth, increased cell proliferation, and decreased cell death (Lai *et al*., 2005).

Briefly, the protein SAV and RASSF bind to the kinase MST1/2 to stabilise it. MST1/2 can phosphorylate MOB1A/B, which binds to and (in conjunction with MST1/2) activates the NDR/LATS kinases. NDR/LATS kinases can then phosphorylate the transcription trans-activator YAP. Phosphorylation inactivates YAP by sequestering it in the cytoplasm. Under normal conditions, Hippo signalling leads to controlled apoptosis and proliferation. Defects in the Hippo pathway can cause YAP to enter the nucleus and activate transcription of targets causing uncontrolled proliferation (Hergovich, 2011).

Other functions for MOB1A and MOB1B have also been reported. MOB1A and MOB1B are involved in centrosome duplication and regulate abscission during cytokinesis (Florindo *et al*., 2012; Hergovich *et al*., 2009). A recent study demonstrated that knockdown MOB1A and MOB1B causes abscission failure in dividing cells and prolonged centriole separation in the G1 phase, indicating that these MOB proteins regulate cytokinesis (Florindo *et al*., 2012).

On the side of MOB1A and MOB1B, that bind to the NDR and LATS kinases, MOB2 does not bind to LATS, but only NDR kinases. MOB3A, MOB3B, MOB3C and MOB4 have not been shown to interact with NDR or LATS kinases (Kohler *et al*., 2010).

Interestingly, although MOB4 is the most divergent of the MOB proteins, significant similarity is still predicted at the structural level. In *D. melanogaster*, dMOB4, along with the rest of STRIPAK, has been identified as a negative regulator of dMOB1 and Hippo signalling (Ribeiro *et al*., 2010). The hMOB4-containing supramolecular STRIPAK complexes have been implicated in Hippo signalling on diverse regulatory levels in human cells. However, the specific contributions of hMOB4 to the crosstalk between Hippo and STRIPAK signalling remain undetermined (Gundogdu & Hergovich, 2019). Nevertheless, the MST4 kinase, a relative of MST1/2, was shown to form a complex with hMOB4, with the overall structure of the hMOB4/MST4 complex resembling the hMOB1/MST1 complex (Chen *et al*., 2018). Nevertheless, one of the key residues (Lys105) that promote hMOB1 binding to MST1 is not conserved in hMOB4. Notably, the phospho-Serine/Threonine binding motif of hMOB1 seems to be present in hMOB4, while key residues such as Glu51 of hMOB1 that mediates NDR/LATS binding are not conserved in hMOB4. Therefore, the binding mode of MST4 and other GCKIIIs to hMOB4 is not understood (Gundogdu & Hergovich, 2019).

Is MOB4 required for mitosis progression?

Chromosome misalignment at metaphase plate is a relatively common phenotype in the absence of constituent kinetochore proteins such as Mis12 and SAC intervening proteins such as Mps1. Incorrect segregation of chromosomes during anaphase, possibly due to misaligned chromosomes in the metaphase plate, leads to aneuploidy, resulting in an irregular distribution of chromosomes across the two daughter cells (Goshima *et al*., 2003).

Chromosome segregation is achieved by the interaction between the spindle microtubules and the kinetochores at the centromeres. Mammalian centromeres are defined epigenetically by nucleosomes containing CENP-A, which marks the place of kinetochore assembly (Gascoigne *et al*., 2011). MOB4 was found to be a new essential element for correct chromosome segregation. Our laboratory determined that CENP-A is lost from mitotic kinetochores in cells depleted of MOB4. When MOB4 is downregulated, several mitotic defects are observed in HeLa cells, and live-cell imaging demonstrated that these defects result in cell death (Florindo, unpublished). Frost *et al*. (2012) observed in HeLa cells,

depleted of MOB4, nearly universal spindle failures followed by death (Frost *et al*., 2012). Together, these results confirm that MOB4 is an essential gene for mitosis progression.

After depletion of MOB4 in Hela cells and analysis, I observed that my non-treated cells represented an equal or higher number of mitotic cells with defects than treated cells.

I can hypothesise that the diminishing of mitotic defects in transfected cells could result from the transfecting protocol by itself. The transfection could have a positive effect on mitotic cells. Moreover, fixed cells were used for analysis, and I cannot confirm that all cells with chromosome misalignment are defective; they could not reach the metaphase plate yet. Additionally, I did not repeat the transfection protocol so that the transfection results could be invalid.

Is MOB4 required for kinetochore-microtubule attachment in mitosis?

Live-cell imaging indicates that MOB4 depleted cells spend five-fold a time in prometaphase compared to control, with problems in the chromosome alignment at the metaphase plate (Florindo, unpublished). Possible causes are chromosome detachment due to its instability or absence of attachment.

Spindle microtubules attached to the chromosomes belong to stable microtubules. Unstable spindle microtubules disassemble when exposed to cold temperatures or a high dose of the tubulin-sequestering drug, nocodazole, or a combination of these two components. Since MOB4 might be required to the kinetochore-microtubule attachment, in the absence of MOB4, it was expected to observe faster microtubule depolymerisation and, possibly, slower repolymerisation.

Is MOB4 localisation altered in the absence of microtubules?

Microtubules and their dynamic behaviour are critical for the correct segregation of chromosomes during mitosis. Nocodazole is widely used for cell synchronisation in mitosis. Nocodazole binds to β-tubulin, sequestering it from dimerisation with α-tubulin, inhibiting the formation of microtubules (Teusel *et al*., 2018).

Twelve-hour nocodazole incubation of cells on Poly-D-Lysine coverslips resulted in a rectangular cell shape. When I analysed these cells, I observed that fluorescence intensity was, apparently, higher than cells seeded on non-treated coverslips. The protein seemed to be compacted.

Previously in our laboratory was observed that MOB4 is spread throughout the cytoplasm and is associated with stress fibres in interphase cells (Santos & Tavares, unpublished). Although Poly-D-Lysine is used for cell adhesion, it resulted in a limitation or inhibition of cell adhesion and the creation of stress fibres in my experiment conditions. This could explain the MOB4-GFP stronger signal in most interphase cells through the cytoplasm. Additionally, if adhesion was limited, it can explain why most mitotic cells were lost. Mitotic cells have a minimal area in contact with the Petri dish, compared to the interphase cells, and slightly disturbs (*e. g*. wash) result in mitotic cell washout.

Short nocodazole incubation allowed to identify MOB4 localisation at centrosomes is stable in the presence or absence of microtubules.

Is MOB4 protein dependent on proteasome degradation?

MG132 is a potent proteasome inhibitor, and it blocks the proteolytic activity of the 26S proteasome. It is a classic drug for studying proteins' degradation through the ubiquitin-proteasome pathway (Teusel *et al*., 2018).

The rise of APC/C^{CDC20} activity initiates mitotic exit by targeting several mitotic determinants for degradation, resulting in the formation and separation of two interphase daughter cells. Of particular importance is securin degradation, which usually inhibits the protease separase. Removal of securin, therefore, allows separase to cleave the sister chromatid cohesion 1 subunit of the cohesin complex to initiate chromosome segregation. Another key mitotic exit event is the APC/C^{CDC20}-induced proteasomal destruction of cyclin B, which inactivates mitotic CDK1 (Wurzenberger & Gerlich, 2011). Since proteasome is inhibited, securin is not degraded, sister chromatids remain together, and cell is blocked at metaphase.

Previous data from our laboratory suggest that depletion of MOB4 results in a loss of kinetochore protein CENP-A. MOB4 can be localised at kinetochores and contribute to CENP-A loading.

MG132 treatment had the purpose of blockage at metaphase and to increase a mitotic index once cyclin B is inhibited of degradation. This could allow observing higher numbers of mitotic cells, specifically metaphases.

Six-hour incubation with MG132 resulted in a mitotic index of 5-6% compared to non-treated cells, 2-3%. Theoretically, 6-hour incubation with MG132 could increase the number of mitotic cells to around 25-30 % if the cell cycle rounds 24 hours.

Different authors have shown that prolonged incubation with MG132 results in non-specific blockage of the cell cycle by inhibiting many cell cycle-dependent proteins, whose degradation results in cell cycle progression. Some of these proteins are Cyclins, A, B, D and E. Cells remain blocked in different phases of the cell cycle (Han *et al*., 2009; Lee & Goldberg, 1998). This observation can explain a low mitotic increase with prolonged incubation.

Cells incubated for 6 hours with MG132 resulted in a high number of interphase cells with MOB4-GFP aggregates on the nucleus periphery (42%). These results suggested that MOB4-GFP is localised in Complex Golgi. These data are in agreement with the previous results in our laboratory in CRAL1 cells (Santos, unpublished) and the results of Baillat *et al*. (2001), where they confirm the localisation of MOB4 to the Golgi complex in HeLa cells. In HeLa cells, MOB4 follow the fate of AP-1 upon Brefeldin A treatment, indicating that their sensitivity to Brefeldin A is comparable to that of known Golgi-associated coat complexes (Baillat *et al*., 2001).

Furthermore, our laboratory data indicate that these aggregates start to accumulate during G2 (Santos, unpublished). This data can explain why not all cells incubated with MG132 present MOB4 aggregates, but only the fraction of cells blocked in the G2 phase. The presence of MOB4 in the Golgi Complex in two different cell lines suggest that MOB4 behaviour can be general for several cell types and not be specific to HeLa cells.

The pre-extraction before cell fixation removes soluble composts present in the cytoplasm through membrane permeabilisation. CRAL1 cells submitted to pre-extraction lost a significant part of the MOB4-GFP signal. These results are concordant with the previous ones about MOB4. It was demonstrated that MOB4 is associated with the cytoplasm (40%) and in particulate, detergent-soluble fraction (60%), where it functions as a protein complex (Baillat *et al*., 2001).

As mentioned previously, MOB4 accumulation in the cytoplasm starts during G2, and its signal intensity increases closer to mitosis (Santos, unpublished). This can explain why non-treated and cells treated for 2 hours with MG132 represented a similar number of cells with MOB4 aggregates.

MOB4 aggregates accumulate during G2, and as mentioned previously, the specific signal of MOB4 is lost when the cell exits mitosis. These results suggested that MOB4 levels can vary

during the cell cycle. Similar protein levels in interphase and mitotic cells observed by Western blot suggest that MOB4 is stable throughout the cell cycle.

Does MOB4 accumulation at Golgi Complex is dependent on motor protein transport?

Several cell processes depend on motor proteins, which generate forces and transport cargoes along cytoskeletal tracks. Dynein and kinesis are two motor proteins that move along microtubules. Dynein drives intracellular transport towards the minus ends of microtubules, which lie in the microtubule organising centre near the nucleus in non-dividing cells, whenever kinesin transports cargoes towards the plus ends (Roberts *et al*., 2013). The microtubule organising centre, also known as centrosome, is located physically with a continuous membranous system called the Golgi ribbon (Sutterlin & Colanzi, 2010).

MOB4 interacts with striatin (Baillat *et al*., 2001) and striatin interacts with dynein motor protein (Goudreault *et al*., 2009). With this data, we hypothesised that MOB4 could interact with dynein indirectly. MOB4 accumulation in Golgi could depend on motor protein dynein and MOB4 traffic throughout the cell towards the microtubule organising centre. Since nocodazole was added 4 hours after the addition of MG132, it is possible to suppose that MOB4 aggregates in Golgi were accumulated before the addition of nocodazole, as well as nocodazole, somehow, can contribute to MOB4 accumulation in Golgi Complex.

Does MOB4 accumulation in Golgi depend on microtubules in interphase cells?

MOB4 is accumulated in Golgi Complex in interphase cells, and its accumulation is not dispersed if microtubules are depolymerised. Incubation with nocodazole, followed by MG132 incubation, was performed to determine if MOB4 accumulates in Golgi when microtubules are depolymerised. Quantitative analysis indicate that control and nocodazole incubation have similar numbers of interphase cells with MOB4-GFP aggregates in the Golgi Complex, around 5%.

Incubation with nocodazole and MG132 indicated a different pattern. Of 146 observed interphase cells, 99 present MOB4-GFP aggregates in the cytoplasm, corresponding to 67% of total interphase cells. The value is 1.5-fold of MG132 treatment. These results suggest that the absence of microtubules can positively affect MOB4-GFP accumulation in Golgi. On the other hand, 35% of all cells blocked at mitosis, as was expected with nocodazole incubation, could contribute to a higher percentage of interphase cells with MOB4-GFP aggregates in Golgi Complex.

Of 99 cells with MOB4-GFP aggregates, 5 present two different accumulations. These cells correspond to 5% of the total cells with MOB4-GFP aggregates. In comparison, in 6-hour MG132 treatment, zero cells with this condition were observed. Additionally, all five cells have an atypical shape of adherent cells in interphase; their cytoskeleton is partially disrupted.

Microtubules are cytoskeletal components and are required to maintain the normal interconnected morphology of the Golgi complex at the microtubule-organising centre of unpolarised mammalian cells and to facilitate membrane traffic to and from the Golgi. Many studies have shown that depolymerisation of microtubules by treatment of cells with nocodazole or colchicine results in the formation of Golgi ministacks that are dispersed throughout the cell periphery and adjacent to endoplasmic reticulum-exit sites (Drecktrah & Brown, 1999). In the presence of nocodazole, Golgi Complex can fragmentate, migrate, and localise in a different part of the cell. These observations suggest that MOB4 is co-transported with Golgi fragments.

Some previous works indicate that the STRIPAK components STRIP and MOB4 act globally to regulate microtubule stability and organisation, potentially through the posttranslational modification of tubulin and microtubule-associated proteins (Schulte *et al*., 2010). Results from this work suggest that MOB4 specific localisation is not dependent on microtubules. More research needs to be performed to understand the interaction of MOB4 and microtubules.

CHAPTER V

CONCLUSIONS

5. Conclusions

One of the objectives of this work was to understand if MOB4 localisation is altered in the absence of microtubules in mitotic cells. Previous data from our laboratory indicate that MOB4 localises at centrosomes in mitotic cells (Florindo, unpublished). MOB4 localises at centrosomes in mitotic cells in the presence and absence of microtubules in my experiment conditions.

MOB4 accumulates in the perinuclear region of interphase cells (CRAL1) treated with MG132. The number of cells with MOB4 aggregates is significantly higher in cells incubated with MG132 than in non-treated cells. It is in agreement with previous results in CRAL1 cells from our laboratory (Santos, unpublished) and the Baillat *et al*. (2001) in HeLa cells, which suggest that MOB4 localises in Golgi Complex. MOB4 accumulation in Golgi has a place during G2.

In order to identify if MOB4 protein levels are altered during the cell cycle, interphase and mitotic cells were analysed. Non-treated and cell blocked in mitosis demonstrated similar levels of MOB4. These results indicate that MOB4 protein levels are stable during the cell cycle.

MOB4 aggregates in Golgi Complex are observable in interphase cells in the presence and absence of microtubules. These results suggest that MOB4 accumulation during G2 is independent of microtubules. Additionally, in the presence of nocodazole and MG132, a high number of cells present MOB4 aggregates in Golgi. Cells with more than one separate accumulation were observed in these working conditions. Golgi Complex can fragmentate in the presence of nocodazole. This observation suggests that MOB4 is co-transported with Golgi fragments.

Whit this work, I did not determine MOB4 function during mitosis. Moreover, I demonstrated that MOB4 accumulates in Golgi during G2. This process is independent of microtubules.

CHAPTER VI

FUTURE PERSPECTIVES

6. Future perspectives

The results obtained throughout this work leave many open questions about MOB4, not allowing confirmation about the *hMOB4* gene function. Previous results indicate *hMOB4* being an essential and uncharacterised gene necessary for a successful outcome of mitosis. However, the exact function of MOB4 is to be determined yet.

Depletion of MOB4 causes strong defects in chromosome congression and alignment, mitotic block, and CENP-A is lost from kinetochores. It is essential to understand how MOB4 affects kinetochore function. For this reason, it is essential to carry out RNAi assays for immunofluorescence in order to understand which other kinetochore proteins are affected, lost or inhibited from being recruited to the kinetochores.

In order to determine if the MOB4-induced metaphase arrest is due to alteration in the stability of kinetochore microtubules, it is critical to identify if MOB4 is localised at microtubules and kinetochores of mitotic cells.

CRAL1 cells, expressing fusion protein, help understand the MOB4 localisation in cells. More cell lines still need to be generated from HCT116 to confirm the results obtained from CRAL1 cells.

One more question to be answered is which are interactors of MOB4 in the STRIPAK complex and how they contribute to Hippo signalling inhibition. The model proposed by Chen *et al*. (2018) suggests that MOB1/MST1 is disrupted by MOB4/MST4 complex, but this model requires more studies to be performed.

MOB4 interacts with PP2A and striatins, and it will be essential to identify what other proteins interact with MOB4 and which protein-protein interactions of MOB4 are essential on the cellular and organism levels. Additionally, it is important to determine if MOB4 is a substrate of PP2A and if MOB4 phosphorylation has a specific time and place during the cell cycle.

CHAPTER VII

REFERENCES

7. References

Addgene plasmid # 72830. (n.d.). Addgene. Retrieved October 11, 2021, from http://n2t.net/addgene:72830

Alberts, B., Bray, D., Hopkin, K., Johnson, A. D., Lewis, J., Raff, M., Roberts, K., & Walter, P. (2014). *Essential Cell Biology, 4th Edition* (4th ed.). Garland Science.

Alberts, B., Johnson, A., Lewis, J., Morgan, D., Raff, M., Roberts, K., & Walter, P. (2015). *Molecular Biology of the Cell* (Sixth ed.). W. W. Norton & Company.

Bai, S. W., Herrera-Abreu, M. T., Rohn, J. L., Racine, V., Tajadura, V., Suryavanshi, N., Bechtel, S., Wiemann, S., Baum, B., & Ridley, A. J. (2011). Identification and characterization of a set of conserved and new regulators of cytoskeletal organization, cell morphology and migration. *BMC Biology*, *9*(1). https://doi.org/10.1186/1741-7007-9-54

Baillat, G., Gaillard, S., Castets, F., & Monneron, A. (2002). Interactions of Phocein with Nucleoside-Diphosphate Kinase, Eps15, and Dynamin I. *Journal of Biological Chemistry*, *277*(21), 18961–18966. https://doi.org/10.1074/jbc.m108818200

Baillat, G., Moqrich, A., Castets, F., Baude, A., Bailly, Y., Benmerah, A., & Monneron, A. (2001). Molecular Cloning and Characterization of Phocein, a Protein Found from the Golgi Complex to Dendritic Spines. *Molecular Biology of the Cell*, *12*(3), 663–673. https://doi.org/10.1091/mbc.12.3.663

Ban, R., Irino, Y., Fukami, K., & Tanaka, H. (2004). Human Mitotic Spindle-associated Protein PRC1 Inhibits MgcRacGAP Activity toward Cdc42 during the Metaphase. *Journal of Biological Chemistry*, *279*(16), 16394–16402. https://doi.org/10.1074/jbc.m313257200

Bane, B., MacRae, T., Xiang, H., Bateman, J., & Slepecky, N. (2002). Microtubule cold stability in supporting cells of the gerbil auditory sensory epithelium: correlation with tubulin post-translational modifications. *Cell and Tissue Research*, *307*(1), 57–67. https://doi.org/10.1007/s00441-001-0483-x

Benmerah, A., Bègue, B., Dautry-Varsat, A., & Cerf-Bensussan, N. (1996). The Ear of α-Adaptin Interacts with the COOH-terminal Domain of the Eps15 Protein. *Journal of Biological Chemistry*, *271*(20), 12111–12116. https://doi.org/10.1074/jbc.271.20.12111

Bianconi, E., Piovesan, A., Facchin, F., Beraudi, A., Casadei, R., Frabetti, F., Vitale, L., Pelleri, M. C., Tassani, S., Piva, F., Perez-Amodio, S., Strippoli, P., & Canaider, S. (2013). An estimation of the number of cells in the human body. *Annals of Human Biology*, *40*(6), 463–471. https://doi.org/10.3109/03014460.2013.807878

Bichsel, S. J., Tamaskovic, R., Stegert, M. R., & Hemmings, B. A. (2004). Mechanism of Activation of NDR (Nuclear Dbf2-related) Protein Kinase by the hMOB1 Protein. *Journal of Biological Chemistry*, *279*(34), 35228–35235. https://doi.org/10.1074/jbc.m404542200

Black, B. E. (2017). *Centromeres and Kinetochores: Discovering the Molecular Mechanisms Underlying Chromosome Inheritance (Progress in Molecular and Subcellular Biology, 56)* (1st ed. 2017 ed.). Springer. https://doi.org/10.1007/978-3-319-58592-5

Bodakuntla, S., Jijumon, A., Villablanca, C., Gonzalez-Billault, C., & Janke, C. (2019). Microtubule-Associated Proteins: Structuring the Cytoskeleton. *Trends in Cell Biology*, *29*(10), 804–819. https://doi.org/10.1016/j.tcb.2019.07.004

Boggiano, J., Vanderzalm, P., & Fehon, R. (2011). Tao-1 Phosphorylates Hippo/MST Kinases to Regulate the Hippo-Salvador-Warts Tumor Suppressor Pathway. *Developmental Cell*, *21*(5), 888–895. https://doi.org/10.1016/j.devcel.2011.08.028

Bowne-Anderson, H., Zanic, M., Kauer, M., & Howard, J. (2013). Microtubule dynamic instability: A new model with coupled GTP hydrolysis and multistep catastrophe. *BioEssays*, *35*(5), 452–461. https://doi.org/10.1002/bies.201200131

Brinkley, B. R., & Cartwright, J. (1975). COLD-LABILE AND COLD-STABLE MICROTUBULES IN THE MITOTIC SPINDLE OF MAMMALIAN CELLS. *Annals of the New York Academy of Sciences*, *253*(1 The Biology o), 428–439. https://doi.org/10.1111/j.1749-6632.1975.tb19218.x

Cheeseman, I. M. (2014). The Kinetochore. *Cold Spring Harbor Perspectives in Biology*, *6*(7), a015826. https://doi.org/10.1101/cshperspect.a015826

Cheeseman, I. M., Chappie, J. S., Wilson-Kubalek, E. M., & Desai, A. (2006). The Conserved KMN Network Constitutes the Core Microtubule-Binding Site of the Kinetochore. *Cell*, *127*(5), 983–997. https://doi.org/10.1016/j.cell.2006.09.039

Cheeseman, I. M., & Desai, A. (2008). Molecular architecture of the kinetochore–microtubule interface. *Nature Reviews Molecular Cell Biology*, *9*(1), 33–46. https://doi.org/10.1038/nrm2310

Chen, M., Zhang, H., Shi, Z., Li, Y., Zhang, X., Gao, Z., Zhou, L., Ma, J., Xu, Q., Guan, J., Cheng, Y., Jiao, S., & Zhou, Z. (2018). The MST4–MOB4 complex disrupts the MST1–MOB1 complex in the Hippo–YAP pathway and plays a pro-oncogenic role in pancreatic cancer. *Journal of Biological Chemistry*, *293*(37), 14455–14469. https://doi.org/10.1074/jbc.ra118.003279

Cherry Biotech | Temperature control for live cell imaging. (2020). Cherry Biotech. Retrieved October 11, 2021, from https://www.cherrybiotech.com/

Chiang, T. W. W., le Sage, C., Larrieu, D., Demir, M., & Jackson, S. P. (2016). CRISPR-Cas9D10A nickase-based genotypic and phenotypic screening to enhance genome editing. *Scientific Reports*, *6*(1). https://doi.org/10.1038/srep24356

Chow, A., Hao, Y., & Yang, X. (2010). Molecular characterization of human homologs of yeast MOB1. *International Journal of Cancer*, NA. https://doi.org/10.1002/ijc.24878

Cong, L., Ran, F. A., Cox, D., Lin, S., Barretto, R., Habib, N., Hsu, P. D., Wu, X., Jiang, W., Marraffini, L. A., & Zhang, F. (2013). Multiplex Genome Engineering Using CRISPR/Cas Systems. *Science*, *339*(6121), 819–823. https://doi.org/10.1126/science.1231143

Cooper, G. M., & Hausman, R. E. (2013). *The Cell: A Molecular Approach, Sixth Edition* (6th ed.). Sinauer Associates, Inc.

Dana, H., Mahmoodi, G., Mahmoodzadeh, H., Karimloo, R., Rezaiean, O., Moradzadeh, A., Mehmandoost, N., Moazzen, F., Mazraeh, A., Marmari, V., Ebrahimi, M., Rashno, M. M., Abadi, S. J., & Gharagouzlo, E. (2017). Molecular Mechanisms and Biological Functions of siRNA. *International Journal of Biomedical Science*, *13*(2).

Desai, A., & Mitchison, T. J. (1997). MICROTUBULE POLYMERIZATION DYNAMICS. *Annual Review of Cell and Developmental Biology*, *13*(1), 83–117. https://doi.org/10.1146/annurev.cellbio.13.1.83

do Carmo Avides, M., & Glover, D. M. (1999). Abnormal Spindle Protein, Asp, and the Integrity of Mitotic Centrosomal Microtubule Organizing Centers. *Science*, *283*(5408), 1733–1735. https://doi.org/10.1126/science.283.5408.1733

Dobbelaere, J., Josué, F., Suijkerbuijk, S., Baum, B., Tapon, N., & Raff, J. (2008). A Genome-Wide RNAi Screen to Dissect Centriole Duplication and Centrosome Maturation in Drosophila. *PLoS Biology*, *6*(9), e224. https://doi.org/10.1371/journal.pbio.0060224

Donaldson, J. G., Finazzi, D., & Klausner, R. D. (1992). Brefeldin A inhibits Golgi membrane-catalysed exchange of guanine nucleotide onto ARF protein. *Nature*, *360*(6402), 350–352. https://doi.org/10.1038/360350a0

Dong, J., Feldmann, G., Huang, J., Wu, S., Zhang, N., Comerford, S. A., Gayyed, M., Anders, R. A., Maitra, A., & Pan, D. (2007). Elucidation of a Universal Size-Control Mechanism in Drosophila and Mammals. *Cell*, *130*(6), 1120–1133. https://doi.org/10.1016/j.cell.2007.07.019

Drecktrah, D., & Brown, W. J. (1999). Phospholipase A2Antagonists Inhibit Nocodazole-induced Golgi Ministack Formation: Evidence of an ER Intermediate and Constitutive Cycling. *Molecular Biology of the Cell*, *10*(12), 4021–4032. https://doi.org/10.1091/mbc.10.12.4021

Duhart, J. C., & Raftery, L. A. (2020). Mob Family Proteins: Regulatory Partners in Hippo and Hippo-Like Intracellular Signaling Pathways. *Frontiers in Cell and Developmental Biology*, *8*. https://doi.org/10.3389/fcell.2020.00161

Duncan, T., & Wakefield, J. G. (2011). 50 ways to build a spindle: the complexity of microtubule generation during mitosis. *Chromosome Research*, *19*(3), 321–333. https://doi.org/10.1007/s10577-011-9205-8

Emami, S., Zhang, D., & Yang, X. (2020). Interaction of the Hippo Pathway and Phosphatases in Tumorigenesis. *Cancers*, *12*(9), 2438. https://doi.org/10.3390/cancers12092438

Etemad, B., Kuijt, T. E. F., & Kops, G. J. P. L. (2015). Kinetochore–microtubule attachment is sufficient to satisfy the human spindle assembly checkpoint. *Nature Communications*, *6*(1). https://doi.org/10.1038/ncomms9987

Fakruddin, M., Mannan, K. B., Hossain, M., Islam, S., Mazumdar, R., Chowdhury, A., & Chowdhury, M. (2013). Nucleic acid amplification: Alternative methods of polymerase chain reaction. *Journal of Pharmacy and Bioallied Sciences*, *5*(4), 245. https://doi.org/10.4103/0975-7406.120066

Florindo, C., Perdigão, J., Fesquet, D., Schiebel, E., Pines, J., & Tavares, L. A. (2012). Human Mob1 proteins are required for cytokinesis by controlling microtubule stability. *Journal of Cell Science*. Published. https://doi.org/10.1242/jcs.097147

Frost, A., Elgort, M., Brandman, O., Ives, C., Collins, S., Miller-Vedam, L., Weibezahn, J., Hein, M., Poser, I., Mann, M., Hyman, A., & Weissman, J. (2012). Functional Repurposing Revealed by Comparing S. pombe and S. cerevisiae Genetic Interactions. *Cell*, *149*(6), 1339–1352. https://doi.org/10.1016/j.cell.2012.04.028

Gascoigne, K., Takeuchi, K., Suzuki, A., Hori, T., Fukagawa, T., & Cheeseman, I. (2011). Induced Ectopic Kinetochore Assembly Bypasses the Requirement for CENP-A Nucleosomes. *Cell*, *145*(3), 410–422. https://doi.org/10.1016/j.cell.2011.03.031

Gayek, A. S., & Ohi, R. (2014). Kinetochore-microtubule stability governs the metaphase requirement for Eg5. *Molecular Biology of the Cell*, *25*(13), 2051–2060. https://doi.org/10.1091/mbc.e14-03-0785

GeneCards. (2011, February). Gene Cards. Retrieved September 1, 2021, from https://www.genecards.org

Giuliano, C. J., Lin, A., Girish, V., & Sheltzer, J. M. (2019). Generating Single Cell–Derived Knockout Clones in Mammalian Cells with CRISPR/Cas9. *Current Protocols in Molecular Biology*, *128*(1). https://doi.org/10.1002/cpmb.100

Gonzalez, C., Saunders, R., Casal, J., Molina, I., Carmena, M., Ripoll, P., & Glover, D. (1990). Mutations at the asp locus of Drosophila lead to multiple free centrosomes in syncytial embryos, but restrict centrosome duplication in larval neuroblasts. *Journal of Cell Science*, *96*(4), 605–616. https://doi.org/10.1242/jcs.96.4.605

Gordon, J., Hwang, J., Carrier, K. J., Jones, C. A., Kern, Q. L., Moreno, C. S., Karas, R. H., & Pallas, D. C. (2011). Protein phosphatase 2a (PP2A) binds within the oligomerization domain of striatin and regulates the phosphorylation and activation of the mammalian Ste20-Like kinase Mst3. *BMC Biochemistry*, *12*(1). https://doi.org/10.1186/1471-2091-12-54

Goshima, G., Kiyomitsu, T., Yoda, K., & Yanagida, M. (2003). Human centromere chromatin protein hMis12, essential for equal segregation, is independent of CENP-A loading pathway. *Journal of Cell Biology*, *160*(1), 25–39. https://doi.org/10.1083/jcb.200210005

Goudreault, M., D'Ambrosio, L. M., Kean, M. J., Mullin, M. J., Larsen, B. G., Sanchez, A., Chaudhry, S., Chen, G. I., Sicheri, F., Nesvizhskii, A. I., Aebersold, R., Raught, B., & Gingras, A. C. (2009). A PP2A Phosphatase High Density Interaction Network Identifies a Novel Striatin-interacting Phosphatase and Kinase Complex Linked to the Cerebral Cavernous Malformation 3 (CCM3) Protein. *Molecular & Cellular Proteomics*, *8*(1), 157–171. https://doi.org/10.1074/mcp.m800266-mcp200

Green, R. A., Paluch, E., & Oegema, K. (2012). Cytokinesis in Animal Cells. *The Annual Review of Cell and Developmental Biology*, *28*, 29–58.

Grimaldi, A. D., Fomicheva, M., & Kaverina, I. (2013). Ice Recovery Assay for Detection of Golgi-Derived Microtubules. *Methods for Analysis of Golgi Complex Function*, 401–415. https://doi.org/10.1016/b978-0-12-417164-0.00024-0

Gu, F., Crump, C., & Thomas, G. (2001). Trans-Golgi network sorting. *Cellular and Molecular Life Sciences*, *58*(8), 1067–1084. https://doi.org/10.1007/pl00000922

Gudimchuk, N. B., & McIntosh, J. R. (2021). Regulation of microtubule dynamics, mechanics and function through the growing tip. *Nature Reviews Molecular Cell Biology*. Published. https://doi.org/10.1038/s41580-021-00399-x

Guizetti, J., & Gerlich, D. W. (2010). Cytokinetic abscission in animal cells. *Seminars in Cell & Developmental Biology*, *21*(9), 909–916. https://doi.org/10.1016/j.semcdb.2010.08.001

Gundogdu, & Hergovich. (2019). MOB (Mps one Binder) Proteins in the Hippo Pathway and Cancer. *Cells*, *8*(6), 569. https://doi.org/10.3390/cells8060569

Haeberlé, A. M., Castets, F., Bombarde, G., Baillat, G., & Bailly, Y. (2006). Immunogold localization of phocein in dendritic spines. *The Journal of Comparative Neurology*, *495*(3), 336–350. https://doi.org/10.1002/cne.20895

Hagting, A., den Elzen, N., Vodermaier, H. C., Waizenegger, I. C., Peters, J. M., & Pines, J. (2002). Human securin proteolysis is controlled by the spindle checkpoint and reveals when the APC/C switches from activation by Cdc20 to Cdh1. *Journal of Cell Biology*, *157*(7), 1125–1137. https://doi.org/10.1083/jcb.200111001

He, Y., Emoto, K., Fang, X., Ren, N., Tian, X., Jan, Y. N., & Adler, P. N. (2005). DrosophilaMob Family Proteins Interact with the Related Tricornered (Trc) and Warts (Wts) Kinases. *Molecular Biology of the Cell*, *16*(9), 4139–4152. https://doi.org/10.1091/mbc.e05-01-0018

Hendry, J. H., & Scott, D. (1987). *Loss of reproductive integrity of irradiated cells, and its importance in tissues, in Perspectives on mammalian cell death*. Oxford Scientific Publications.

Hergovich, A. (2011). MOB control: Reviewing a conserved family of kinase regulators. *Cellular Signalling*, *23*(9), 1433–1440. https://doi.org/10.1016/j.cellsig.2011.04.007

Hergovich, A. (2016). The Roles of NDR Protein Kinases in Hippo Signalling. *Genes*, *7*(5), 21. https://doi.org/10.3390/genes7050021

Hergovich, A., Kohler, R. S., Schmitz, D., Vichalkovski, A., Cornils, H., & Hemmings, B. A. (2009). The MST1 and hMOB1 Tumor Suppressors Control Human Centrosome Duplication by Regulating NDR Kinase Phosphorylation. *Current Biology*, *19*(20), 1692–1702. https://doi.org/10.1016/j.cub.2009.09.020

Homepage | Bio-Rad Laboratories. (2021). BIO-RAD. Retrieved October 10, 2021, from https://www.bio-rad.com/

Hori, T., Amano, M., Suzuki, A., Backer, C. B., Welburn, J. P., Dong, Y., McEwen, B. F., Shang, W. H., Suzuki, E., Okawa, K., Cheeseman, I. M., & Fukagawa, T. (2008). CCAN Makes Multiple Contacts with Centromeric DNA to Provide Distinct Pathways to the Outer Kinetochore. *Cell*, *135*(6), 1039–1052. https://doi.org/10.1016/j.cell.2008.10.019

Huang, J., Wu, S., Barrera, J., Matthews, K., & Pan, D. (2005). The Hippo Signaling Pathway Coordinately Regulates Cell Proliferation and Apoptosis by Inactivating Yorkie, the Drosophila Homolog of YAP. *Cell*, *122*(3), 421–434. https://doi.org/10.1016/j.cell.2005.06.007

The Human Protein Atlas. (2021, November 18). The Protein Atlas. Retrieved November 20, 2021, from https://www.proteinatlas.org/

Hwang, J., & Pallas, D. C. (2014). STRIPAK complexes: Structure, biological function, and involvement in human diseases. *The International Journal of Biochemistry & Cell Biology*, *47*, 118–148. https://doi.org/10.1016/j.biocel.2013.11.021

Hyman, A. A., & Mitchison, T. J. (1990). Modulation of microtubule stability by kinetochores in vitro. *Journal of Cell Biology*, *110*(5), 1607–1616. https://doi.org/10.1083/jcb.110.5.1607

Ishino, Y., Shinagawa, H., Makino, K., Amemura, M., & Nakata, A. (1987). Nucleotide sequence of the iap gene, responsible for alkaline phosphatase isozyme conversion in Escherichia coli, and identification of the gene product. *Journal of Bacteriology*, *169*(12), 5429–5433. https://doi.org/10.1128/jb.169.12.5429-5433.1987

Jinek, M., Chylinski, K., Fonfara, I., Hauer, M., Doudna, J. A., & Charpentier, E. (2012). A Programmable Dual-RNA–Guided DNA Endonuclease in Adaptive Bacterial Immunity. *Science*, *337*(6096), 816–821. https://doi.org/10.1126/science.1225829

Jokelainen, P. T. (1967). The ultrastructure and spatial organization of the metaphase kinetochore in mitotic rat cells. *Journal of Ultrastructure Research*, *19*(1–2), 19–44. https://doi.org/10.1016/s0022-5320(67)80058-3

Jordan, M., Thrower, D., & Wilson, L. (1992). Effects of vinblastine, podophyllotoxin and nocodazole on mitotic spindles. Implications for the role of microtubule dynamics in mitosis. *Journal of Cell Science*, *102*(3), 401–416. https://doi.org/10.1242/jcs.102.3.401

Karp, G., Iwasa, J., & Marshall, W. (2016). *Karp's Cell and Molecular Biology: Concepts and Experiments* (8th ed.). Wiley.

Khodjakov, A., Copenagle, L., Gordon, M. B., Compton, D. A., & Kapoor, T. M. (2003). Minus-end capture of preformed kinetochore fibers contributes to spindle morphogenesis. *Journal of Cell Biology*, *160*(5), 671–683. https://doi.org/10.1083/jcb.200208143

Khodjakov, A., Gabashvili, I. S., & Rieder, C. L. (1999). ?Dumb? versus ?smart? kinetochore models for chromosome congression during mitosis in vertebrate somatic cells. *Cell Motility and the Cytoskeleton*, *43*(3), 179–185.

Kirschner, M., & Mitchison, T. (1986). Beyond self-assembly: From microtubules to morphogenesis. *Cell*, *45*(3), 329–342. https://doi.org/10.1016/0092-8674(86)90318-1

Kohler, R. S., Schmitz, D., Cornils, H., Hemmings, B. A., & Hergovich, A. (2010). Differential NDR/LATS Interactions with the Human MOB Family Reveal a Negative Role for Human MOB2 in the Regulation of Human NDR Kinases. *Molecular and Cellular Biology*, *30*(18), 4507–4520. https://doi.org/10.1128/mcb.00150-10

Kück, U., Radchenko, D., & Teichert, I. (2019). STRIPAK, a highly conserved signaling complex, controls multiple eukaryotic cellular and developmental processes and is linked with human diseases. *Biological Chemistry*, *400*(8), 1005–1022. https://doi.org/10.1515/hsz-2019-0173

Kwon, H., Kim, J., & Jho, E. (2021). Role of the Hippo pathway and mechanisms for controlling cellular localization of YAP/TAZ. *The FEBS Journal*. Published. https://doi.org/10.1111/febs.16091

Lai, Z. C., Wei, X., Shimizu, T., Ramos, E., Rohrbaugh, M., Nikolaidis, N., Ho, L. L., & Li, Y. (2005). Control of Cell Proliferation and Apoptosis by Mob as Tumor Suppressor, Mats. *Cell*, *120*(5), 675–685. https://doi.org/10.1016/j.cell.2004.12.036

Lambrus, B. G., Moyer, T. C., & Holland, A. J. (2018). Applying the auxin-inducible degradation system for rapid protein depletion in mammalian cells. *Mitosis and Meiosis Part A*, 107–135. https://doi.org/10.1016/bs.mcb.2018.03.004

Lampson, M. A., Renduchitala, K., Khodjakov, A., & Kapoor, T. M. (2004). Correcting improper chromosome–spindle attachments during cell division. *Nature Cell Biology*, *6*(3), 232–237. https://doi.org/10.1038/ncb1102

Lane, M. E., Sauer, K., Wallace, K., Jan, Y. N., Lehner, C. F., & Vaessin, H. (1996). Dacapo, a Cyclin-Dependent Kinase Inhibitor, Stops Cell Proliferation during Drosophila Development. *Cell*, *87*(7), 1225–1235. https://doi.org/10.1016/s0092-8674(00)81818-8

Lee, D. H., & Goldberg, A. L. (1998). Proteasome inhibitors: valuable new tools for cell biologists. *Trends in Cell Biology*, *8*(10), 397–403. https://doi.org/10.1016/s0962-8924(98)01346-4

Li, D., Musante, V., Zhou, W., Picciotto, M. R., & Nairn, A. C. (2018). Striatin-1 is a B subunit of protein phosphatase PP2A that regulates dendritic arborization and spine development in striatal neurons. *Journal of Biological Chemistry*, *293*(28), 11179–11194. https://doi.org/10.1074/jbc.ra117.001519

Li, X., Bai, H., Wang, X., Li, L., Cao, Y., Wei, J., Liu, Y., Liu, L., Gong, X., Wu, L., Liu, S., & Liu, G. (2011). Identification and validation of rice reference proteins for western blotting. *Journal of Experimental Botany*, *62*(14), 4763–4772. https://doi.org/10.1093/jxb/err084

Lodish, H., Berk, A., Kaiser, C. A., Kreiger, M., Bretscher, A., Ploegh, H., Amon, A., & Martin, K. C. (2016). *Molecular Cell Biology* (8th ed.). W.H. Freeman and Company.

Lorenz, T. C. (2012). Polymerase Chain Reaction: Basic Protocol Plus Troubleshooting and Optimization Strategies. *Journal of Visualized Experiments*, *63*. https://doi.org/10.3791/3998

Luca, F. C., Mody, M., Kurischko, C., Roof, D. M., Giddings, T. H., & Winey, M. (2001). Saccharomyces cerevisiae Mob1p Is Required for Cytokinesis and Mitotic Exit. *Molecular and Cellular Biology*, *21*(20), 6972–6983. https://doi.org/10.1128/mcb.21.20.6972-6983.2001

Luca, F. C., & Winey, M. (1998). MOB1, an Essential Yeast Gene Required for Completion of Mitosis and Maintenance of Ploidy. *Molecular Biology of the Cell*, *9*(1), 29–46. https://doi.org/10.1091/mbc.9.1.29

Lüders, J., & Stearns, T. (2007). Microtubule-organizing centres: a re-evaluation. *Nature Reviews Molecular Cell Biology*, *8*(2), 161–167. https://doi.org/10.1038/nrm2100

Maiato, H., Rieder, C. L., & Khodjakov, A. (2004). Kinetochore-driven formation of kinetochore fibers contributes to spindle assembly during animal mitosis. *Journal of Cell Biology*, *167*(5), 831–840. https://doi.org/10.1083/jcb.200407090

Maiato, H., & Schuh, M. (2018). *Mitosis and Meiosis Part A (Volume 144) (Methods in Cell Biology, Volume 144)* (1st ed.). Academic Press.

Mali, P., Yang, L., Esvelt, K. M., Aach, J., Guell, M., DiCarlo, J. E., Norville, J. E., & Church, G. M. (2013). RNA-Guided Human Genome Engineering via Cas9. *Science*, *339*(6121), 823–826. https://doi.org/10.1126/science.1232033

Marumoto, T., Hirota, T., Morisaki, T., Kunitoku, N., Zhang, D., Ichikawa, Y., Sasayama, T., Kuninaka, S., Mimori, T., Tamaki, N., Kimura, M., Okano, Y., & Saya, H. (2002). Roles of aurora-A kinase in mitotic entry and G2 checkpoint in mammalian cells. *Genes to Cells*, *7*(11), 1173–1182. https://doi.org/10.1046/j.1365-2443.2002.00592.x

McKinley, K. L., & Cheeseman, I. M. (2015). The molecular basis for centromere identity and function. *Nature Reviews Molecular Cell Biology*, *17*(1), 16–29. https://doi.org/10.1038/nrm.2015.5

Meng, Z., Moroishi, T., & Guan, K. L. (2016). Mechanisms of Hippo pathway regulation. *Genes & Development*, *30*(1), 1–17. https://doi.org/10.1101/gad.274027.115

Mitchison, T., & Kirschner, M. (1984). Dynamic instability of microtubule growth. *Nature*, *312*(5991), 237–242. https://doi.org/10.1038/312237a0

Moreno, C. S., Lane, W. S., & Pallas, D. C. (2001). A Mammalian Homolog of Yeast MOB1 Is Both a Member and a Putative Substrate of Striatin Family-Protein Phosphatase 2A Complexes. *Journal of Biological Chemistry*, *276*(26), 24253–24260. https://doi.org/10.1074/jbc.m102398200

Moreno, C. S., Park, S., Nelson, K., Ashby, D., Hubalek, F., Lane, W. S., & Pallas, D. C. (2000). WD40 Repeat Proteins Striatin and S/G2 Nuclear Autoantigen Are Members of a Novel Family of Calmodulin-binding Proteins That Associate with Protein Phosphatase 2A. *Journal of Biological Chemistry*, *275*(8), 5257–5263. https://doi.org/10.1074/jbc.275.8.5257

Musacchio, A., & Salmon, E. D. (2007). The spindle-assembly checkpoint in space and time. *Nature Reviews Molecular Cell Biology*, *8*(5), 379–393. https://doi.org/10.1038/nrm2163

Nasmyth, K. (2000). Splitting the Chromosome: Cutting the Ties That Bind Sister Chromatids. *Science*, *288*(5470), 1379–1384. https://doi.org/10.1126/science.288.5470.1379

National Academies of Sciences, Engineering, and Medicine, National Academy of Medicine, National Academy of Sciences, & Committee on Human Gene Editing: Scientific, Medical, and Ethical Considerations. (2017). *Human Genome Editing: Science, Ethics, and Governance* (Illustrated ed.). National Academies Press.

Natsume, T., Kiyomitsu, T., Saga, Y., & Kanemaki, M. T. (2016). Rapid Protein Depletion in Human Cells by Auxin-Inducible Degron Tagging with Short Homology Donors. *Cell Reports*, *15*(1), 210–218. https://doi.org/10.1016/j.celrep.2016.03.001

Nicklas, R. B., & Ward, S. C. (1994). Elements of error correction in mitosis: microtubule capture, release, and tension. *Journal of Cell Biology*, *126*(5), 1241–1253. https://doi.org/10.1083/jcb.126.5.1241

Nishimura, K., Fukagawa, T., Takisawa, H., Kakimoto, T., & Kanemaki, M. (2009). An auxin-based degron system for the rapid depletion of proteins in nonplant cells. *Nature Methods*, *6*(12), 917–922. https://doi.org/10.1038/nmeth.1401

Oh, H., & Irvine, K. D. (2008). In vivo regulation of Yorkie phosphorylation and localization. *Development*, *135*(6), 1081–1088. https://doi.org/10.1242/dev.015255

Oh, H., & Irvine, K. D. (2010). Yorkie: the final destination of Hippo signaling. *Trends in Cell Biology*, *20*(7), 410–417. https://doi.org/10.1016/j.tcb.2010.04.005

Oliver, C., & Jamur, M. C. (Eds.). (2010). Immunocytochemical Methods and Protocols. *Methods in Molecular Biology*. Published. https://doi.org/10.1007/978-1-59745-324-0

Pan, D. (2010). The Hippo Signaling Pathway in Development and Cancer. *Developmental Cell*, *19*(4), 491–505. https://doi.org/10.1016/j.devcel.2010.09.011

Park, S., & Guo, X. (2014). Adaptor protein complexes and intracellular transport. *Bioscience Reports*, *34*(4). https://doi.org/10.1042/bsr20140069

Paweletz, N. (2001). Walther Flemming: pioneer of mitosis research. *Nature Reviews Molecular Cell Biology*, *2*(1), 72–75. https://doi.org/10.1038/35048077

Perpelescu, M., & Fukagawa, T. (2011). The ABCs of CENPs. *Chromosoma*, *120*(5), 425–446. https://doi.org/10.1007/s00412-011-0330-0

Poon, R. Y. (2015). Cell Cycle Control☆. *Reference Module in Biomedical Sciences*. Published. https://doi.org/10.1016/b978-0-12-801238-3.98748-8

Praskova, M., Xia, F., & Avruch, J. (2008). MOBKL1A/MOBKL1B Phosphorylation by MST1 and MST2 Inhibits Cell Proliferation. *Current Biology*, *18*(5), 311–321. https://doi.org/10.1016/j.cub.2008.02.006

Ren, F., Wang, B., Yue, T., Yun, E. Y., Ip, Y. T., & Jiang, J. (2010). Hippo signaling regulates Drosophila intestine stem cell proliferation through multiple pathways. *Proceedings of the National Academy of Sciences*, *107*(49), 21064–21069. https://doi.org/10.1073/pnas.1012759107

Ribeiro, P. S., Josué, F., Wepf, A., Wehr, M. C., Rinner, O., Kelly, G., Tapon, N., & Gstaiger, M. (2010). Combined Functional Genomic and Proteomic Approaches Identify a PP2A Complex as a Negative Regulator of Hippo Signaling. *Molecular Cell*, *39*(4), 521–534. https://doi.org/10.1016/j.molcel.2010.08.002

Rieder, C. L. (1981). The structure of the cold-stable kinetochore fiber in metaphase PtK1 cells. *Chromosoma*, *84*(1), 145–158. https://doi.org/10.1007/bf00293368

Rieder, C. L. (1982). The Formation, Structure, and Composition of the Mammalian Kinetochore and Kinetochore Fiber. *International Review of Cytology*, 1–58. https://doi.org/10.1016/s0074-7696(08)61672-1

Roberts, A. J., Kon, T., Knight, P. J., Sutoh, K., & Burgess, S. A. (2013). Functions and mechanics of dynein motor proteins. *Nature Reviews Molecular Cell Biology*, *14*(11), 713–726. https://doi.org/10.1038/nrm3667

Roos, U. P. (1973). Light and electron microscopy of rat kangaroo cells in mitosis. *Chromosoma*, *41*(2), 195–220. https://doi.org/10.1007/bf00319696

Sambrook, J., Fritsch, E. F., & Maniatis, T. (1989). *Molecular Cloning: A Laboratory Manual (3 Volume Set)* (2nd ed.). Cold Spring Harbor Laboratory Pr.

Schatten, H. (2008). The mammalian centrosome and its functional significance. *Histochemistry and Cell Biology*, *129*(6), 667–686. https://doi.org/10.1007/s00418-008-0427-6

Schulte, J., Sepp, K. J., Jorquera, R. A., Wu, C., Song, Y., Hong, P., & Littleton, J. T. (2010). DMob4/Phocein Regulates Synapse Formation, Axonal Transport, and Microtubule Organization. *Journal of Neuroscience*, *30*(15), 5189–5203. https://doi.org/10.1523/jneurosci.5823-09.2010

Shi, Z., Jiao, S., & Zhou, Z. (2016). STRIPAK complexes in cell signaling and cancer. *Oncogene*, *35*(35), 4549–4557. https://doi.org/10.1038/onc.2016.9

Sütterlin, C., & Colanzi, A. (2010). The Golgi and the centrosome: building a functional partnership. *Journal of Cell Biology*, *188*(5), 621–628. https://doi.org/10.1083/jcb.200910001

Tang, L. (2019). Investigating heterogeneity in HeLa cells. *Nature Methods*, *16*(4), 281. https://doi.org/10.1038/s41592-019-0375-1

Tang, N., & Marshall, W. F. (2012). Centrosome positioning in vertebrate development. *Journal of Cell Science*, *125*(21), 4951–4961. https://doi.org/10.1242/jcs.038083

Tang, N., Marshall, W. F., McMahon, M., Metzger, R. J., & Martin, G. R. (2011). Control of Mitotic Spindle Angle by the RAS-Regulated ERK1/2 Pathway Determines Lung Tube Shape. *Science*, *333*(6040), 342–345. https://doi.org/10.1126/science.1204831

Teusel, F., Henschke, L., & Mayer, T. U. (2018). Small molecule tools in mitosis research. *Mitosis and Meiosis Part A*, 137–155. https://doi.org/10.1016/bs.mcb.2018.03.005

Trammell, M. A., Mahoney, N. M., Agard, D. A., & Vale, R. D. (2008). Mob4 plays a role in spindle focusing in Drosophila S2 cells. *Journal of Cell Science*, *121*(8), 1284–1292. https://doi.org/10.1242/jcs.017210

University of Cambridge. (2003). *Characterization of the Drosophila melanogaster MOB homologues*. Wainman.

Vichalkovski, A., Gresko, E., Cornils, H., Hergovich, A., Schmitz, D., & Hemmings, B. A. (2008). NDR Kinase Is Activated by RASSF1A/MST1 in Response to Fas Receptor Stimulation and Promotes Apoptosis. *Current Biology*, *18*(23), 1889–1895. https://doi.org/10.1016/j.cub.2008.10.060

Vigneron, S., Prieto, S., Bernis, C., Labbé, J. C., Castro, A., & Lorca, T. (2004). Kinetochore Localization of Spindle Checkpoint Proteins: Who Controls Whom? *Molecular Biology of the Cell*, *15*(10), 4584–4596. https://doi.org/10.1091/mbc.e04-01-0051

Vitulo, N., Vezzi, A., Galla, G., Citterio, S., Marino, G., Ruperti, B., Zermiani, M., Albertini, E., Valle, G., & Barcaccia, G. (2007). Characterization and Evolution of the Cell Cycle-Associated Mob Domain-Containing Proteins in Eukaryotes. *Evolutionary Bioinformatics*, *3*, 117693430700300. https://doi.org/10.1177/117693430700300007

Walczak, C. E., & Heald, R. (2008). Mechanisms of Mitotic Spindle Assembly and Function. *International Review of Cytology*, 111–158. https://doi.org/10.1016/s0074-7696(07)65003-7

Walker, J. M. (1996). SDS Polyacrylamide Gel Electrophoresis of Proteins. *Springer Protocols Handbooks*, 55–61. https://doi.org/10.1007/978-1-60327-259-9_11

Walker, J. M. (2002). SDS Polyacrylamide Gel Electrophoresis of Proteins. *Protein Protocols Handbook, The*, 61–68. https://doi.org/10.1385/1-59259-169-8:61

Wang, T., Birsoy, K., Hughes, N. W., Krupczak, K. M., Post, Y., Wei, J. J., Lander, E. S., & Sabatini, D. M. (2015). Identification and characterization of essential genes in the human genome. *Science*, *350*(6264), 1096–1101. https://doi.org/10.1126/science.aac7041

Weeks, D. P., Spalding, M. H., & Yang, B. (2015). Use of designer nucleases for targeted gene and genome editing in plants. *Plant Biotechnology Journal*, *14*(2), 483–495. https://doi.org/10.1111/pbi.12448

Wei, X., Shimizu, T., & Lai, Z. C. (2007). Mob as tumor suppressor is activated by Hippo kinase for growth inhibition in Drosophila. *The EMBO Journal*, *26*(7), 1772–1781. https://doi.org/10.1038/sj.emboj.7601630

Wheatley, S. P., Kandels-Lewis, S. E., Adams, R. R., Ainsztein, A. M., & Earnshaw, W. C. (2001). INCENP Binds Directly to Tubulin and Requires Dynamic Microtubules to Target to the Cleavage Furrow. *Experimental Cell Research*, *262*(2), 122–127. https://doi.org/10.1006/excr.2000.5088

Wheatley, S. P., & Wang, Y. (1996). Midzone microtubule bundles are continuously required for cytokinesis in cultured epithelial cells [published erratum appears in J Cell Biol 1996 Dec;135(6 Pt 1):1679]. *The Journal of Cell Biology*, *135*(4), 981–989. https://doi.org/10.1083/jcb.135.4.981

Witt, P. L., Ris, H., & Borisy, G. G. (1980). Origin of kinetochore microtubules in Chinese hamster ovary cells. *Chromosoma*, *81*(3), 483–505. https://doi.org/10.1007/bf00368158

Wurzenberger, C., & Gerlich, D. W. (2011). Phosphatases: providing safe passage through mitotic exit. *Nature Reviews Molecular Cell Biology*, *12*(8), 469–482. https://doi.org/10.1038/nrm3149

Xie, R., Wen, F., & Qin, Y. (2020). The Dysregulation and Prognostic Analysis of STRIPAK Complex Across Cancers. *Frontiers in Cell and Developmental Biology*, *8*. https://doi.org/10.3389/fcell.2020.00625

Yang, D., Xu, J., Zhu, T., Fan, J., Lai, L., Zhang, J., & Chen, Y. E. (2014). Effective gene targeting in rabbits using RNA-guided Cas9 nucleases. *Journal of Molecular Cell Biology*, *6*(1), 97–99. https://doi.org/10.1093/jmcb/mjt047

Yesbolatova, A., Natsume, T., Hayashi, K. I., & Kanemaki, M. T. (2019). Generation of conditional auxin-inducible degron (AID) cells and tight control of degron-fused proteins using the degradation inhibitor auxinole. *Methods*, *164–165*, 73–80. https://doi.org/10.1016/j.ymeth.2019.04.010

Yu, F. X., & Guan, K. L. (2013). The Hippo pathway: regulators and regulations. *Genes & Development*, *27*(4), 355–371. https://doi.org/10.1101/gad.210773.112

Zhang, L., Luo, J., Wan, P., Wu, J., Laski, F., & Chen, J. (2011). Regulation of cofilin phosphorylation and asymmetry in collective cell migration during morphogenesis. *Development*, *138*(3), 455–464. https://doi.org/10.1242/dev.046870

Zhao, B., Tumaneng, K., & Guan, K. L. (2011). The Hippo pathway in organ size control, tissue regeneration and stem cell self-renewal. *Nature Cell Biology*, *13*(8), 877–883. https://doi.org/10.1038/ncb2303

Zhou, J., Yao, J., & Joshi, H. C. (2002). Attachment and tension in the spindle assembly checkpoint. *Journal of Cell Science*, *115*(18), 3547–3555. https://doi.org/10.1242/jcs.00029

Zimmerman, W. C., Sillibourne, J., Rosa, J., & Doxsey, S. J. (2004). Mitosis-specific Anchoring of γ Tubulin Complexes by Pericentrin Controls Spindle Organization and Mitotic Entry. *Molecular Biology of the Cell*, *15*(8), 3642–3657. https://doi.org/10.1091/mbc.e03-11-0796

CHAPTER VIII

ANNEX

8. Annex

ANNEX

Table VIII.1 – Solutions for preparing 10 % resolving and 5 % stacking gels for Tris-glycine SDS-polyacrylamide gel electrophoresis (Sambrook et al., 1989).

10% Resolving gel	ml	5% Stacking gel	ml
Deionized H_2O	1,9	Deionized H_2O	1,4
30% Acrylamide/Bis solution (29:1)	1,7	30% Acrylamide/Bis solution (29:1)	0,33
1,5 M Tris (pH 8,8)	1,3	1,0 M Tris (pH 6,8)	0,25
10% SDS	0,05	10% SDS	0,02
10% Ammonium persulfate	0,05	10% Ammonium persulfate	0,02
TEMED	0,002	TEMED	0,002